University of Alberta

Ultrasensitive Assays for Proteins

by

Hongquan Zhang

A thesis submitted to the Faculty of Graduate Studies and Research
in partial fulfillment of the requirements for the degree of

Doctor of Philosophy

Medical Sciences - Laboratory Medicine and Pathology

Fall 2009
Edmonton, Alberta

Your file Votre référence
ISBN: 978-0-494-55837-9
Our file Notre référence
ISBN: 978-0-494-55837-9

Examining Committee

Dr. X. Chris Le (Supervisor), Laboratory Medicine and Pathology

Dr. Xing-Fang Li (Co-Supervisor), Laboratory Medicine and Pathology

Dr. Liang Li, Chemistry

Dr. Jonathan W. Martin, Laboratory Medicine and Pathology

Dr. Gregory J. Tyrrell, Laboratory Medicine and Pathology

Dr. Robert Kennedy, Chemistry, University of Michigan

Abstract

Important protein biomarkers for cancer, infectious diseases, and various biochemical processes are usually present at trace levels, making their detection analytically challenging. The primary objective of this thesis was to develop highly sensitive and specific techniques enabling the detection of minute amounts of proteins. Three bioanalytical techniques have been developed and described in this thesis.

A tunable aptamer capillary electrophoresis assay enabled highly sensitive fluorescence detection of multiple proteins and protein isomers. The electrophoretic mobility of proteins was tuned with DNA aptamers binding to the target proteins. Fluorescently labeled aptamers of varying nucleotide lengths served as both charge modulators for CE separation and as fluorescent affinity probes for ultrasensitive laser-induced fluorescence detection. Simultaneous determination of pM concentrations of human immunodeficiency virus reverse transcriptase (HIV-RT), thrombin, human immunoglobulin E (IgE), and two isomers of platelet-derived growth factor (PDGF) was achieved in a single analysis.

An affinity aptamer amplification assay was based on an integration of affinity aptamer recognition, CE separation, and amplification by polymerase chain reaction (PCR). A specific aptamer was first introduced to bind to the target protein, forming a protein-aptamer complex. The protein–aptamer complex was then separated from the unbound aptamer by CE. Fractions were collected and subjected to PCR amplification. The assay was able to detect as

few as 180 molecules of HIV-RT. Simultaneous determination of HIV-RT, thrombin, and IgE demonstrated the capability of the assay for multiple protein detection.

A binding-induced hairpin assay was able to measure trace amounts of proteins in homogeneous solutions. Two affinity ligands were each conjugated to a custom-designed oligonucleotide so that these two oligonucleotides could provide complementary stem sequences at their free ends. Binding of both affinity ligands to a specific target brought the complementary sequences together for their hybridization, inducing the formation of a hairpin structure. DNA ligation resulted in a unique DNA sequence that was subsequently detected by real-time PCR. Detection of the DNA sequence provided an indirect measure of the target protein. Streptavidin, PDGF-BB, and prostate specific antigen were determined with an improvement in detection limit by 10^3-10^5 folds better than those with immunoassays.

Acknowledgement

I would like to express my gratitude to all those who have helped and inspired me during my doctoral study.

My deepest gratitude goes to my supervisor, Dr. X. Chris Le, for his expertise, kindness, and most of all, for his patience. His help, stimulating suggestions and encouragement helped me in all the time of research for and writing of this thesis. His mentorship and scholarship really impress me and will benefit me for the rest of my life. I wish to express my sincere thanks to my co-supervisor, Dr. Xing-Fang Li, for her invaluable guidance and support throughout this work. Her perpetual energy and enthusiasm in research had motivated all her students, including me.

My thanks and appreciation also goes to my thesis committee members, Dr. Liang Li and Dr. Jonathan Martin for their kind assistance, wise advices, constructive comments, and so on. I am delighted to interact with Dr. Steve Hrudey by attending his class. His kind assistance with writing letters and with various applications is appreciated.

The generous support from Ms. Katerina Carastathis and Ms. Dianne Sergy is greatly appreciated.

I am indebted to many postdoctoral fellows and my fellow graduate students in AET division for providing a stimulating and fun environment in

which to learn and grow. I am especially grateful to Dr. Shengwen Shen, Dr. Jeff Guthrie, Dr. Zhilong Gong, Dr. Hailin Wang, Dr. Qiang Zhao, Dr. Vichaya Charoensuk, and Ms. Alevtina Goulko for their tremendous help and cherished friendship.

Lastly, and most importantly, I wish to thank my parents, my parents-in-law, and my sisters for their continuous encouragement and boundless support. I owe my loving thanks to my wife, Zhongwen, and my lovely son, Ryan. Without their patient love and understanding it would have been impossible for me to complete this work.

Table of Contents

List of Tables

List of Figures

List of Abbreviations

BoNT/A	Botulinum toxin type A
BSA	bovine serum albumin
CE	capillary electrophoresis
CZE	capillary zone electrophoresis
FAM	carboxyfluorescein
CTBS	Cholera toxin beta subunit
Captamer	circular DNA aptamer
C_t	cycle threshold
Kd	dissociation constant
EOF	electroosmotic flow
μ_{EOF}	electroosmotic mobility
μ_{EP}	electrophoretic mobility
ELISA	enzyme-linked immunosorbent assay
FRET	fluorescent resonance energy transfer
HSA	Human serum albumin
Ig	Immunoglobulin
IL	Interleukin
IS	internal standard
LIF	laser-induced fluorescence
LPS	lipopolysaccharide
MW	molecular weight

NV	Noroviruses
rNVLP	Norwalk viral-like particle
nt	Nucleotide
μ_{OBS}	observed electrophoretic mobility
PBS	Phosphate buffered saline
PDGF	platelet-derived growth factor
PCR	polymerase chain reaction
PSA	prostate-specific antigen
PLA	proximity ligation assay
RIA	radioimmunoassay
HIV-RT	reverse transcriptase of the human immunodeficiency virus type 1
RCA	rolling circle amplification
scFv	single chain variable fragment
SPT	skin prick test
SELEX	systematic evolution of ligands by exponential enrichment
TSE	transmissible spongiform encephalopathies
TG	Tris and glycine
TBE	Tris-borate-EDTA
T_m	melting temperature
TNF	tumor necrosis factor
VEGF	vascular endothelial growth factor

Chapter One*

General Introduction: Ultrasensitive Assays for Proteins

1.1 Introduction

Proteins carry out many biological functions, including, but not limited to, catalyzing reactions in living organisms, decoding information in cells, regulating biochemical activities, storing and transporting small molecules, providing mechanical support, and serving many other specialized functions (1). The occurrence of various cancers and diseases usually involves altered protein expression and distribution (2). The detection of certain protein biomarkers can be useful for the diagnosis of specific diseases in clinical research.

Tremendous advances have been achieved in the development of analytical technology for protein detection. These range from the traditional immunological techniques, such as enzyme-linked immunosorbent assays (ELISA), radioimmunoassays (RIA) and immunosensors, to protein microarrays and mass spectrometry-based techniques (3-8). Although some of these techniques are able to provide relatively high sensitivity and low limits of detection, most of them are only capable of detecting abundant proteins. There is substantial interest in detection of proteins at ultra-low concentrations, e.g. below pM, because numerous important biological markers for cancer, infectious diseases, or biochemical processes are present at very low concentrations during the early stages of the disease development. Moreover, a few molecules of a pathologic protein are sufficient to trigger a disease or to affect the biological functions of

*A portion of this chapter has been published in H. Zhang, Q. Zhao, X. -F. Li, X. C. Le, *Analyst,* 2007, 132, 724-737.

cells. Therefore, methods with extreme sensitivity and high specificity are required.

This chapter reviews the recent developments of novel technologies for ultrasensitive protein detection, focusing on protein detection methods based on amplification of nucleic acids using polymerase. The major techniques used in this thesis, including capillary electrophoresis (CE) and polymerase chain reaction (PCR), were also introduced.

1.2 Protein Assays Based on Amplification of Nucleic Acids Using Polymerase

A polymerase is an enzyme whose central function is to catalyze the synthesis of new DNA or RNA from an existing DNA or RNA template. Polymerase-based technologies, such as polymerase chain reaction (PCR), have been widely used for amplification and detection of specific nucleic acid sequences with excellent sensitivity and specificity. When protein targets are recognized by affinity ligands (antibodies or aptamers) conjugated with DNA nucleotides, the amplification of the DNA tags by polymerase converts the detection of proteins into detection of nucleic acids, improving the sensitivity of protein detection dramatically. A variety of polymerase-based protein detection methods have been developed, and here immuno-PCR, affinity aptamer PCR, proximity ligation assay, immuno-rolling circle amplification, and immuno-T7 RNA polymerase amplification techniques are summarized.

1.2.1 Immuno-PCR

Immuno-PCR, first described in 1992 by Sano *et al.* (9), is a hybrid

technology that combines antibody recognition and PCR amplification. In immuno-PCR, the recognition of an antigen by an antibody that is conjugated to a DNA fragment results in the formation of a specific complex of the antigen with the antibody-DNA conjugate. The subsequent amplification of the attached DNA molecule by PCR allows for the indirect detection of the antigen with very high sensitivity. Owing to the PCR amplification, immuno-PCR can lead to a 100-10,000-fold increase in sensitivity over the conventional ELISA for proteins (10).

1.2.1.1 Antibody-DNA conjugates

In immuno-PCR, the antibody-DNA conjugates are required to recognize targets and serve as the template for PCR. In an initial work, a streptavidin-protein A chimera produced by protein recombinant technology was employed as a linker molecule to attach the DNA molecule to the antibody (9). This protein chimera contained two affinity units, the streptavidin moiety that could bind to biotin and the protein A moiety that could bind to the Fc portion of the antibody. Therefore, this bifunctional binding affinity enabled the conjugation of the biotinylated DNA molecule to the antibody. Although this protein chimera had been used successfully in several studies, the application of this technique was limited due to the limited availability of the chimeric proteins. To overcome this limitation and extend the application of immuno-PCR, streptavidin or avidin was used to join both the biotinylated DNA reporter and the biotinylated antibody, since streptavidin (avidin) and biotinylated antibodies are readily available (11, 12). This approach was easily carried out in simple successive incubation steps, and thus it has become the most commonly used format of the immuno-PCR

applications. However, the requirement of multiple incubation steps led to incomplete formation of the antibody-streptavidin-DNA complex, which reduced the sensitivity of immuno-PCR (13).

Another strategy for constructing antibody-DNA conjugates was direct covalent linkage of the DNA to the antibody (14). Covalent DNA-labeled antibodies have been employed for simultaneous detection of three analytes (hTSH, hCG and β-Gal) by immuno-PCR (14). Unique DNA nucleotides were covalently coupled to each of the analyte-specific antibodies, enabling the analysis of multiple analytes.

DNA-streptavidin nanostructures were assembled from the bisbiotinylated double-stranded DNA and the tetravalent biotin-binding protein streptavidin (15, 16). The self-assembly of these nanostructures could be controlled by the alteration of concentrations and ratios of reagents. The optimized conditions predominantly produced linear DNA-streptavidin nanostructures by using streptavidin molecules to bridge two adjacent DNA fragments. These unsaturated streptavidin molecules in nanostructures offered a number of binding sites for biotinylated antibodies. The incubation of these DNA-streptavidin networks with biotinylated antibodies resulted in the formation of supermolecular reagents, each containing multiple antibodies. The employment of these supermolecular reagents provided a 100-fold increase in sensitivity compared to conventional immuno-PCR (15).

1.2.1.2 Assay format

Immuno-PCR assays have been performed in formats similar to

conventional ELISA, including both the direct immuno-PCR format and the sandwich format. In the direct format, analytes were first captured directly onto a solid surface by adsorption (17-19). These adsorbed analytes were then recognized by antibodies conjugated to DNA nucleotides. Following washing to remove unbound species, PCR amplification of the DNA led to indirect detection of the analyte of interest. An interesting application was the detection of surface proteins in intact cells or tissue sections (20-22). However, the application of this format was limited to analytes that could be adsorbed onto the solid phase. In addition, other non-specifically adsorbed sample components could cross-react with the detection antibodies, resulting in interference. In the sandwich format, a capture antibody was attached onto the solid surface and was used to specifically capture the analyte. Then the antibody conjugated with DNA was used to bind with the captured analyte (23-25). Thus, the analyte was sandwiched between the two antibody molecules, enhancing the specificity of the assay (26-28).

Traditional PCR was used for amplification in the initial applications of the immuno-PCR. The detection of PCR amplification products was carried out at the end of PCR cycles by using gel electrophoresis or microplate-based methods (9, 29-31). Immuno-PCR assays using traditional PCR were time-consuming, and not quantitative. Real-time PCR led to significant improvements over the traditional PCR (32-34). Consequently, immuno-PCR assays adapting real-time PCR have achieved quantification for many practical applications (35-37).

1.2.1.3 Applications

Two comprehensive reviews (10, 38) have summarized the applications of

immuno-PCR to clinical diagnostics, biomedical research, and environmental analysis. Herein, the recent development of immuno-PCR is only discussed for protein detection, summarized in **Table 1.1**.

The detection of disease-related proteins represents a main application of immuno-PCR. The pathologic prion protein, implicated in transmissible spongiform encephalopathies (TSE), has been determined by immuno-PCR in two different studies (39, 40). Although both studies employed the similar sandwich immunoassay and real-time PCR, different sensitivities were observed due to variations in the operating process. The first study demonstrated the validity of immuno-PCR as a test method for the detection of the pathologic prion protein in bovine brain extract (39). The method was used to detect the pathologic prion protein in Sporadic Creutzfeldt-Jakob disease (41). Due to the insufficient washing process for removing the non-specific binding, the sensitivity of the assay was only 10-fold higher than that of ELISA. In contrast, the second study introduced a more efficient washing buffer and additional blocking steps to decrease the background signal from non-specific binding (40). The limit of detection was 1 fg/mL for recombinant hamster prion protein and 70-700 fg/mL for scrapie-infected hamster brain homogenate, which represented an improvement of one million times in sensitivity over conventional ELISA.

Three different formats of sandwich real-time immuno-PCR were compared for detection of prostate-specific antigen (PSA), a biomarker for prostate cancer (42). The capture antibodies were adsorbed directly onto the solid phase in the first two formats, while in the third format, the capture antibodies were linked to

the solid phase through streptavidin-biotin conjugation. In the first format, the DNA reporter was linked to the detection antibodies through streptavidin and biotin, but in the second and third formats, the covalent DNA-labeled antibodies were employed for detection. The results showed that the second format had the highest sensitivity and also high reproducibility. Another sandwich immuno-PCR assay was conducted to detect *Staphylococcus aureus* (*S. aureus*) through its specific product protein A (43). The detection limit was 0.01 fg/mL. The method was also successfully applied to the analysis of patient samples.

Immuno-PCR has also been used in environmental analysis. The detection of noroviruses (NV) was achieved through detection of NV capsid protein by real-time immuno-PCR (44). A sandwich format was employed, and the NV capsid proteins were detected in fecal and food samples with a sensitivity >1000-fold higher than conventional ELISA. The detection of Cry1Ac toxin by immuno-PCR was demonstrated (45), using antibodies covalently linked to DNA nucleotide. Two types of solid phase, microtiter plates and streptavidin-coated polystyrene particles, were employed. The detection using microtiter plates resulted in the lower limit of detection, 1×10^{11} molecules or 21.6 ng of toxin. Dianthin and ricin, two ribosome-inactivating proteins, were detected by immuno-PCR in the direct format (46). After the protein targets were adsorbed onto the solid surface, they were recognized by the primary antibody, which in turn bound to the secondary antibody that was linked with DNA nucleotides through biotin-streptavidin interaction. This assay was able to detect 10 fg/mL of dianthin and ricin due to an improvement in sensitivity by one-million-fold over ELISA.

Table 1.1. Summary of recent applications of immuno-PCR

Analyte	Assay format	PCR amplification	Detection limit	Sensitivity increase over ELISA	Ref.
Pathologic prion protein	Sandwich	Real-time PCR	0.75 ng/mL	10-fold	39, 41
Pathologic prion protein	Sandwich	Real-time PCR	1 fg/mL	1,000,000-fold	40
Prostate-specific antigen (PSA)	Sandwich	Real-time PCR	4.8×10^5 molecules (1 pg/mL)	100-fold	42
Protein A produced by *S. aureus*	Sandwich	Conventional PCR	0.01 fg/mL	NA	43
Norwalk viral-like particles (rNVLPs)	Sandwich	Real-time PCR	10 fg rNVLPs (0.13 pg/mL)	>1000-fold	44
Cry1Ac toxin	Direct format	Conventional PCR	21.6 ng (216 ng/mL)	NA	45
Dianthin and ricin	Direct format	Conventional PCR	10 fg/mL	1,000,000-fold	46
Cholera toxin beta subunit (CTBS)	Liposome-PCR	Real-time PCR	0.02 fg/mL	10, 000-fold	47
Botulinum toxin type A (BoNT/A)	Liposome-PCR	Real-time PCR	0.02 fg/mL	450-fold	47
Hanttaan virus nucleocapsid protein	Phage display mediated immuno-PCR	Real-time PCR	10 pg/mL	10, 000-fold	48
Pathologic prion protein	Phage display mediated immuno-PCR	Real-time PCR	NA	1,000-fold	48

NA: not available

1.2.1.4 Recent development of immuno-PCR analogous methods

The liposome-PCR assay (47) and phage display mediated immuno-PCR (48) represent two recent developments that further improve on immuno-PCR. The liposome-PCR assay employed the sandwich ELISA format (47). To detect cholera toxin beta subunit (CTBS), CTBS was sandwiched by a capture antibody and liposome encapsulated detection probe. The liposome detection probe was constructed by the incorporation of approximately 2,500 non-specific receptor molecules for CTBS into the bilayer of the single liposome in which about 60 copies of an 80 bp dsDNA reporter were encapsulated. Amplification of DNA reporters by real-time PCR afforded the detection and quantification of the corresponding biotoxin target. The limit of detection of this assay for both CTBS and botulinum toxin type A (BoNT/A) was 0.02 fg/mL, which was 2–3 orders of magnitude lower than those of the most sensitive assays in use. The higher sensitivity was achieved because of the multiple reporters per binding event. In addition, the DNA reporters encapsulated in the liposome were protected from chemical or enzymatic degradation, while background contamination was removed by the use of DNase I. It is conceivable that antibodies in place of toxin receptors may be used in this assay for the analysis of other targets. The extension of this technology to other targets remains to be demonstrated.

Another modification of the immuno-PCR was the use of a recombinant phage particle instead of the antibody-DNA conjugate (48). On the surface of the phage particle, a single chain variable fragment (scFv) was displayed, serving as a recognition element. Therefore, this technology opened up a new approach to

create a ready-to-use reagent for immuno-PCR through bacterial activity. However, the sensitivity of this technology was lower than that of antibody-based immuno-PCR, because the binding affinity of scFv was usually lower compared to its parent antibody.

1.2.2 Protein detection by PCR amplification of affinity aptamers

Aptamers are short oligonucleotides that have high affinity for specific target molecules. They are usually generated by an *in vitro* selection process known as systematic evolution of ligands by exponential enrichment (SELEX) (49, 50). Many aptamers bind specifically to their targets with affinity equivalent to the binding of monoclonal antibodies to antigens (51, 52). As affinity reagents, aptamers have been used in a range of bioanalytical techniques (53-55).

Recently, an exonuclease protection assay has been established for protein detection, coupling target recognition by aptamers and PCR amplification. In the exonuclease protection assay, exonuclease I was used to degrade the unbound aptamer while leaving the protein-bound aptamer protected (56). When thrombin was bound to its aptamer, the aptamer was protected from degradation by exonuclease I, while the unbound aptamer was degraded by 20 units of exonuclease I. The bound aptamer was then released from thrombin by a heating step at 80 °C for 15 min and used as a connector to form a longer oligonucleotide for real-time PCR amplification. This method offered exquisite sensitivity, enabling detection of as few as several hundred thrombin molecules. A potential caveat of this assay is that any incomplete degradation of the unbound aptamer will result in high background signals, compromising the detection limit.

Application of this technique to the detection of other proteins remains to be demonstrated.

1.2.3 Proximity ligation assay

In the proximity ligation assay (PLA), DNA oligonucleotides were attached to affinity probes (e.g. antibodies or aptamers) for the target protein (**Figure 1.1**) (57). When two or more such affinity probes bound to the same target protein molecule, these DNA tags were brought sufficiently close to hybridize together to a subsequently added connector oligonucleotide. The new DNA strands were formed by enzymatic DNA ligation. These ligation products were then amplified and detected by real-time PCR.

1.2.3.1 Affinity probes and assay formats

DNA aptamers were attractive affinity probes in proximity ligation, and attachment of DNA oligonucleotides to DNA aptamers was simple and straightforward (58). However, due to the limited availability of two aptamers for a single target protein molecule, both monoclonal and polyclonal antibodies have also been used for proximity ligation. Through direct covalent attachment or using streptavidin-biotin recognition, the antibodies were attached to DNA oligonucleotides, and these antibody-DNA conjugates have been successfully used in PLA (59). Recently, a peptide aptamer was also used as the affinity probe for PLA (60).

PLA has been carried out in the homogenous and the solid phase formats (58, 61). Partitioning procedures, such as washing, were not required for the homogenous assay format. Affinity recognition, DNA ligation and PCR

amplification were conducted in a single tube, facilitating high-throughput analysis. In the solid phase format, target proteins were first captured by the affinity probes attached to a solid phase. Pairs of proximity probes were then employed to recognize the captured protein molecules. After washing off the excess probes, the protein-bound DNA probes were ligated and amplified. Although more complicated than the homogenous assay, the solid phase format required three specific binding events, resulting in reduced cross-reactive detection. The solid phase also provided a better detection limit due to the washing step that decreased the background signal.

PLA has two-binder and three-binder formats, depending on the number of affinity probes binding to individual target proteins (62). In two-binder PLA (2PLA), the simultaneous binding of two affinity probes to individual protein molecules brought DNA tags into proximity, and a connector oligonucleotide was then used as a template for the subsequent DNA ligation. Three-binder PLA (3PLA) involved the simultaneous binding of three affinity probes to the same protein molecule, and the DNA tag of the third affinity probe served as the template for ligation of the other two DNA tags. The 3PLA assay required three independent binding events and allowed the use of lower concentrations of template strands and higher concentrations of affinity probes, which greatly improved its specificity and sensitivity over those of the 2PLA method.

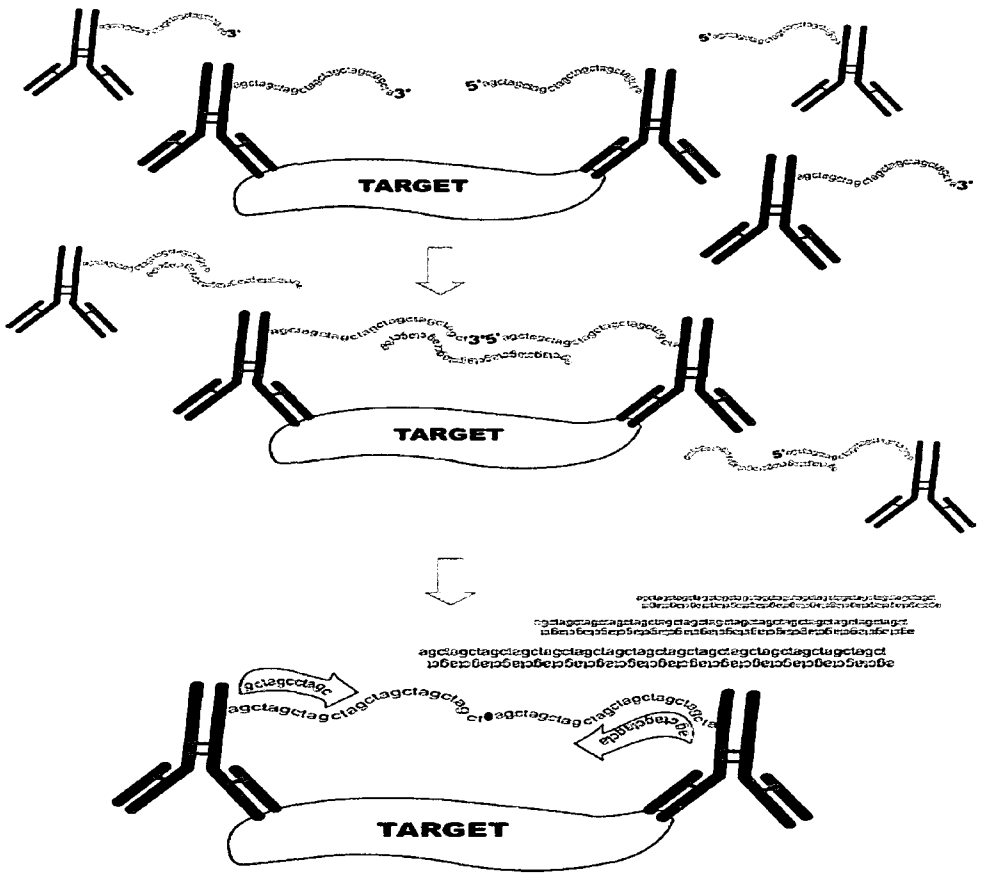

Figure 1.1. Schematic of proximity ligation assay. Adapted from ref. 57. An oligonucleotide tag is conjugated with an affinity ligand (e.g. antibody) that recognizes the target protein. When two or more such ligands bind to the same target protein molecule, the oligonucleotide tags are brought sufficiently close to hybridize together to a subsequently added connector oligonucleotide. The new DNA strands are created by enzymatic DNA ligation. These ligation products can be detected and quantified by real-time PCR.

1.2.3.2 Applications

PLA was first developed and applied to the analysis of cytokine platelet-derived growth factor (PDGF-BB) and thrombin (58). Affinity DNA aptamers were attached to DNA oligonucleotides for ligation, and the analysis of PDGF-BB was conducted in both the homogenous and solid phase formats. The detection of as few as 24,000 PDGF-BB molecules represented an increase in sensitivity of three orders of magnitude over the conventional ELISA. The method also offered a broad dynamic range and high specificity. The measurement of PDGF-BB by this technique has been used in two other studies on PDGF function (63, 64). Several other cytokines were also analyzed by PLA in which DNA-conjugated antibodies were employed as binding reagents (59). PLA has also been applied to detect only active prostate-specific antigen (PSA), in which a peptide that specifically bound to enzymatically active PSA was employed as an affinity probe (65). The detection limit of 0.07 μg/L active PSA was achieved.

3PLA presented higher sensitivity in protein detection than 2PLA. As few as several hundred molecules of the vascular endothelial growth factor (VEGF), tropoin I, and PSA were detected by 3PLA in cell lysate or in dilute plasma (62). The detection of 300 PSA molecules in 5 μL buffer represented 4×10^4 fold higher sensitivity than the corresponding 2PLA.

PLA enabled multiplexed protein detection because the sequence of DNA tags in affinity probes could be specifically designed to different protein targets. Six cytokines (VEGF, interleukin-4 (IL-4), IL-10, IL-7, IL-1α, and tumor necrosis factor-α (TNFα)) were simultaneously detected by PLA with low-femtomolar

detection limit as well as a five-order-of-magnitude linear dynamic range (66).

PLA also enabled sensitive detection of cell surface proteins, which was demonstrated in a recent study for the detection of individual microbial pathogens (61). When DNA-conjugated antibodies were bound to cell surface proteins in close proximity, the DNA conjugates were ligated together to form a unique template for PCR amplification. The detection of proteins on the cell surface did not require the binding of a pair of antibodies to a single protein molecule. The DNA-conjugate antibodies were needed to bind to two adjacent protein molecules on the cell surface. Since different cells express specific proteins on their surfaces, the detection of cell surface proteins can be used to detect specific cells. A very small number of bacteria were readily detected in 1μL samples, showing much higher sensitivity than ELISA (61). In another study, a peptide aptamer was attached to a DNA oligonucleotide through the fluorescent protein phycoerythrin, and was used for sensitive detection of a spore by PLA (60).

In addition to ultrasensitive detection of proteins, PLA was also applied to study protein-protein and DNA-protein interactions, in which proximity ligation was conducted with DNA strands from different molecules in protein-protein and DNA-protein complexes (67, 68). These DNA strands were extended from the DNA sequences in complexes, or conjugated to antibodies that bound to proteins in complexes.

1.2.4 Immuno-recognition and rolling circle amplification

Immuno-recognition and rolling circle amplification (RCA) were combined to achieve protein detection with high sensitivity (**Figure 1.2**) (69). RCA involved

rolling replication of short circular DNA sequences by using certain DNA polymerases at constant temperature (70, 71). The DNA polymerases used in RCA had special strand displacement or duplex unwinding activity, allowing them to perform the rolling synthesis of the repeat DNA sequences. In immuno-RCA, the antibody was labeled with an oligonucleotide primer that was complementary to the circular DNA probe. The labeled antibody bound specifically to the analyte of interest. After removal of the unbound antibody, DNA polymerase was employed to extend the single primer along the circular probe, producing a longer single-stranded DNA that consisted of many tandem repeats (typically 10^2-10^3) of the complement to the circular DNA. The increased length of DNA (by up to one-thousand-fold the length of the probe) resulted in substantial enhancement in detection sensitivity. For example, when fluorescently labeled nucleotides were incorporated into the RCA products, the longer DNA contained more fluorescent nucleotides, yielding higher sensitivity (72). In the initial study, the immuno-RCA sandwich assay for Immunoglobulin E (IgE) yielded an improvement in sensitivity of two to three orders of magnitude over the conventional ELISA (69).

Because the replication products of linear RCA were synthesized at a uniform rate, immuno-RCA usually provided a broad dynamic range and good reproducibility. Unlike traditional PCR, the RCA reaction did not require thermal cycling because the RCA reactions were performed under constant and moderate temperature. The complexes of the conjugated antibodies to their antigens were not dissociated during the RCA amplification process. Therefore, the reaction products remained localized to the antibody-antigen complexes. These features

have made immno-RCA ideally suitable for protein microarray applications (69, 72).

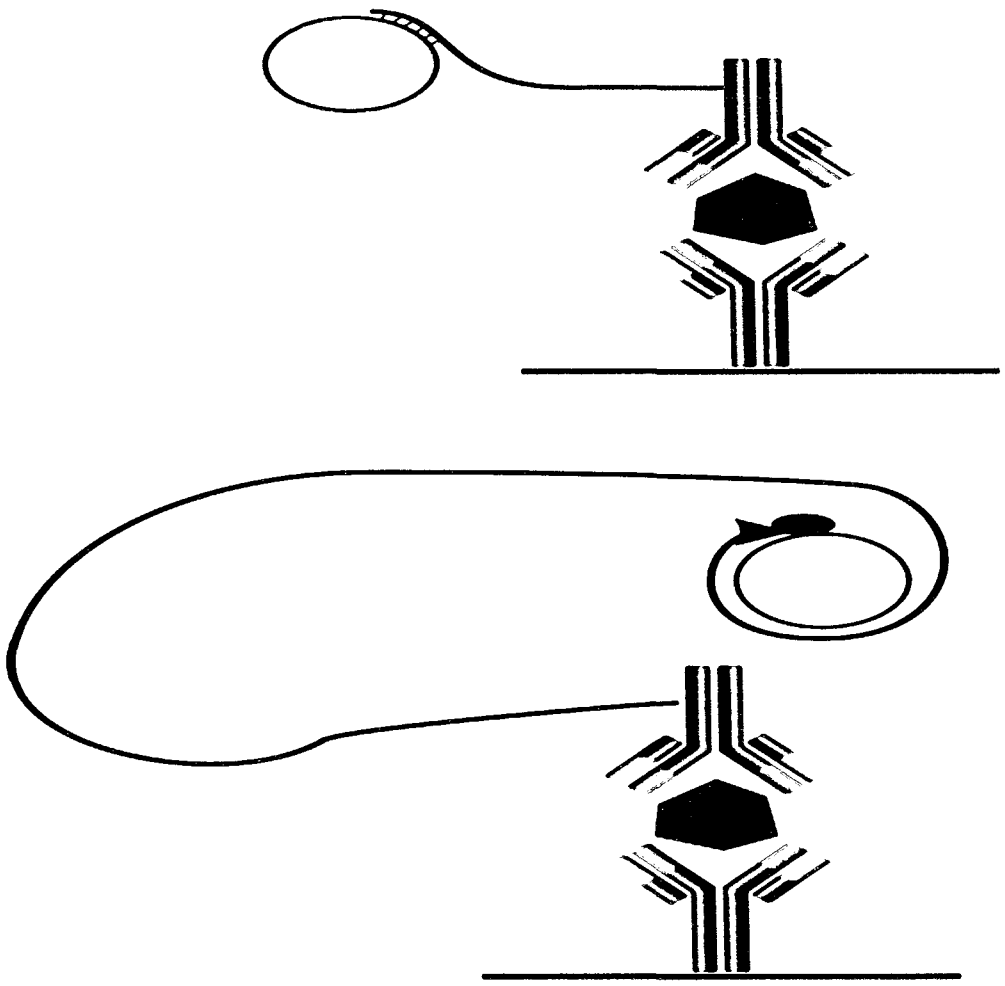

Figure 1.2. Schematic of immuno-rolling circle amplification. The analyte is captured onto a solid surface by a capture antibody. The captured analyte is then recognized by a reporter antibody that is covalently attached to an oligonucleotide primer. In the presence of circular DNA and DNA polymerase, the oligonucleotide primer is extended by RCA, resulting in a longer DNA molecule containing multiple repeats of the circle DNA sequence. The detection of the longer single-stranded DNA provides improved sensitivity.

The adaptation of immuno-RCA to protein microarray enabled multiple protein detection with high sensitivity and good reproducibility, and offered a promising prospect in proteomics and clinical diagnostics (72). The immuno-RCA mircoarray has been used to detect multiple allergen-specific IgEs in two studies (73, 74). Four allergens were spotted on activated glass slides to capture their specific IgEs, which were detected by the anti-IgE antibody DNA conjugate through RCA. Serum samples from 30 patients were tested by the immuno-RCA microarray and the results were compared with those from the skin prick test (SPT), the gold standard (73). The results from the microarray assay were in excellent agreement with those obtained from SPT. The immuno-RCA microarray assay was also compared with three commercial methods for testing allergen-specific IgEs *in vitro* (74). The RCA microarry assay produced correlation coefficients > 0.9 with each commercial test.

An immuno-RCA microassay has been developed for multiplexed protein profiling (72). It was able to measure a total of 75 cytokines simultaneously with femtomolar sensitivity, a quantitative range of three orders of magnitude, and small sample consumption. The expression of 51 cytokines was determined in secretion from human dendritic cells induced by lipopolysaccharide (LPS) or TNF-α. This RCA microarray was later extended to enable the detection of 150 cytokines simultaneously in a sandwich immunoassay format (75). By choosing optimal capture and detection antibody pairs and optimizing the assay procedures, more than half of these proteins were detected at sensitivities in the pg/mL range. In a recent study, the immuno-RCA microassay enabled the determination of 78

cytokines, growth factors, and soluble receptors in human serum and demonstrated differences in their profiles between patients with inflammatory bowel disease and those in remission (76).

A two-color RCA microarray immunoassay was developed that offered a 30-fold improvement in sensitivity over two other methods using antibody microassays (77). Replicate measurements of 51 proteins from sets of 24 serum samples were highly reproducible. The two-color RCA microassay has been applied to profile the serum proteins of lung and pancreatic cancer patients in two recent studies (78, 79).

The substitution of aptamers for antibodies in immuno-RCA has recently led to the proximity extension assay (**Figure 1.3**) (80). This method used two aptamers for thrombin, each recognizing a distinct binding site of thrombin. A multivalent circular aptamer, or captamer, was constructed to possess two functionalities: binding to one site of thrombin and also serving as the template of RCA. The other aptamer had an extended length so that it could bind to the thrombin at one end while its tail served as a primer for the RCA of the circular aptamer. Upon binding to the target protein, the tail of the linear aptamer was hybridized to the complementary loop of the captamer, allowing RCA to start. A detection limit of 30 pM was obtained, and this value was almost three orders of magnitude lower than the dissociation constants of the two aptamer-thrombin complexes. Moreover, the analysis was carried out in a one-step homogeneous format. The requirement of two aptamers binding to the same target makes this method very specific. However, this same requirement restricts its application to

the target molecules that have two aptamer-binding sites available.

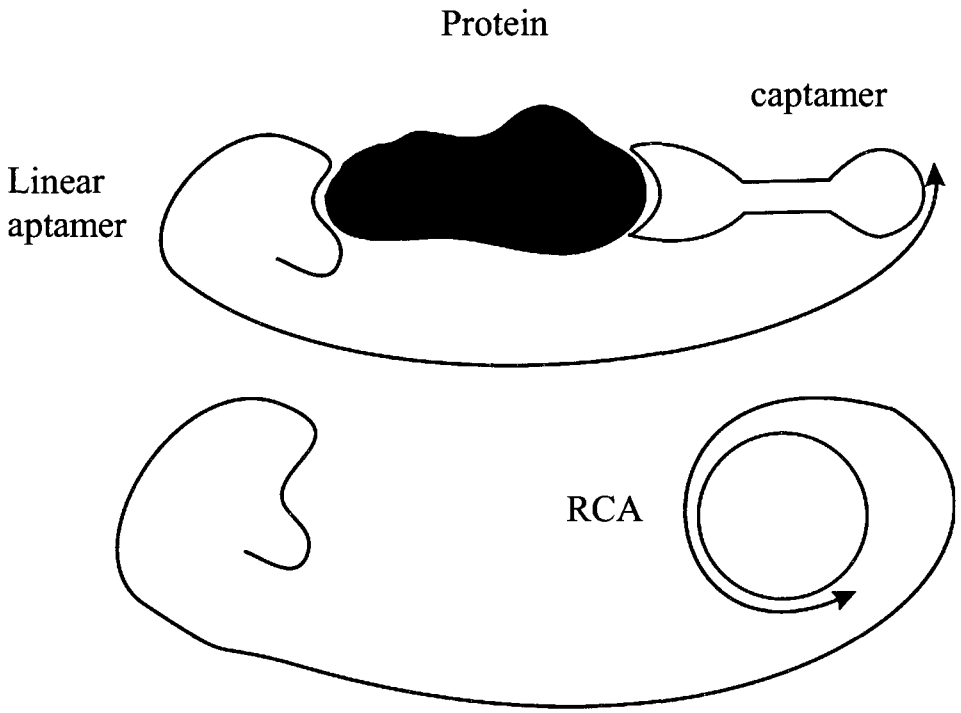

Figure 1.3. Schematic of proximity extension assay. A circular DNA aptamer (captamer) binds to one site of the target protein and also serves as the template of rolling circle amplification (RCA). Another linear aptamer binds to the other site of the target protein, and this linear aptamer is long enough to reach the captamer. Upon target binding, the tail of the linear aptamer is then able to hybridize to the complementary loop of the captamer, allowing RCA to start. Polymerase-mediated extension of RCA dissociates the captamer from the target protein and converts the captamer from a functional binding element into a structural template.

Although immuno-RCA assays are very useful for protein detection, the ultimate sensitivity of any immuno-RCA assay may be limited by the following factors. The extra time used for RCA amplification will lead to some dissociation of the antibody-antigen complexes, and the dissociated antibodies will be removed by the washing step before detection. The large RCA product attached to the antibody may decrease the binding affinity of the antibody, inducing the dissociation of the antibody-antigen complexes.

1.2.5 Immuno recognition and T7 RNA polymerase amplification

T7 RNA polymerase, instead of DNA polymerase, was used to amplify the DNA reporter for the protein analysis (81). In a sandwich format, the analyte was bound to both the capture antibody on a solid phase and to the detection antibody that was conjugated to a double-stranded DNA containing the T7 promoter. The T7 RNA polymerase was employed to amplify RNA from the dsDNA (82, 83). By incorporating the ^{32}P-labeled CTP to the RNA synthesis by T7 RNA polymerase, this method exhibited a 10^9-fold increase in sensitivity over the ELISA for detection of a tumor-related protein $p185^{her2/neu}$. The method offered a broad dynamic range due to the linear amplification by T7 RNA polymerase. Recently, this method was modified by using RNA intercalating fluorescent dye in place of the radioactive isotopes for RNA detection (84). The major drawbacks of this method include the longer amplification time and the relatively lower amplification efficiency of T7 RNA polymerase compared to PCR amplification.

1.3 Capillary Electrophoresis

Two major techniques, CE and PCR, were employed in this thesis research to develop novel bioanalytical techniques for ultrasensitive protein analysis. Therefore, these two techniques are briefly introduced here.

1.3.1 Capillary zone electrophoresis

Capillary zone electrophoresis (CZE), also referred to as free solution CE, is the most commonly utilized form of CE because it is relatively simple and applicable to separations of a diverse array of analytes varying in size and character (85-88). In CZE, the capillary is filled with a homogenous buffer, and analytes are separated on the basis of their relative charge and size.

A typical CZE system consists of a sample vial, two buffer vials (source and destination vials), a fused silica capillary, a high-voltage power supply, electrodes connected to the power supply, a detector, and a data output and handling device (**Figure 1.4**). The capillaries employed in CZE usually have a very small internal diameter (typically 5–100 μm), which imparts capillaries with a high surface-to-volume ratio allowing very efficient dissipation of Joule heat generated from large applied fields. Therefore, much higher voltages, up to 30 kV, can be employed than those used in slab gel electrophoresis, leading to faster, more efficient separations. To perform a CZE separation, the source vial, capillary, and destination vial are filled with an appropriate separation buffer at the desired pH and the sample is introduced at the inlet. An electric field is applied between the source and destination vials. The ionic species in the sample plug migrate through the capillary with an electrophoretic mobility determined by their charge and size,

and are detected by the detector. The output of the detector is sent to a data output and handling device such as an integrator or computer. The output is then displayed as an electropherogram, which represents detector response as a function of time. In an electropherogram, separated compounds appear as peaks with different retention times.

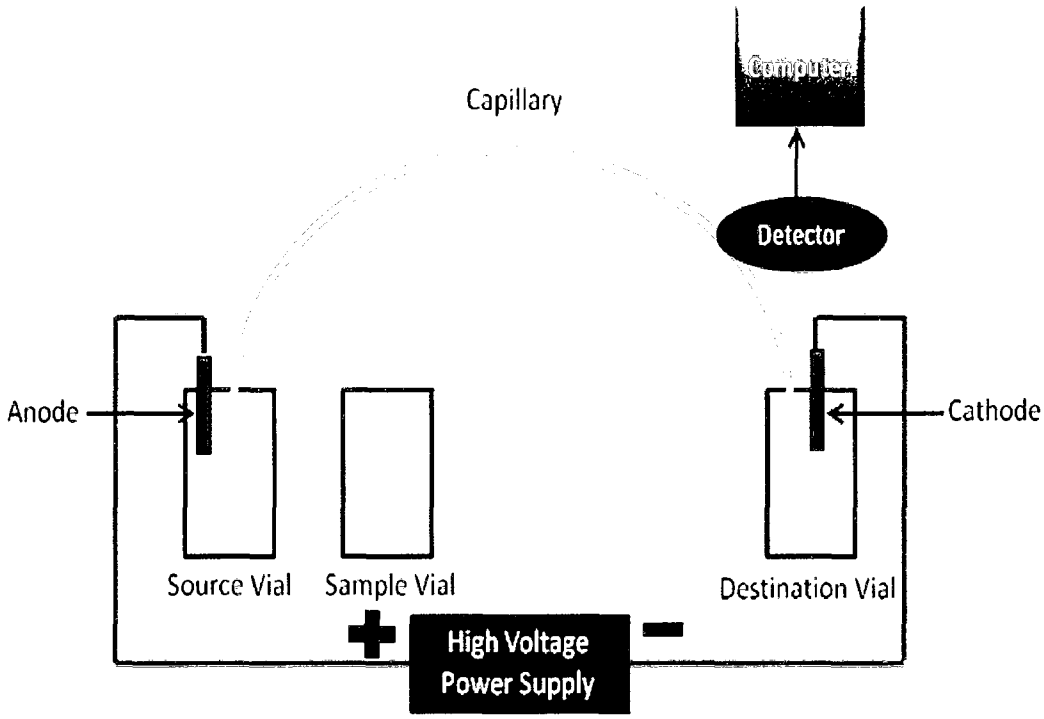

Figure 1.4. Schematic of capillary zone electrophoresis

In CZE, in addition to ionic species, the buffer solution is also pulled through the capillary under an applied electric field. This phenomenon, termed electroosmotic flow (EOF), is responsible for the bulk flow in CE. When a buffer is filled inside a fused silica capillary, an electrical double layer is created at the interface between a solid and a liquid phase due to the adsorption of positively

charged cations in the buffer to the ionized silanol groups on the capillary wall. In the presence of an electric field, the cations in the diffuse portion of this double layer migrate toward the negatively charged cathode and drag the bulk buffer solution with them, causing an EOF. The EOF profile is flat rather than the parabolic shape characteristic of press-induced flow. The advantage of this flat flow profile is that analytes migrate through the capillary in very narrow bands leading to highly efficient separations. The EOF can be changed by various parameters, including applied electric voltage, buffer pH, concentration or ionic strength of the buffer, temperature, and modification of the capillary wall.

The EOF acts as an electric-field-driven pump analogous to the mechanical pump used in liquid chromatography. In most cases, the EOF is the strongest driving force propelling all analytes, regardless of charge, toward the cathode. Therefore, it is possible to separate and detect positive, negative, and neutral molecules in a single electrophoretic run. In CZE, the separation is ultimately determined by differences in the electrophoretic mobility of the individual analytes. An analyte's velocity passing through the capillary is dependent on both EOF and its electrophoretic mobility, and the observed electrophoretic mobility μ_{OBS} of the analyte is represented by its electrophoretic mobility (μ_{EP}) plus the electroosmotic mobility (μ_{EOF}):

$$\mu_{OBS} = \mu_{EP} + \mu_{EOF}$$

The EOF adds the same mobility to all analytes, regardless of their ionic status. Positively charged analytes have electrophoretic mobilities in the same direction as the electroosmotic flow, and so move faster than the EOF. Negatively charged

compounds are attracted to the anode but are swept up by the electroosmotic flow, and they move at a rate that is lower than the EOF. Neutral molecules, which are not separated from each other in capillary zone electrophoresis, elute as a single band with the same velocity as the electroosmotic flow. Therefore, the order in which analytes migrate through the capillary is cations, neutrals, and then anions.

1.3.2 Capillary electrophoresis with laser-induced fluorescence detection

One of the greatest challenges in CE instrumentation development is the design and development of the detectors that possess the desired detection limits. CE has been coupled with a wide of variety of detection techniques, including ultraviolet absorbance, fluorescence, mass spectrometry, conductivity, amperometry, and refractive index. Among these detection techniques, laser-induced fluorescence (LIF) detection produces the best detection limits. Detection limits of 10^{-18}–10^{-21} mol have been reported with on-column LIF detection (89-92).

Several unique characteristics contribute to the success of LIF detection for CE. A laser can be focused near the diffraction limit of light so that it is particularly suitable for focusing to the small inner diameter of a capillary. The monochromaticity of laser results in simpler Raman spectra that are filtered more easily than the spectral background produced by a general light source. Moreover, the laser intensity can be varied to a wide range and can be optimized to achieve very high sensitivity without photodecomposition of the analytes.

Zare and coworkers reported the first application of lasers to fluorescence detection for CE (93). A number of improvements in LIF detection have since been made in the past few years. A variety of lasers have been used in LIF

detection, including argon ion, helium-cadmium, helium-neon, and diode lasers. In order to achieve high sensitivity, many efforts have been made to improve the collection of fluorescence and decrease the background signal. A large amount of background signal due to reflection and refraction at capillary walls is generated when on-column fluorescence detection is adapted. To avoid the disadvantages of on-column detection, Dovichi's group has designed a post-column fluorescence detector based on the sheath flow cuvette (94-98). In this system, the capillary outlet is inserted into the cuvette. Sheath flow, identical to the separation buffer, is introduced into the flow chamber at a rate which prevents mixing of the two flowing streams. The laser is then focused at the outlet of the capillary, not on the capillary. Because the sheath flow cuvette is made from optically flat quartz, much less light scattering is produced than from a capillary. Therefore, the background from light scattering is greatly minimized, and much lower detection limits are obtained compared to on-column detection. Detection limits of hundreds of molecules have been reported by using sheath flow cuvette in LIF detection (99, 100).

CE-LIF has been demonstrated for biological and environmental applications, including DNA sequencing, detection of peptides and proteins, studies of antibody-antigen interactions, determination of therapeutic drugs and natural toxins, assays for DNA and DNA damage, and analysis of single cells.

1.4 PCR

PCR is a widely used technique that amplifies a piece of DNA by *in vitro* enzymatic replication (101-103). With PCR it is possible to amplify a few copies

of a DNA, generating millions or more copies of the same DNA molecule. PCR has become an integral tool in molecular biology, and it is highly versatile and readily adaptable for a wide variety of applications.

Several components and reagents are required to carry out a PCR experiment, including a DNA template that contains the DNA region to be amplified, a thermostable DNA polymerase, two primers that are complementary to the DNA template at the 5' or 3' ends of the amplified DNA region, four deoxyribonucleoside triphosphates (dNTPs) that provide the building blocks for synthesis of the new DNA strand, magnesium ion which is very important for the specificity and efficiency of the reaction, and buffer solution that provides a suitable chemical environment for optimum activity of the DNA polymerase.

PCR is commonly carried out with cycles that have three distinct steps performed at different temperatures. These three steps are denaturation, annealing and extension (**Figure 1.5**). In the denaturation step, the complementary strands of DNA are separated by heating the reaction to 94-98 °C for 20-30 seconds. This allows melting of DNA template by disrupting the hydrogen bonds between complementary bases of the DNA strands, yielding single stranded DNA. In the annealing step, the reaction is cooled to 50-65 °C for 20-40 seconds, allowing the oligonucleotide primers to hybridize to the template. The annealing temperature is typically about 3-5 °C below the T_m of the primers. Therefore, the primers are able to track down and bind to the complementary regions within the long DNA template by forming stable DNA-DNA hydrogen bonds. The polymerase begins to extend the primers as soon as they anneal to the DNA template. In the

extension step, the reaction is heated to a temperature close to the optimal polymerization temperature, depending on the DNA polymerase used. Taq polymerase presents its optimum activity at a temperature range of 70-75 °C, and an extension temperature of 72 °C is commonly used with this enzyme. At this step the DNA polymerase synthesizes a new DNA strand complementary to the DNA template strand by adding four dNTPs that are complementary to the template in 5' to 3' direction. The extension time is determined both by the DNA polymerase used and depending on the length of the DNA fragment to be amplified. The three steps are usually repeated for 20-45 times, as necessary for the specific application. Under optimum conditions, the amount of the DNA target is doubled at each cycle, leading to exponential amplification of the specific DNA fragment.

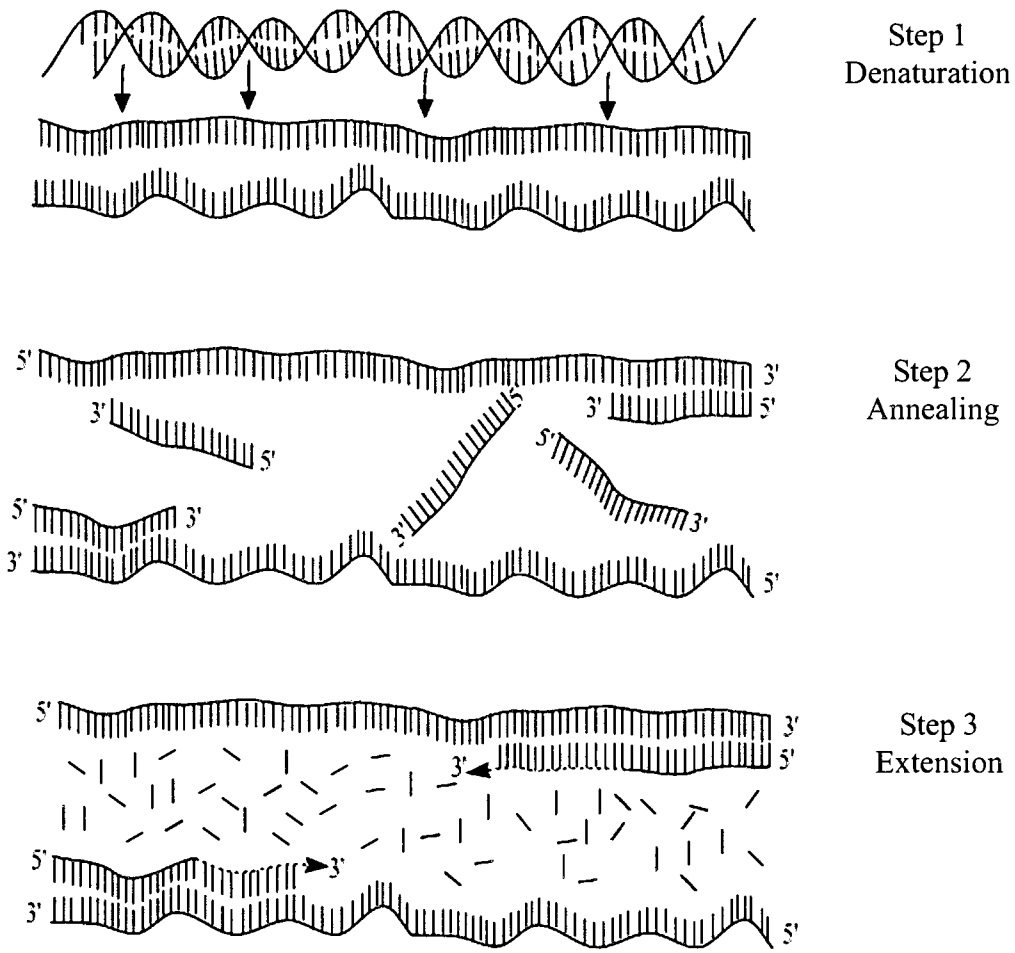

Figure 1.5. Schematic of polymerase chain reaction. Step 1, the template DNA is denatured to separate the complementary stands; step 2, the reaction is cooled to allow the oligonucleotide primers to hybridize to the template; step 3, the DNA polymerase synthesizes a new DNA strand complementary to the DNA template strand by adding four dNTPs.

One major technical advance that has allowed PCR to become such a routine and accessible technique is automation of the temperature cycling process. After the reagents required for PCR are mixed in a reaction volume of 10-200 μL, the PCR reaction is carried out in a thermal cycler that automatically regulates the temperature of the reaction cycles according to the preprogrammed set of instructions.

Because PCR allows amplification of any short sequence of DNA without the necessity of cloning it, it has been widely applied in molecular biology, microbiology, genetics, diagnostics, clinical laboratories, forensic science, environmental science, hereditary studies, paternity testing, and many other applications.

1.4.1 Real-time PCR

Traditional PCR uses gel electrophoresis for separation and detection of PCR products at the final phase or end-point of the PCR reaction. This approach is not quantitative for the following reason. A whole PCR run can be broken up into three distinct phases, the exponential, linear, and plateau phases. Given well-optimized conditions of a PCR experiment, all reaction components are present in their optimum concentration in the exponential phase, allowing the reaction to be very specific and precise. Exact doubling of DNA product is obtained at each cycle. As the reaction proceeds, some of the components are being consumed as a result of amplification in the linear phase. The reactions start to slow down and the PCR product is no longer being doubled at each cycle. Eventually, the reactions stop and reach a plateau phase. The plateau phase is reached at different

points depending on the different reaction kinetics for each sample.

Real-time PCR, on the other hand, is able to quantify the amplified DNA during the process of amplification (104-108). Although real-time PCR follows the general principles of PCR, its key feature that enables it to amplify and simultaneously quantify a target DNA molecule is that the amplified DNA is quantified after each amplification cycle. This is typically done by including fluorescent reporter probes in the reaction mixture and by measuring fluorescence at each PCR cycle. In order to accurately quantify the initial amount of DNA templates, it is necessary to determine the amount of amplified DNA in the exponential phase, which can only be achieved by real-time PCR not traditional PCR.

Two common approaches are applied to generate the fluorescence signals that are proportional to the amount of PCR product. Double-stranded DNA dyes, such as SYBR Green, are able to intercalate all double-stranded DNA. Once the DNA binding dye binds to double-stranded DNA, the intensity of the fluorescent emissions is increased. As more double-stranded DNA are produced in PCR, the fluorescent signal increases, providing quantitative measures of the amplified DNA. The major disadvantage of this approach is that DNA intercalating dyes also bind to non-specific PCR products, interfering with accurate quantification of the intended target sequence. The use of fluorescent reporter probes is an alternative approach to performing real-time PCR analysis. Fluorescent reporter probes are modified DNA oligonucleotide probes that fluoresce when hybridized to a complementary DNA. There are also a number of strand-specific probes that

use the phenomenon of fluorescent resonance energy transfer (FRET), including TaqMan probe, molecular beacon, and scorpion primers. Using fluorescent reporter probes is the most accurate and most reliable of these methods, but also the most expensive.

Real-time PCR offers a number of advantages compared with traditional PCR, including higher precision in quantitation, wider dynamic range, faster analysis, and higher sensitivity. Real-time PCR has numerous applications for both diagnostic and research purposes. Some of the applications include gene expression analysis, diagnosis of infectious disease, human genetic testing, and environmental microbiology.

1.5 Rationale and Scope of the Thesis

Many challenges remain for the detection of specific proteins at ultra-low levels. The abundance of a variety of proteins present in cells can vary by as much as 10^{10}-fold. Therefore, the determination of specific proteins at ultra-low levels usually has to be carried out in the presence of a huge excess of other more abundant molecules. Affinity-based protein detection takes advantage of the specific binding of an affinity ligand, for example, antibody and aptamer, to their targets. The antibodies and aptamers can be labeled by various probes, including enzymes, radioisotopes and fluorophores, enabling highly sensitive detection. In addition, the tremendous progress in nanotechnology also offers excellent prospects for developing highly sensitive bioassays for proteins (109).

While nucleic acids can be amplified by PCR to improve the sensitivity, there is no comparable technique to chemically amplify proteins. However, if an

affinity ligand is a nucleic acid, e.g. DNA aptamer, or the affinity ligand is conjugated to a nucleic acid, PCR amplification of the specific nucleic acid bound to the target protein could provide an indirect measure of the protein with improved sensitivity. Therefore, it is hypothesized that combinations of aptamer affinity binding, CE separation, PCR amplification, LIF detection, and real-time PCR could lead to development of ultrasensitive and specific assays for minute amounts of proteins. The objective of this research was to develop novel bioanalytical techniques enabling the detection of proteins by taking advantage of affinity binding and by designing unique separation and signal amplification.

This thesis consists of seven chapters. **Chapter 1** reviews the recent developments of novel technology enabling ultrasensitive protein detection. The chapter focuses on protein detection methods based on amplification of nucleic acids using polymerase. The basic principles, performances, applications, merits and limitations of these techniques have been discussed and highlighted. **Chapter 2** describes a tunable aptamer capillary electrophoresis (CE) assay enabling the ultrasensitive analysis of multiple proteins. In addition to serving as affinity molecules binding to the specific proteins, the use of aptamers as charge modulators is explored. The theoretical basis of the application of aptamers as charge modulators to modify the electrophoretic mobility of proteins is discussed. Four target proteins, human IgE, the reverse transcriptase of the human immunodeficiency virus type 1 (HIV-RT), thrombin, and platelet derived growth factor BB (PDGF-BB) are chosen to demonstrate the ability of tunable aptamer capillary electrophoresis to determine the multiple proteins in a single analysis.

The applicability of the assay for sample analysis is examined by the detection of four proteins in dilute human serum matrix. **Chapter 3** demonstrates the ability of tunable aptamer capillary electrophoresis to differentiate and detect protein isomers. The protein isomers PDGF-AB and PDGF-BB are chosen as target proteins because the sequences of PDGF A and B chains are ~60% identical, and the molecular weights of PDGF-AB (27 kDa) and PDGF-BB (25 kDa) are similar, making their separation difficult. The detection of PDGF receptors α and β is also studied based on the interaction of isomers with their receptors. **Chapter 4** describes an ultrasensitive aptamer-based affinity PCR technique for the determination of minute amounts of proteins. Because this affinity aptamer PCR technique fulfills the ultrasensitive protein detection through PCR amplification of the aptamer bound to the target protein, it is termed "affinity aptamer amplification assay". The principle of the assay is demonstrated by choosing HIV-RT as the initial target. The experimental conditions for binding, separation, and detection are optimized to achieve the ultrasensitive detection of the target protein. The quantitation, detection limit, and selectivity of the technique are assessed. **Chapter 5** demonstrates the affinity aptamer amplification assay as a generalized approach for multiple protein detection. Beside HIV-RT, thrombin and human IgE are chosen as the additional target proteins. The adaptation of real-time PCR technique to yield accurate quantitative information is assessed. The detection of three target proteins in the complex matrix of cell lysate is examined. **Chapter 6** describes a new principle for construction of probes that can be used for analysis of proteins and other macromolecules in homogeneous solutions. Since the

hairpin structures are induced upon binding of probes to target molecules, the method is termed "binding-induced hairpin assay". Design and construction of binding-induced hairpin probes are investigated by using streptavidin as initial targets. The detection of trace amounts of PDGF-BB and PSA is further explored. **Chapter 7** summarizes the conclusions generated from this research, discusses the implications of the research, and suggests further research directions.

1.6 References

1. G. A. Petsko, and D. Ringe, *Protein Structure and Function*, New Science Press, London, 2004.
2. S. Hanash, *Nature*, 2003, 422, 226-232.
3. R. Aebersold and M. Mann, *Nature*, 2003, 422, 198-207.
4. R. S. Yalow and S. A. Berson, *Clin. Invest.,* 1960, 39, 1157-1175.
5. E. Engvall and P. Perimann, *Immunochemistry*, 1971, 8, 871-874.
6. P. B. Luppa, L. J. Sokoll and D. W. Chan, *Clin. Chim. Acta*, 2001, 314, 1-26.
7. A. Bange, H. B. Halsall and W. R. Heineman, *Biosens. Bioelectron.*, 2005, 20, 2488-2503.
8. M. F. Templin, D. Stoll, M. Schrenk, P. C. Traub, C. F. Vohringer and T. O. Joos, *Trends Biotechnol.,* 2002, 20, 160-166.
9. T. Sano, C. L. Smith and C. R. Cantor, *Science*, 1992, 258, 120-121.
10. C. M. Niemeyer, M. Adler and R. Wacker, *Trends Biotechnol.*, 2005, 23, 208-216.
11. V. Ruzicka, W. Marz, A. Russ and W. Ross, *Science*, 1993, 260, 698-699.
12. H. Zhou, R. J. Fisher and T. S. Papas, *Nucleic Acids Res.*, 1993, 21, 25-26.
13. T. Sano, C. L. Smith and C. R. Cantor, *Science*, 1993, 260, 699.
14. E. R. Hendrichson, T. M. H. Truby, R. D. Joerger, W. R. Majarian and R. C. Ebersole, *Nucleic Acids Res.*, 1995, 23, 522-529.
15. C. M. Niemeyer, M. Adler, B. Pignataro, S. Lenhert, S. Gao, L. Chi, H. Fuchs and D. Blohm, *Nucleic Acids Res.*, 1999, 27, 4553-4561.
16. C. M. Niemeyer, *Trends Biotechnol.*, 2002, 20, 395-401.

17. A. S. Mweene, T. I. K. Okazaki, E. Ono, Y. Shimizu and H. Kida, *J. Clin. Microbiol.,* 1996, 34, 748-750.

18. H. C. Wu, Y. L. Huanf, S. C. Lai, Y. Y. Huang and M. F. Shaio, *Lett. Appl. Microbiol.*, 2001, 32, 321-325.

19. N. Henterich, A. A. Osman, E. Mendez and T. Mothes, *Nahrung/Food*, 2003, 5, 345-348.

20. A.S. McElhinny and C. M. Warner, *BioTechniques*, 1997, 23, 660-662.

21. X. Ke and C. M. Warner, *J. Reprod. Immunol.,* 2000, 46, 1-15.

22. Y. Cao, K. Kopplow and G. Liu, *Lancet*, 2000, 356, 1002-1003.

23. M. Maia, H. Takahashi, K. Alder, R. K. Garlick and J. R. Wands, *J. Virol. Methods*, 1995, 52, 273-286.

24. M. Adler, R. Wacher and C. M. Niemeyer, *Biochem. Biophys. Res. Commun.*, 2003, 308, 240-250.

25. M. Adler, S. Schulz, R. Fischer and C. M. Niemeyer, *Biochem. Biophys. Res. Commun.*, 2005, 333, 1289-1294.

26. A. Mckie, D. Samuel, B. Cohen and N. A. Saunders, *J. Immunol. Methods*, 2002, 270, 135-141.

27. K. Sugawara, D. Kobayashi, K. Saito, D. Furuya, H. Araake, A. Yagihashi, T. Yajima, K. Hosoda, T. Kamimura and N. Watanabe, *Clin. Chim. Acta,* 2000, 299, 45-54.

28. D. Furuya, A. Yagihashi, T. Yajima, D. Kobayashi, K. Orita, M. Kurimoto and N. Watanabe, *J. Immunol. Methods*, 2000, 238, 173-180.

29. P. P. Sanna, F. Weiss, M. E. Samson, F. E. Bloom and E. M. Pich, *Proc. Natl.*

Acad. Sci. USA, 1995, 92, 272-275.

30. C. M. Niemeyer, M. Alder and D. Blohem, *Anal. Biochem.*, 1997, 246, 140-145.

31. M. Adler, M. Langer, K. Witthohn, J. Eck, D. Blohm and C. M. Niemeyer, *Biochem. Biophys. Res. Commun.*, 2003, 300, 757-763.

32. Y.-L. Ong and A. Irvine, *Hematology*, 2002, 7, 59-67.

33. D. Klein, *Trends Mol. Med.*, 2002, 8, 257-259.

34. J. Wilhelm and A. Pingoud, *ChemBioChem*, 2003, 4, 1120-1128.

35. P. W. Sims, M. Vasser, W. L. Wong, P. M. Williams and Y. G. Meng, *Anal. Biochem.*, 2000, 281, 230-232.

36. A. Mckie, D. Samuel, B, Cohen and N. A. Saunders, *J. Immunol. Methods,* 2002, 261, 167-175.

37. J. M. Barletta, D. C. Edelman and N. T. Constantine, *Am. J. Clin. Pathol.*, 2004, 122, 20-27.

38. J. Barletta, *Mol. Aspects Med.*, 2006, 27, 224-253.

39. S. Gofflot, B. El Moualij, D. Zorzi, L. Melen, S. Roels, D. Quatpers, J. Grassi, E. Vanopdenbosch, E. Heinen and W. Zorzi, *J. Immunoassay Immunochem.,* 2004, 25, 241-258.

40. J. M. Barletta, D. C. Edelman, W. E. Highsmith and N. T. Constantine, *J. Virol. Methods*, 2005, 127, 154-164.

41. S. Gofflot, M. Deprez, B. E. Moualij, A. Osman, J-F. Thonnart, O. Hougrand, E. Heinen and W. Zorzi, *Clin. Chem.*, 2005, 51, 1605-1611.

42. K. Lind and M. Kubista, *J. Immunol. Methods,* 2005, 304, 107-116.

43. S.-H. Huang and T.-C. Chang, *Clin. Chem.*, 2004, 50, 1673.

44. P. Tian and R. Mandrell, *J. Appl. Microbiol.*, 2006, 100, 564-574.

45. R. C. Allen, S. Rogeli, S. E. Cordova and T. L. Kieft, *J. Immunol. Methods,* 2006, 308, 109-115.

46. C. Lubelli, A. Chatgilialoglu, A. Bolognesi, P. Strocchi, M. Colombatti and F. Stirpe, *Anal. Biochem.*, 2006, 355, 102-109.

47. J. T. Mason, L. Xu, Z.-M. Sheng and T. J. O'Leary, *Nat. Biotechnol.*, 2006, 24, 555-557.

48. Y.-C. Guo, Y.-F. Zhou, X.-E. Zhang, Z.-P. Zhang, Y.-M. Qiao, L.-J. Bi, J.-K. Wen, M.-F. Liang and J.-B. Zhang, *Nucleic Acids Res.*, 2006, 34, e62.

49. C. Tuerk and L. Gold, *Science*, 1990, 249, 505-510.

50. A. D. Ellington and J. Szostak, *Nature,* 1990, 346, 818-822.

51. L. Gold, B. Polisky, O. Uhlenbeck and M. Yarus, *Annu. Rev. Biochem.*, 1995, 64, 763-797.

52. S. E. Osborne and A. D. Ellington, *Chem. Rev.*, 1997, 97, 349-370.

53. S. D. Jayasena, *Clin. Chem.*, 1999, 45, 1628-1650.

54. C. L. A. Hamula, J. W. Guthrie, H. Zhang, X.-F. Li and X. C. Le, *Trends Anal. Chem.*, 2006, 25, 681-691.

55. S. Tombelli, M. Minunni, and M. Mascini, *Biosens. Bioelectron.,* 2005, 20, 2424-2434..

56. X.-L. Wang, F. Li, Y.-H. Li, X. Sun, X.-B. Li, H. J. Schluesener, F. Tang and S.-Q. Xu, *Anal. Chem.*, 2004, 76, 5605-5610.

57. S. M. Gustafsdottir, E. Schallmeiner, S. Fredriksson, M. Gullberg, O.

Söderberg, M. Jarvius, J. Jarvius, M. Howell, U. Landegren, *Anal. Biochem.*, 2005, 345, 2-9.

58. S. Fredriksson, M. Gullberg, J. Jarvius, C. Ollson, K. Pietras, S. M. Gustafsdottir, A. Ostman and U. Landergren, *Nat. Biotechnol.*, 2002, 20, 473-477.

59. M. Gullberg, S. M. Gustafsdottir, E. Schallmeiner, J. Jarvius, M. Bjarnegard, C. Betsholtz, U. Landegren and S. Fredriksson, *Proc. Natl. Acad. Sci. USA*, 2004, 101, 8420-8424.

60. S. Pai, A. D. Ellington and M. Levy, *Nucleic Acids Res.*, 2005, 33, e162.

61. S. M. Gustafsdottir, A. Nordengrahn, S. Fredriksson, P. Wallgren, E. Rivera, E. Schallmeiner, M. Merza and U. Landegren, *Clin. Chem.*, 2006, 52, 1152-1160.

62. E. Schallmeiner, E. Oksanen, O. Ericsson, L. Spångberg, S. Eriksson, U. Stenman, K. Pettersson, U. Landegren, *Nat. Methods*, 2007, 4, 135-137.

63. O. Rollman, U. B. Jensen, A. Ostman, L. Bolund, S. M. Gustafsdottir and T. G. Jensen, *J. Invest. Dermatol.*, 2003, 120, 742-749.

64. M. Bjarnegard, M. Enge, J. Norlin, S. Gustafsdottir, S. Fredriksson, A. Abramsson, M. Takemoto, E. Gustafsson, R. Fassler and C. Betsholtz, *Dev. Dis.*, 2003, 131, 1847-1857.

65. L. Zhu, H. Koistinen, P.Wu, A. Närvänen, E. Schallmeiner, S. Fredriksson, U. Landegren, U. Stenman, *Biol. Chem.* 2006, 387, 769-772.

66. S. Fredriksson, W. Dixon, H. Ji, A. C. Koong, M. Mindrinos, R. W. Davis, *Nat. Methods*, 2007, 4, 327-329.

67. O. Söderberg, M. Gullberg, M. Jarvius, K. Ridderstråle, K. Leuchowius, J. Jarvius, K. Wester, P. Hydbring, F. Bahram, L. Larsson, U. Landegren, *Nat. Methods*, 2006, 3, 995-1000.

68. S. M. Gustafsdottir, J. Schlingemann, A. Rada-Iglesias, E. Schallmeiner, M. Kamali-Moghaddam, C. Wadelius, U. Landegren, *Proc. Natl. Acad. Sci. USA,* 2007, 104, 3067-3072.

69. B. Schweitzer, S. Wiltshire, J. Lambert, S. O'Malley, K. Kukanskis, Z. Zhu, S. F. Kingsmore, P. M. Lizardi and D. C. Ward, *Proc. Natl. Acad. Sci. USA*, 2000, 97, 10113-10119.

70. A. Fire and S.-Q. Xu, *Proc. Natl. Acad. Sci. USA*, 1995, 92, 4641-4645.

71. J. Baner, M. Nilsson, M. Mendel-Hartvig and U. Landergren, *Nucleic Acids Res.*, 1998, 26, 5073-7078.

72. B. Schweitzer, S. Roberts, B. Grimwade, W. Shao, M. Wang, Q. Fu, Q. Shu, I. Laroche, Z. Zhou, V. T. Tchenev, J. Christiansen, M. Velleca and S. F. Kingsmore, *Nat. Biotechnol.*, 2002, 20, 359-365.

73. S. Wiltshire, S. O'Malley, J. Lambert, K. Kukanskis, D. Edgar, S. F. Kingsmore and B. Schweitzer, *Clin. Chem.*, 2000, 46, 1991-1993.

74. M. C. Mullenix, S. Wiltshire, W. Shao, G. Kitos and B. Schweitzer, *Clin. Chem.,* 2001, 47, 1927-1929.

75. W. Shao, Z. Zhou, I. Laroche, H. Lu, Q. Zong, D. D. Patel, S. Kingsmore and S. P. Piccoli, *J. Biomed. Biotechnol.*, 2003, 5, 299-307.

76. H. A. Kader, V. T. Tchernev, E. Satyaraj, S. Lejnine, G. Kotler, S. F. Kingsmore and D. D. Patel, *Am. J. Gastroenterol.*, 2005, 100, 414-423.

77. H. Zhou, K. Bouwman, M. Schotanous, C. Verweij, J. A. Marrero, D. Dillon, J. Costa, P. Lizard and B. B. Haab, *Genome Biol.*, 2004, 5, R28.

78. R. Orchekowski, D. Hamelink, L. Li, E. Gliwa, M. VanBrocklin, J. A. Marrero, G. F. V. Woude, Z. Feng, R. Brand and B. B. Haab, *Cancer Res.*, 2005, 65, 11193-11202.

79. W.-M. Gao, R. Kuick, R. P. Orchekowski, D. E. Misek, J. Qiu, A.K. Greenberg, W. N. Rom, D. E. Brenner, G. S. Omenn, B. B. Haab and S. M. Hanah, *BMC Cancer*, 2005, 5, 110-119.

80. D. A. D. Giusto, W. A. Wlassoff, J. J. Gooding, B. A. Messerie and G. C. King, *Nucleic Acids Res.*, 2005, 33, e64.

81. H.-T. Zhang, J. E. Kacharmina, K. Miyashiro, M. I. Greene and J. Eberwine, *Proc. Natl. Acad. Sci. USA*, 2001, 98, 5497-5502.

82. R. N. V. Gelder, M. E. V. Zastrow, A. Yool, W. C. Dement, J. D. Barchas and J. H. Eberwine, *Proc. Natl. Acad. Sci. USA*, 1990, 87, 1663-1667.

83. J. Eberwine, H. Yeh, K. Miyashiro, Y. Cao, S. Nair, R. Finnell, M. Zettel and P. Coleman, *Proc. Natl. Acad. Sci. USA*, 1992, 89, 3010-3014.

84. H. Zhang, X. Cheng, M. Richter and M. I. Greene, *Nat. Med.*, 2006, 12, 473-477.

85. D. R. Baker, *Capillary electrophoresis*. John-Wiley & Sons, New York, *NY*, 1995.

86. J. P. Lander, *Handbook of Capillary Electrophoresis (2nd ed),* CRC Press, Boca Raton, FL, 1996.

87. P.G. Righetti, *Capillary Electrophoresis in Analytical Biotechnology,* CRC Press, Boca Raton, FL, 1996.

88. P. Camilleri, *Capillary Electrophoresis: Theory and Practice (2nd ed),* CRC Press, Boca Raton, FL, 1997.

89. T. T. Lee and E. S. Yeung, *J. Chromatogr.,* 1992, 595, 319-325.

90. S. M. Nie, R. Dadoo and R. N. Zare, *Anal. Chem.,* 1993, 65, 3571-3575.

91. L. Tao and R. T. Kennedy, *Anal. Chem.,* 1996, 68, 3899-3907.

92. X.C. Le, J. Z. Xing, J. Lee, S. A. Leadon and M. Weinfeld, *Science,* 1998, 280,1066-1069.

93. E. Gassman, J. E. Kuo and R. N. Zare, *Science,* 1985, 230, 813-814.

94. Y. F. Cheng and N. J. Dovichi, *Science,* 1988, 242, 562-564.

95. S. Wu and N. J. Dovichi, *J. Chromotogr.,* 1989, 480, 141-155.

96. D. Y. Chen, H. P. Swerdlow, H. R. Harke, J. Z. Zhang and N. J. Dovichi, *J. Chromatogr.* 1991, 559, 237-246.

97. J. Z. Zhang, D. Y. Chen, S. Wu, H. R, Harke and N. J. Dovichi, *Clin. Chem.*, 1991, 37, 1492-1496.

98. S. Wu and N.J. Dovichi, *Talanta*, 1992, 39, 173-178.

99. H. Swerdlow, J. Z. Zhang, D.Y. Chen, H. R. Harke, R. Grey, S. L. Wu, N. J. Dovichi and C. Fuller, *Anal. Chem.*, 1991, 63, 2835-2841.

100. D.Y. Chen and N. J. Dovichi, *J. Chromatogr. B*, 1994, 657, 265-269.

101. R. K. Saiki, S. Scharf, F. Faloona, K. B. Mullis, G. T. Horn, H. A. Erlich and N. Arnheim, *Science,* 1985, 230, 1350-1354.

102. R. K. Saiki, D. H. Gelfand, S. Stoffel, S. J. Scharf, R. Higuchi, G. T. Horn, K. B. Mullis and H. A. Erlich, *Science*, 1988, 239, 487-491.

103. M. J. McPherson and S. G. MØller, *PCR-The Basics from Background to Bench*, Springer, New York, NY, 2000.

104. M. T. Dorak, *Real-Time PCR*, Taylor & Francis, New York, NY, 2006.

105. C. A. Heid, J. Stevens, K. J. Livak and P. M. Williams, *Genome Res.,* 1996, 6, 986-994

106. S. Mocellin, C. R. Rossi, P. Pilati, D. Nitti and F. M. Marincola, *Trends Mol. Med.,* 2003, 9, 189-195.

107. J. Wilhelm and A. Pingoud, *ChemBioChem,* 2003, 4, 1120-1128.

108. D. Klein, *Trends Mol. Med.,* 2002, 8: 257-260.

109. H. Zhang, Q. Zhao, X. -F. Li, X. C. Le, *Analyst,* 2007, 132, 724-737.

Chapter Two*

Tunable Aptamer Capillary Electrophoresis and its Application to Multiple Protein Analysis

2.1 Introduction

Affinity capillary electrophoresis has been applied mostly to the analysis of a single protein at a time (1-7).

Development of protein biomarkers for disease diagnosis and treatment often requires the determination of multiple proteins that are present at trace levels. This chapter describes a tunable aptamer capillary electrophoresis assay enabling the ultrasensitive analysis of multiple proteins (**Figure 2.1**). The key concept is tuning the electrophoretic mobility of proteins with DNA aptamers to achieve efficient separation of multiple proteins or protein isomers. We introduce aptamers of varying nucleotide length as charge modulators to modify the electrophoretic mobility of proteins, tailored for the separation of the various protein-aptamer complexes in free solution. This systematic approach extends the applications of charge modulation in affinity assays (8, 9) and end-labeled free-solution electrophoresis of DNA (10).

* A portion of this chapter has been published in H. Zhang, X.-F. Li, and X. C. Le, *J. Am. Chem. Soc.* 2008, 130, 34-35.

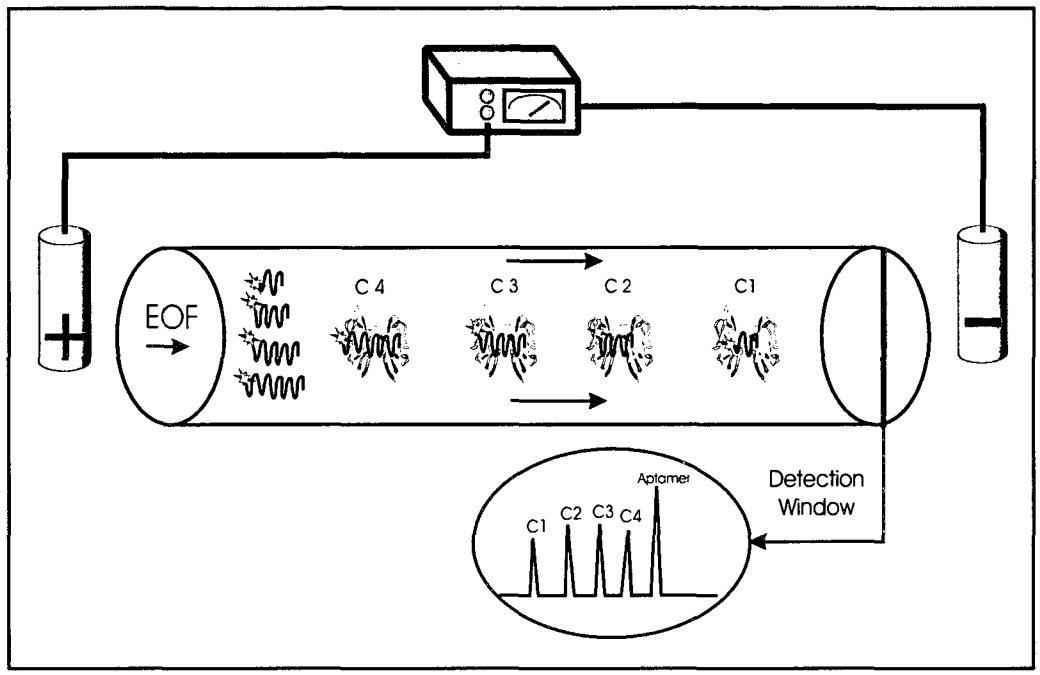

Figure 2.1. Concept of tunable aptamer electrophoretic assay for proteins. Four fluorescent aptamers of variable length are bound to proteins forming complexes (C1, C2, C3, and C4) that have sufficiently different mobilities appropriate for the separation and detection of multiple proteins.

2.2 Experimental

2.2.1 Reagents

Human IgE, HIV-RT, thrombin, PDGF-BB, and PDGF-AB were obtained from Athens Research & Technology (Athens, GA), Worthington Biochemical (Lakewood, NJ), Haematologic Technologies (Essex Junction, VT), and R&D Systems (Minneapolis, MN), respectively. Aptamers were synthesized by

Integrated DNA Technologies (Corarville, IA). They were fluorescently labeled at the 5' end with 6'-Carboxyfluorescein (6'-FAM) and purified by reversed-phase HPLC. Aptamer (both full-length and truncated) sequences are listed in **Table 2.1** (11-14). Human serum was obtained from Sigma-Aldrich (Oakville, ON). 1×TG buffer (25 mM Tris and 192 mM glycine, pH 8.3) was diluted with deionized water from 10×TG buffer (from Bio-Rad Laboratories, Mississauga, ON) and was then adjusted by 1 M acetic acid to pH below 8.3 or 1M NaOH to pH above 8.3. The pH-adjusted TG buffer was appropriately diluted by deionized water to maintain the same conductivity as TG buffer (pH 8.3). All other reagents were commercially available analytical grade.

Table 2.1. Summary of proteins and their aptamers used in this study

Proteins	Mol. Wt. (kDa)	pI	Aptamer size	Aptamer sequence(5'–3')
IgE	200	~9.0	38 nt	TGGGGCACGTTTATCCGTCCCTCCTAGT GGCGTGCCCC
			53 nt	AGGGGCACGTTTATCCGTCCCTCCTAGT GGCGTGCCCCTGTCTGACTGTCTCG
HIV-RT	120	~8.2	49 nt	ATCCGCCTGATTAGCGATACTCAGAAGG ATAAACTGTCCAGAACTTGGA
			80 nt	ATCCGCCTGATTAGCGATACTCAGAAGG ATAAACTGTCCAGAACTTGGAACTCATC ACTACAATACATCATACTTCACTA
			2X81 nt	ATCCGCCTGATTAGCGATACTTACGTGA GCGTGCTGTCCCCTAAAGGTGATACGTC ACTTGAGCAAAATCACCTGCAGGGG
Thrombin	36	6.35-7.6	38 nt	CAGTCCGTGGTAGGGCAGGTTGGGGTG ACTTCGTGGAA
			76 nt	AGATGCCTGTCGAGCATGCTCTTTGGAG ACAGTCCGTG GTAGGGCAGGTTGGGGTGACTTCGTGG AAGAAGCGAGA
PDGF-BB	25	9.5-10.5	37 nt	TGGGAGGGCGCGTTCTTCGTGGTTACTT TTAGTCCCG
Non-specific			49 nt	TGGTCTTGTGTGGCTGTGGCTATGTCTG ATCTTAATCCACGAAGTCACC

2.2.2 Apparatus

A laboratory-built CE-LIF system was used in this work (15-17). A schematic of a CE-LIF system is shown in **Figure 2.2**. The system's main components are a sample vial, source and destination vials, electrodes, a CE power supply (model CZE 1000R, Spellman, Plainview, NY), a fused-silica

capillary (Polymicro Technologies, Phoenix, AZ), a laser-induced fluorescence detector, and a data output and handling device. To introduce the sample, the capillary inlet is placed into a vial containing the sample and a voltage is applied to inject the sample electrokinetically. The capillary inlet is then placed back to the source buffer vial. The migration of the analytes is then driven by an electric field supplied to the electrodes by the high-voltage power supply. All ions, positive or negative, are pulled through the capillary due to electroosmotic flow. The analytes separate as they migrate due to their electrophoretic mobility and are detected at a sheath flow cuvette (NSG Precision Cells, Farmingdale, NY) used as a postcolumn fluorescence detection cell. The 6'-FAM label in aptamers was excited by 488 nm light from an argon ion laser (model 2014-65ML, Uniphase, San Jose, CA). Fluorescence was collected using a high-numerical aperture microscope objective (60×, 0.7 NA, Universe Kogaku, Oster Bay, NY), spectrally filtered through a 515-nm band-pass filter (515DF20) and restricted by a 2-mm pinhole. A polarizing beam splitter (Melles Griot, Nepean, ON) was used to split the beam to two photomultiplier tubes (PMT, R1477, Hamamatsu Photonics, Japan) to measure horizontally and vertically polarized light. The output of PMT is sent to a computer via a PCI-MIO-16XH-18 input/output board and an interface box (I-V converter). The data is then displayed as an electropherogram by the LabVIEW (National Instruments, Austin, TX) program on the computer. All CE data were analyzed using Igor Pro software (version 2.04, WaveMetrics, Lake Oswego, OR).

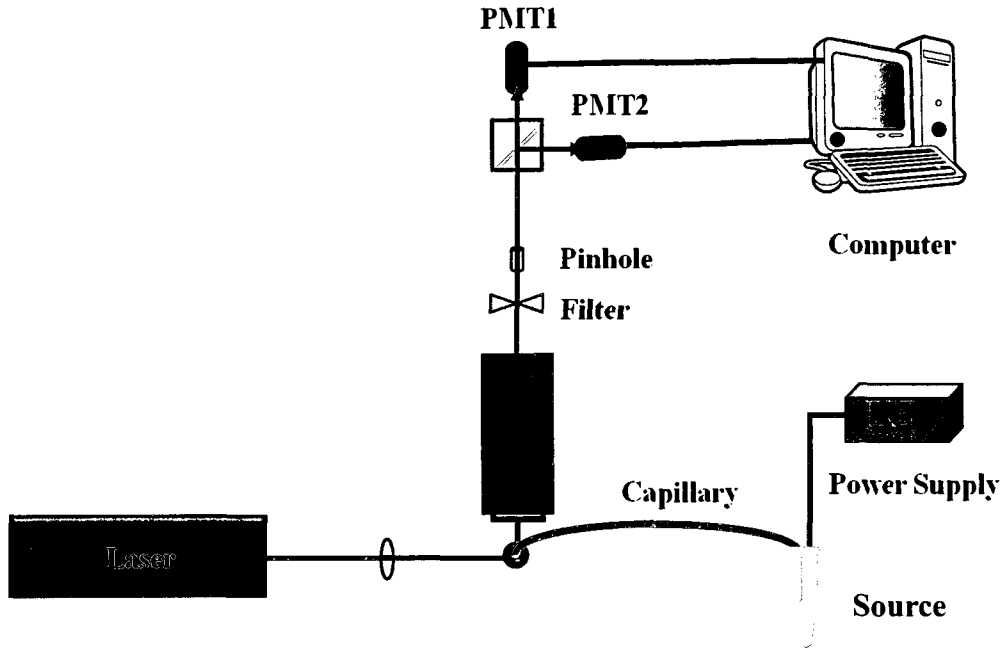

Figure 2.2. Schematic of the laboratory-built capillary electrophoresis with laser-induced fluorescence detection system

2.2.3 Capillary electrophoresis

Uncoated fused-silica capillaries (20 μm inner diameter, 150 μm outer diameter, 40 cm in length, Polymicro Technologies, Phoenix, AZ) were used for CE separation. Samples were electrokinetically injected into the capillary at a voltage of 18 kV for 5 s, and a running voltage of 18 kV (450 V/cm) was employed to drive separation. The running buffer used for all experiments was 1×TG adjusted to pH 8.5 by 1 M NaOH unless otherwise stated. Periodically, the capillaries were treated by running 0.02 M NaOH for 5 min, followed by water for 3 min and running buffer for 5 min at 300-450 V/cm.

2.2.4 Tuning of mobility for HIV-RT and thrombin

To place aptamers in their desired conformation, all the aptamer stock solutions were treated at 80 °C for 5min followed by cooling slowly to room temperature before analysis. To test the mobility of HIV-RT complex with aptamers, 10 nM HIV-RT was incubated with 100 nM of three aptamers separately, a 49-nt (nucleotide) aptamer, an 80-nt aptamer, and an 81-nt aptamer in a buffer of 10 mM Tris·HCl (7.4) + 1 mM $MgCl_2$. The final volume of each incubation solution was 50 μL, and the solution was incubated at 37 °C for 10 min. An aliquot of each incubation solution was injected to CE-LIF to measure the mobility of HIV-RT as tuned by various aptamers of different lengths. To tune the mobility for thrombin, 25 nM thrombin was incubated at 37 °C for 10 min with 100 nM of either a full-length aptamer (76 nt) or a truncated aptamer (38 nt).

2.2.5 Analysis of IgE, HIV-RT, thrombin, and PDGF-BB

To achieve multiple protein analysis by tunable aptamer CE, the experimental conditions for binding, separation, and detection were optimized to maximize the sensitivity and speed of analysis. These optimized parameters included the incubation temperature and time, the separation buffer conditions, and the effects of Mg^{2+} on the formation of specific protein-aptamer complexes. The optimum conditions for multiple protein analysis were as follows: incubation buffer, 10 mM Tris·HCl +1 mM $MgCl_2$ + 100 μg/mL bovine serum albumin (BSA) at pH 7.4; incubation temperature, 37 °C; incubation time, 10 min; separation buffer, 1×TG (pH 8.5).

For calibration, IgE, HIV-RT, thrombin, and PDGF-BB (each 1–100 nM)

were incubated with 200 nM fluorescently labeled 38-nt aptamer for IgE, 200 nM fluorescently labeled 80-nt aptamer for HIV-RT, 200 nM fluorescently labeled 38-nt aptamer for thrombin, and 300 nM fluorescently labeled 37-nt aptamer for PDGF-BB. A 5-nL aliquot of each solution was injected electrokinetically into a 40-cm capillary. Electrophoretic separation was carried out using an applied voltage of 18 kV and running buffer containing 25 mM Tris and 192 mM glycine at pH 8.5. A blue argon ion laser (488 nm) was used for excitation, and fluorescence was detected at 515 nm.

2.2.6 Serum sample preparation

A frozen serum sample was thawed in a water bath at 30 °C, and then kept on ice. Prior to analysis, a 0.5mL serum sample was centrifuged at 10,000 rpm for 10 min to remove precipitate. The desired amount of serum was then diluted 10 times with incubation buffer. The dilute serum was spiked with 25 nM each of IgE, HIV-RT, thrombin, and PDGF-BB. An aliquot (50 μL) of the sample was incubated at 37 °C for 10 min with 100 nM of four fluorescently labeled aptamers for the specific proteins and another 4 μM of non-specific, non-fluorescent 49-mer oligonucleotide. The non-specific oligonucleotide was used to reduce interference from the serum matrix.

2.3 Theoretical Basis

The principle of modulating the mobility of proteins may be expressed in the following equations, showing the dependence of electrophoretic mobility (μ) on the net charge (Z) and the mass (M) of the protein. In free zone CE, the

electrophoretic mobility of a protein is proportional to its net charge, and inversely proportional to the frictional forces acting upon it in solution (18, 19).

$$\mu \approx C_p \frac{Z}{M^\alpha} \qquad (1)$$

where C_p is a constant for a given protein, and α is a factor (0-1) describing the shape of the protein molecule. Upon the binding of an aptamer, the electrophoretic mobility of the protein is shifted to:

$$\mu_c \approx C_p \frac{Z + n\Delta Z}{(M + n\Delta M)^\alpha} \qquad (2)$$

where n is the number of nucleotides making up the aptamer, ΔZ is the change in charge per nucleotide, and ΔM is the change in size per nucleotide. Under the pH conditions (pH 7–9) typically used for CE separation, ΔZ is nearly -1 due to the phosphate group in the nucleotides and the effect of the counter ions in solution (10). Because most proteins carry a small net charge (20), and the change in mass ΔM (~320 amu) per nucleotide is much smaller than the mass of a protein (M), the contribution of nΔZ to the shift in mobility is often much more significant than that of nΔM. Therefore, Eq 2 can be approximated to:

$$\mu_c \approx C_p \left(\frac{Z}{M^\alpha} + \frac{n\Delta Z}{M^\alpha}\right) \qquad (3)$$

Thus, the electrophoretic mobility of the proteins can be rationally controlled by modulating the length of the aptamer (n), taking into account the size of the protein (M), to achieve the desired value of the $n\Delta Z/M^\alpha$ term in Eq 3. Moreover, the aptamer with given length has larger influence on the electophoretic mobility of smaller proteins than of larger ones. The value of electophoretic mobility is

usually greater than that estimated by Eq3 after including the influence of aptamer mass, especially for the smaller proteins bound by longer aptamers.

2.4 Results and Discussion

2.4.1 Tuning the electrophoretic mobility of proteins

To achieve the multiple protein analysis in a single CE operation, the key strategy of tunable aptamer CE is the adaptation of aptamers of varying nucleotide length as charge modulators to tune the electrophoretic mobility of proteins, thereby accomplishing the efficient separation of multiple proteins. To demonstrate the proof of principle, tunable aptamer CE was first employed to modify the electrophoretic mobility of HIV-RT and thrombin. Three aptamers with different lengths were used as charge modulators to tune the mobility of HIV-RT. **Figure 2.3a** shows the tuning of mobility for HIV-RT by binding it with a 49-nt aptamer, an 80-nt aptamer, and two 81-nt aptamers. The aptamers, having a similar mass-to-charge ratio, migrate through the capillary at a similar mobility (-2.81×10^{-4} $cm^2V^{-1}s^{-1}$). Upon binding of HIV-RT to the aptamers of varying length, the mobilities are shifted to -0.58×10^{-4}, -0.83×10^{-4}, and -1.45×10^{-4} $cm^2V^{-1}s^{-1}$, respectively. The binding of longer aptamers drives the mobility of HIV-RT closer to that of aptamers which have the highest negative charge density. An excellent linear association (r^2=0.999) between the mobilities of the three HIV-RT aptamer complexes and the length of aptamers supports the validity of Eq 3. The tuning of the mobility of thrombin was achieved by using a full-length (76 nt) aptamer and a truncated (38 nt) aptamer. Results are shown in **Figure 2.3b**. The mobility of thrombin shifted to -1.68×10^{-4} $cm^2V^{-1}s^{-1}$ when using the 38-nt aptamer and shifted

further to -2.22×10^{-4} $cm^2V^{-1}s^{-1}$ when using the 76-nt aptamer. Similarly, the longer aptamer led to the mobility nearer to that of aptamers. The change in electrophoretic mobility $\Delta\mu_C$ per nucleotide of thrombin is about 2 times larger than that of HIV-RT because of the difference in molecular weight between thrombin (MW, 36 kDa) and HIV-RT (MW, 120 kDa). Aptamers of different lengths can be made by maintaining the core sequence responsible for binding and either extending or truncating the aptamers at the ends. Thus, the mobilities of both large and small proteins can be readily tuned using aptamers of appropriate length, to achieve the desired separation.

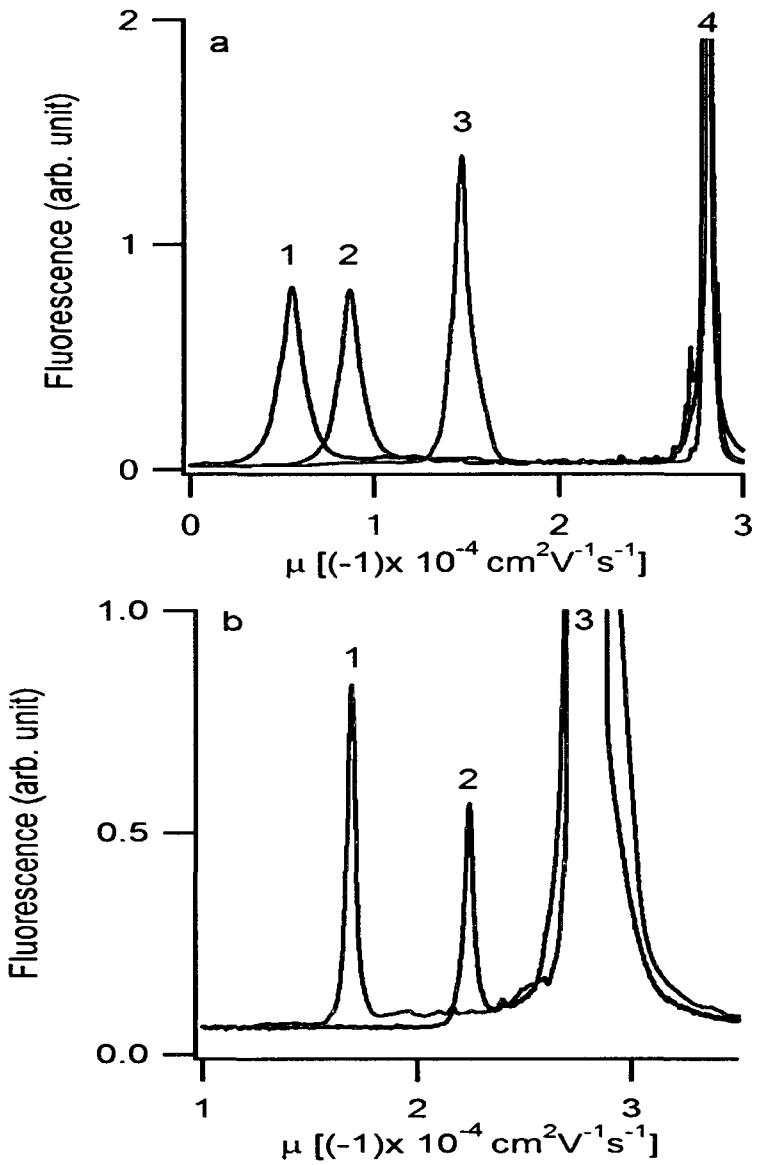

Figure 2.3. Electropherograms showing modulation of mobility of HIV-RT (a) and thrombin (b) by aptamers of variable length. (a). Peak 1 corresponds to the complex of HIV-RT with the 49-nt aptamer; peak 2 corresponds to the complex of HIV-RT with the 80-nt aptamer; peak 3 corresponds to the complex of HIV-RT with two 81-nt aptamers; and peak 4 corresponds to the unbound (free) fluorescent aptamers. (b). Peak 1 is the complex of thrombin with the 38-nt aptamer; peak 2 is the complex of thrombin with the 76-nt aptamer; and peak 3 corresponds to the unbound (free) fluorescent aptamers.

2.4.2 Separation of multiple proteins

Having achieved tunable mobility of proteins through their binding to tailored aptamers, the principle was further applied to the separation of IgE, HIV-RT, thrombin, and PDGF-BB in a single CE operation. Fluorescently labeled aptamers for IgE (38 nt), HIV-RT (80 nt), thrombin (38 nt), and PDGF-BB (37 nt) were utilized as charge modulators for the separation of the four proteins. **Figure 2.4** shows the electropherogram from the separation of IgE, HIV-RT, thrombin, and PDGF-BB in mixture solutions containing aptamers for these proteins. The electrophoretic mobility of proteins is strikingly affected by the binding with aptamers. The migration sequence of proteins through the capillary is determined by the mobility of the protein-aptamer complexes instead of the mobility of free proteins. Although free PDGF-BB presents the largest mobility of the four proteins since it has highest pI (>9.5) and smallest molecular weight, the binding of the aptamer to PDGF-BB shifted its electrophoretic mobility from largest to smallest. The separation of proteins could be improved by employment of the aptamer with appropriate length to rationally control the mobility of the specific protein. For example, the extension of the 49-nt aptamer to 80-nt for binding to HIV-RT decreased the mobility of HIV-RT and resulted in better separation of HIV-RT from IgE. Furthermore, adsorption of the basic proteins (IgE, pI~9.0; PDGF-BB, pI=9.5–10.5) on the negatively charged silica-fused capillary surface would have been a problem, if there were no aptamers binding to these proteins. The binding of the aptamers to the proteins makes the complex negatively charged, thereby eliminating the adsorption problem and focusing the protein-aptamer

complexes into narrow zones. The ability to focus proteins and to tune their electrophoretic mobility using aptamers is the key to the successful analysis of multiple proteins using free zone CE. The specific binding of proteins to their aptamers with optimized lengths results in the formation of protein-aptamer complexes presenting efficient difference in mobility. Therefore, the four protein-aptamer complexes were resolved well from one another and from the free (unbound) aptamers. This is the first time the analysis of multiple proteins is achieved using affinity CE. Previous research has shown only the analysis of a single protein by separating a single protein-aptamer complex from the unbound aptamer. The maximum number of protein-aptamer complexes that can be separated and detected by tunable aptamer CE was estimated based on the electropherogram shown in Figure 2.4. If the separation window is defined as the time interval between the beginning of both the first complex peak and the unbound aptamer peak and the average of four complex peak widths is used as the peak width, approximately eight protein-aptamer complexes can be well resolved in a single analysis.

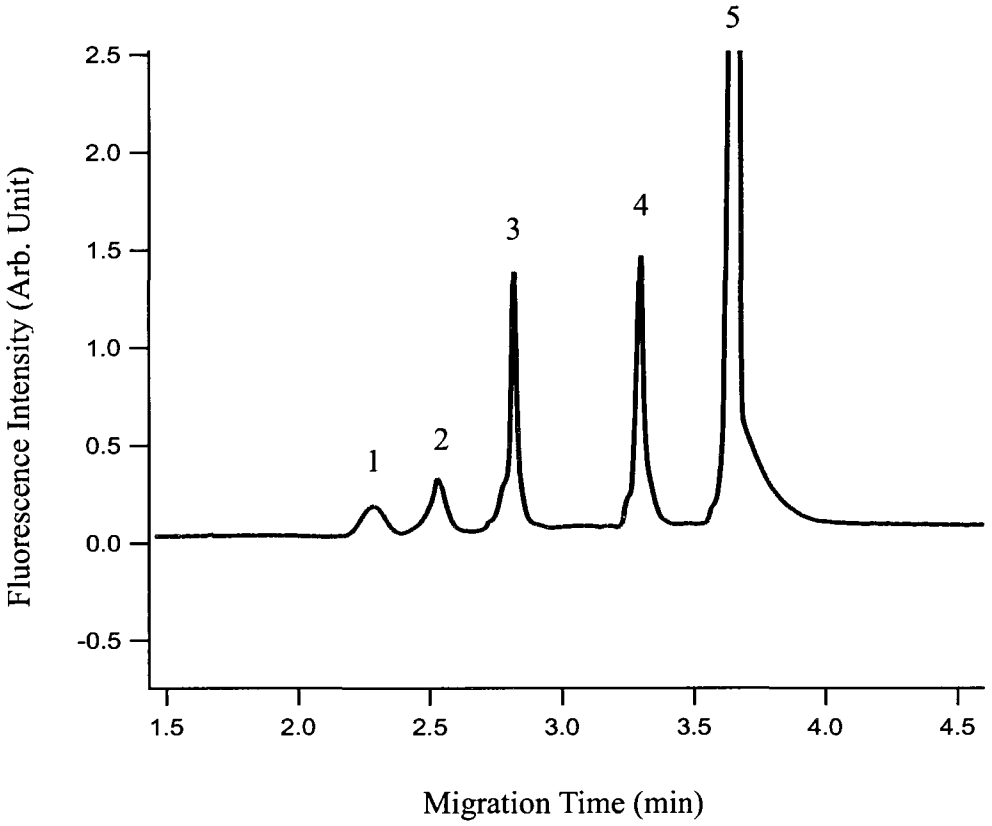

Figure 2.4. Electropherogram showing the separation of IgE, HIV-RT, thrombin, and PDGF-BB in mixture solutions. Peak 1 corresponds to the complex of IgE with the 38-nt aptamer; peak 2 corresponds to the complex of HIV-RT with the 80-nt aptamer; peak 3 corresponds to the complex of thrombin with the 38-nt aptamer; peak 4 corresponds to the complex of PDGF-BB with the 37-nt aptamer; and peak 5 corresponds to the unbound (free) fluorescent aptamers.

In addition to the tuning of mobility of proteins, the pH of the running buffer is another important parameter in the separation of proteins because of its great influence on the shape, and charge of proteins and the surface properties of the capillary wall. A pH range of 7.5-9.0 was used to examine the effect of running buffer pH on the separation of proteins. **Figure 2.5** shows the electropherograms from the separation of IgE, HIV-RT, thrombin, and PDGF-BB when running buffer with various pH values (7.5-9.0) was used. Both the migration time and the peak shape of proteins were affected by pH of running buffer. The lower pH yielded a longer migration time for all proteins and unbound aptamers, because the electroosmotic flow is reduced with the decrease in the pH of running buffer. Under different pH values, the peaks of proteins presented a great variety in their shapes. When using a running buffer pH of 7.5, a sharpest peak was observed for IgE, whereas HIV-RT resulted in a sharpest peak under a running buffer pH of 8.0. In contrast, the sharper peaks were observed for both thrombin and PDGF-BB when the running buffer pH was 8.3, 8.5, or 9.0. The variety in peak shapes under different pH might be determined by changes in protein conformation and the surface charge distribution of proteins. Although pH 7.5 offered the best separation of the four proteins, the wider peak and lower intensity for HIV-RT, thrombin, and PDGF-BB damaged the sensitivity of the method in detection of these proteins. The pH of 8.5 was chosen as optimum running buffer pH because it offered both relatively better separation and peak intensity for all four proteins.

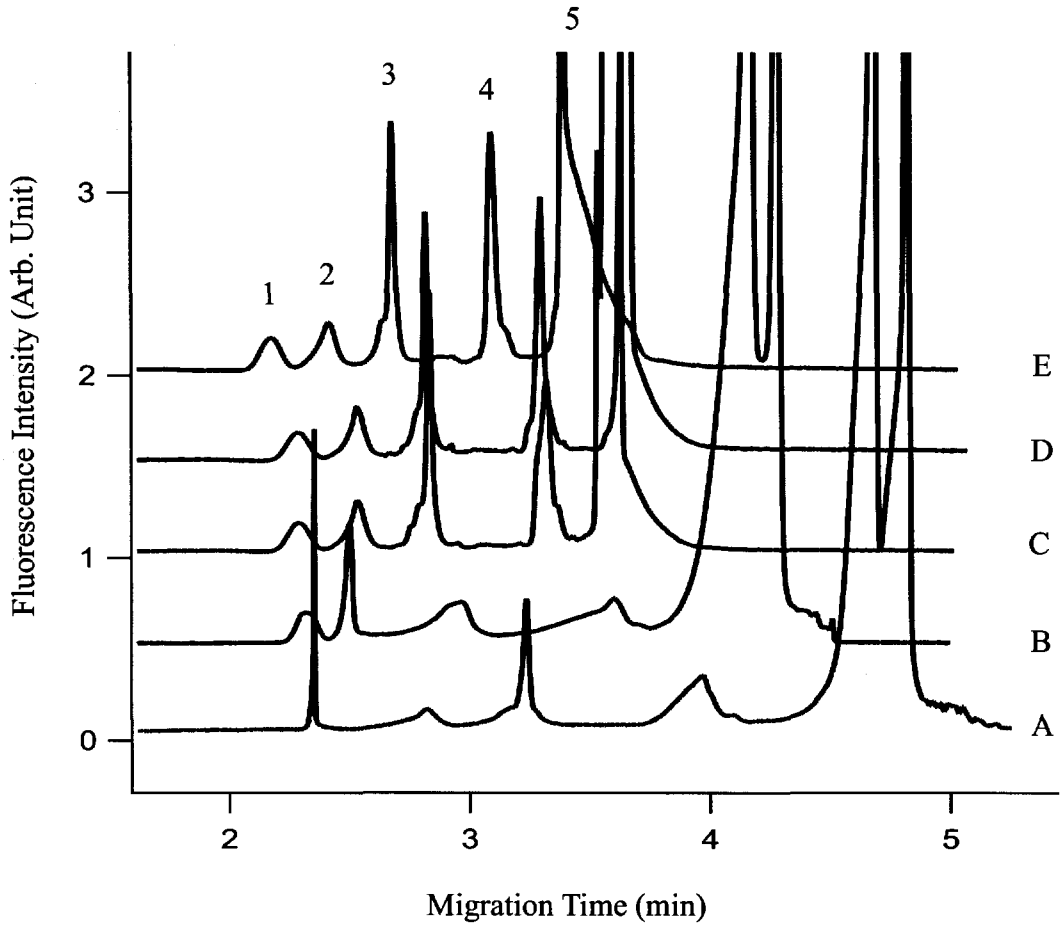

Figure 2.5. Electropherograms showing the effect of the pH of the running buffer on the separation of protein-aptamer complexes. Peaks 1-4 represent aptamer complexes of IgE (peak 1), HIV-RT (peak 2), thrombin (peak 3), and PDGF-BB (peak 4), and peak 5 represents a mixture of fluorescent aptamers for the four proteins. The pH of running buffer is 7.5 (A), 8.0 (B), 8.3 (C), 8.5 (D), and 9.0 (E).

2.4.3 Detection of multiple proteins

Building on the success of the separation of protein-aptamer complexes, tunable aptamer CE was applied to the detection of four proteins. In addition to the adaptation of aptamers as charge modulators, another important benefit of aptamer binding to the proteins is the incorporation of fluorescent aptamers as probes to enable LIF detection of the proteins that are otherwise not amenable to high sensitivity LIF detection. Aptamers were labeled at 5' end with highly fluorescent 6'-FAM which was excited by an argon ion laser (488 nm). The binding of fluorescent aptamers to non-fluorescent proteins makes proteins amenable for highly sensitive LIF detection. In order to maximize the sensitivity and speed of detection, the experimental conditions for binding and detection were first optimized. These optimized parameters included the incubation temperature and time, and the effects of Mg^{2+} and BSA on the formation of specific protein-aptamer complexes.

Incubation temperature and time were optimized to favor the formation of protein-aptamer complexes. To determine the effect of temperature on the formation of protein-aptamer complexes, three mixture solutions each containing 10 nM four proteins and 50 nM corresponding aptamers were incubated for 10 min at 0 °C, 25 °C, or 37 °C, respectively. The amounts of protein-aptamer complexes were determined by tunable aptamer CE. **Figure 2.6a** shows the change profile of the formation of protein-aptamer complexes under different incubation temperatures after analysis of these mixture solutions. The maximum amount of protein-aptamer complexes was formed for all proteins when the

incubation temperature was 37 °C, although incubation temperature has the greatest effect on the formation of PDGF-BB complex and the smallest effect on the formation of IgE complex. Therefore, 37 °C was chosen as final incubation temperature. The effect of incubation time on the formation of protein-aptamer complexes was further determined by conducting another experiment in which three mixture solutions containing the same concentrations of proteins and their aptamers were incubated at 37 °C for 10, 20, or 30 min. **Figure 2.6b** shows the effect of incubation time on the formation of protein-aptamer complexes. Although the increase of incubation time assists the formation of protein-aptamer complexes for IgE, thrombin, and PDGF-BB, the formation of HIV-RT-aptamer complexes decreases with longer incubation time. Therefore, an incubation time of 10 min was used for detection of these four proteins.

The presence of Mg^{2+} in the incubation buffer can usually facilitate the aptamers to present their desired secondary conformation, thereby favoring the formation of protein-aptamer complexes. To examine the effect of Mg^{2+} on the formation of protein-aptamer complexes, the five mixture solutions, each containing 10 nM four proteins and 50 nM corresponding aptamers, were added with 0, 0.5, 1, 2, or 3 nM Mg^{2+}, respectively. The solutions were incubated at 37 °C for 10 min, and the amount of protein-aptamer complexes was determined by tunable aptamer CE. **Figure 2.7** shows results from the analysis of these solutions. Mg^{2+} has various effects on the formation of different complexes. The formation of thrombin and PDGF-BB complexes reached a plateau after 1 nM Mg^{2+}, whereas the formation of IgE complexes increased continuously with the

increase in concentration of Mg^{2+}. However, the increase of Mg^{2+} from 0 nM to 1 nM resulted in a moderate decrease in the formation of the HIV-RT complex, and further increase of Mg^{2+} from 1 nM to 3 nM led to a substantial decrease in the formation of the HIV-RT complex. Therefore, 1 nM was chosen as the final concentration of Mg^{2+} for the analysis of the four proteins.

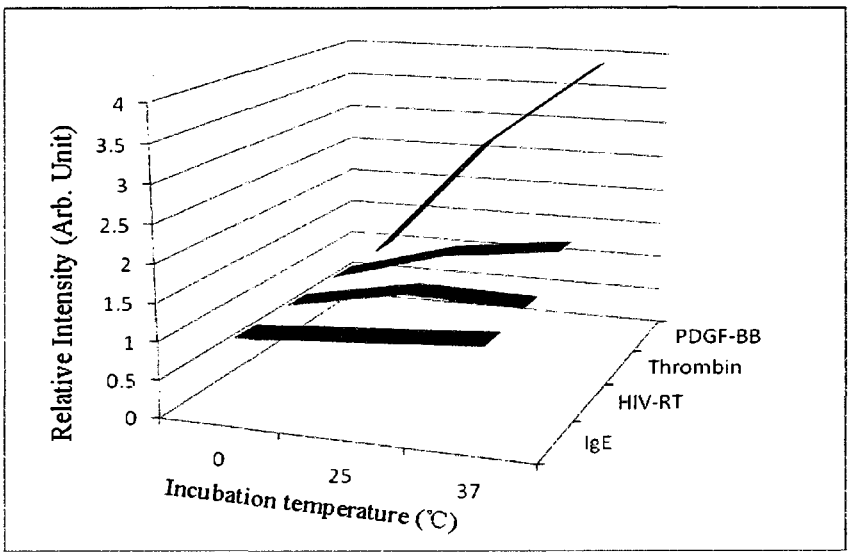

Figure 2.6a Effect of incubation temperature on the formation of protein-aptamer complexes. Standard deviation: 0.04 -0.34.

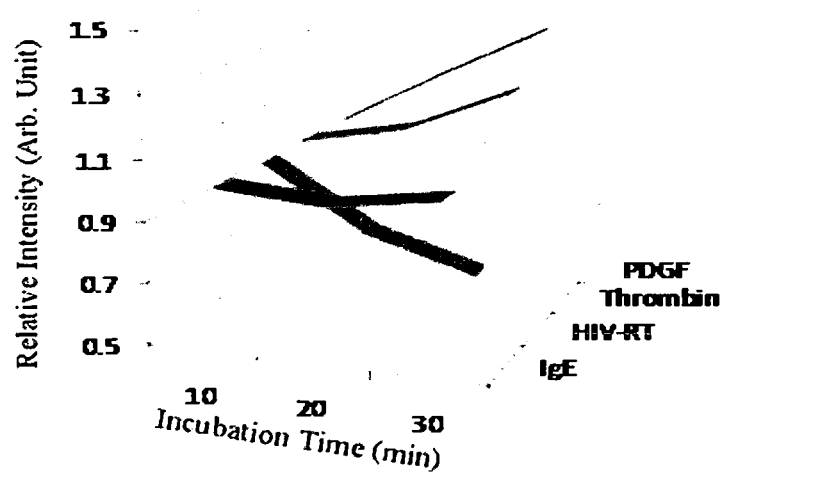

Figure 2.6b Effect of incubation time on the formation of protein-aptamer complexes. Standard deviation: 0.03 -0.12.

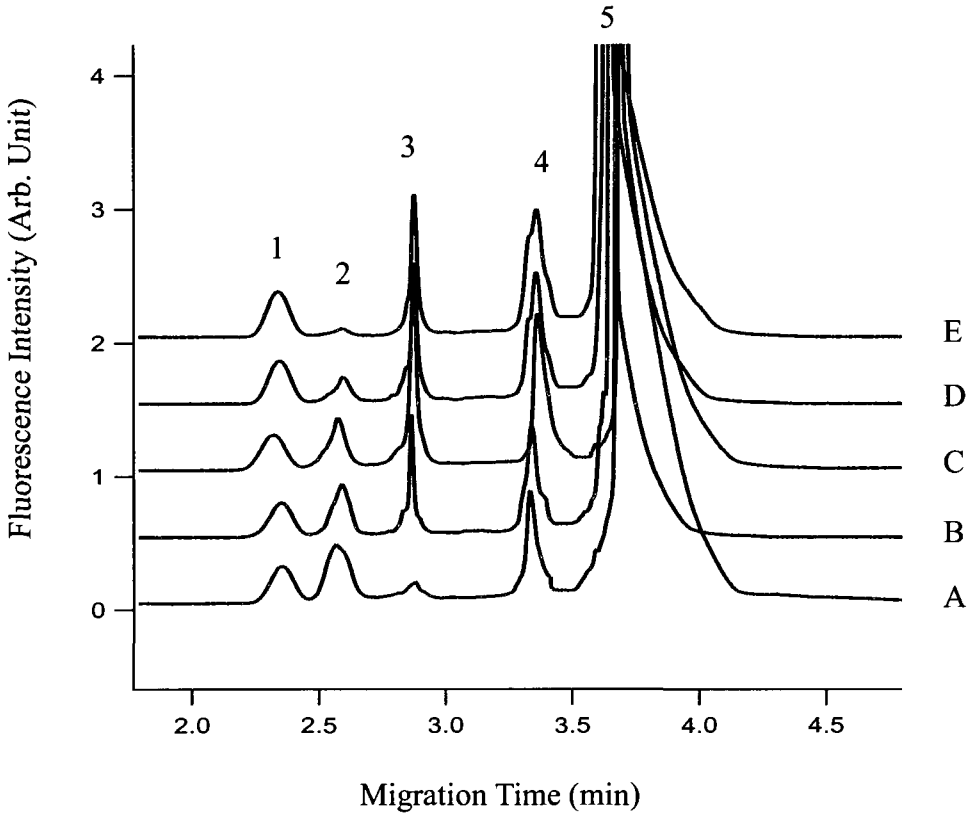

Figure 2.7a Electropherograms showing the effect of Mg2+ on the formation of protein-aptamer complexes. Peaks 1-4 represent aptamer complexes of IgE (peak 1), HIV-RT (peak 2), thrombin (peak 3), and PDGF-BB (peak 4), and peak 5 represents a mixture of fluorescent aptamers for the four proteins. The concentration of Mg^{2+} is 0 (A), 0.5 (B), 1 (C), 2 (D), or 3 mM (E).

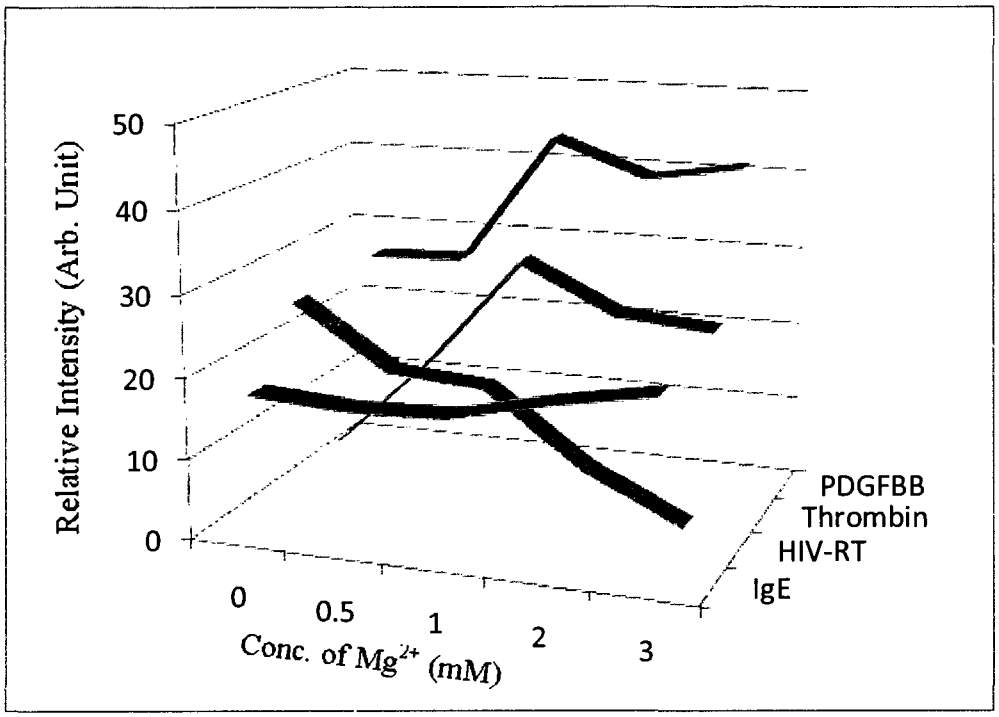

Figure 2.7b Effect of Mg^{2+} on the formation of protein-aptamer complexes. Standard deviation: 0.56 - 2.43.

It has been reported that the presence of general proteins in the incubation buffer is able to stabilize and enhance the protein-DNA complex (17). The effect of general proteins on the formation of protein-aptamer complexes was examined by addition of different concentrations of BSA (0-500 μg/mL) into mixture solutions containing 10 nM of the four proteins and 50 nM of their aptamers. **Figure 2.8** demonstrates that the addition of BSA into the incubation buffer is able to enhance the formation of protein-aptamer complexes for all four proteins. Because the formation of protein-aptamer complexes reached plateau after the use of 100 nM BSA, this was determined as the optimum concentration for BSA.

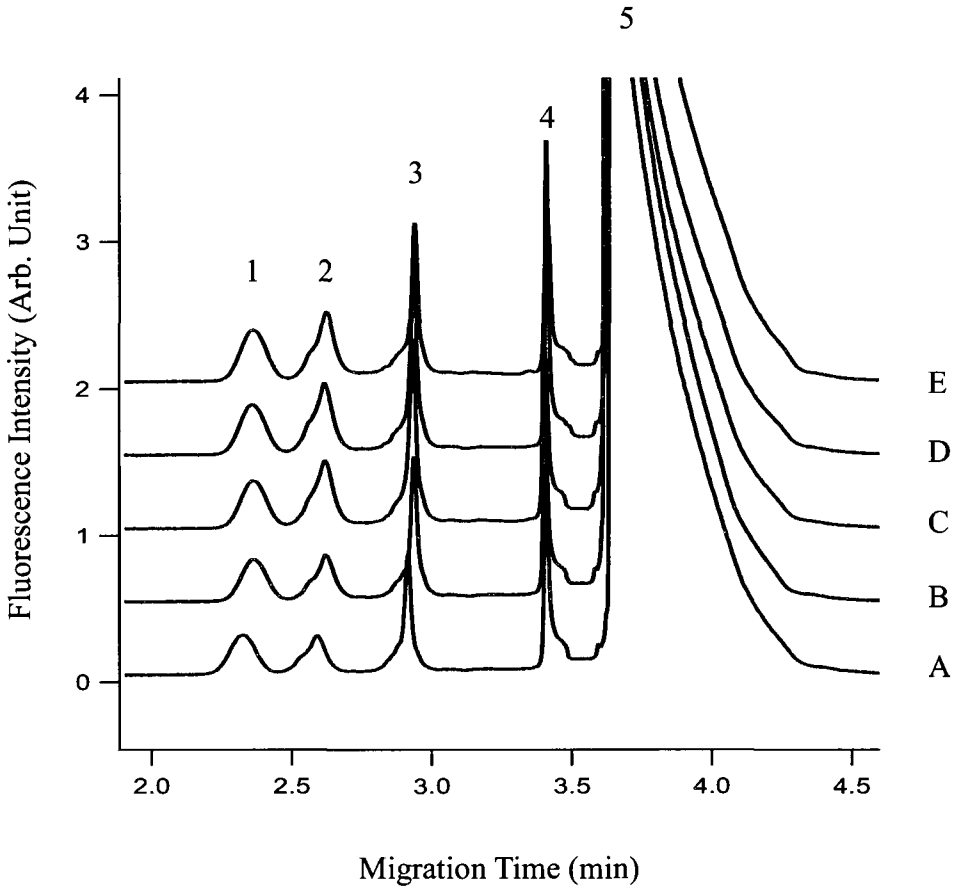

Figure 2.8a Electropherograms showing the effect of BSA on the formation of protein-aptamer complexes. Peaks 1-4 represent aptamer complexes of IgE (peak 1), HIV-RT (peak 2), thrombin (peak 3), and PDGF-BB (peak 4), and peak 5 represents a mixture of fluorescent aptamers for the four proteins. The concentration of BSA is 0 (A), 50 (B), 100 (C), 200 (D), or 500 μg/mL (E).

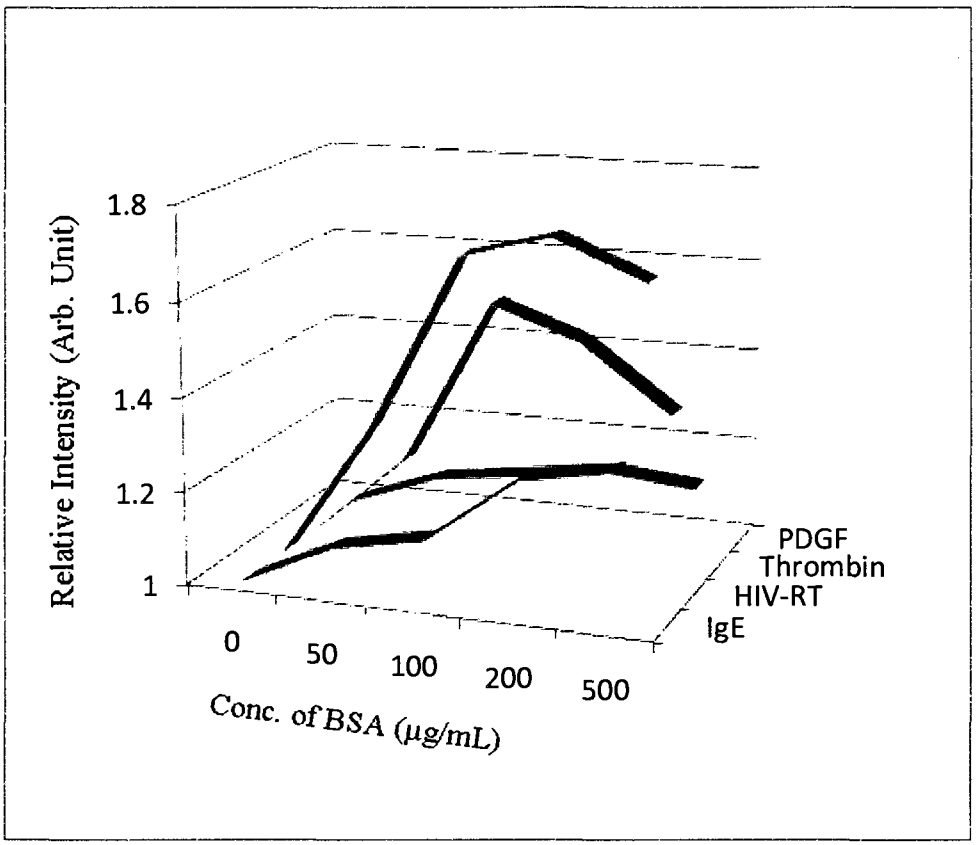

Figure 2.8b Effect of BSA on the formation of protein-aptamer complexes.

Standard deviation: 0.04 -0.11.

Under the optimized binding and detection conditions, the tunable aptamer CE was applied to the detection of four proteins. The method exhibited excellent sensitivity for detection of these proteins. Detection limits were 250 pM for IgE, 100 pM for HIV-RT and thrombin, and 50 pM for PDGF-BB (**Figure 2.9**). Although Craig and Dovichi *et al.* (23) have demonstrated ultimate detection of single β-galactosidase molecule by using a CE enzyme assay, the detection limits shown here are best ever reported for the simultaneous determination of multiple proteins by affinity CE. The calibrations were linear for the determination of IgE (r^2=0.991), HIV-RT (r^2=0.985), thrombin (r^2=0.984), and PDGF-BB (r^2=0.988) (**Figure 2.10**). A linear dynamic range of two orders of magnitude (1-100 nM) in the low concentration region was obtained for all four proteins, and this dynamic range could be extended to higher concentrations of proteins by using proportionally higher concentrations of aptamers.

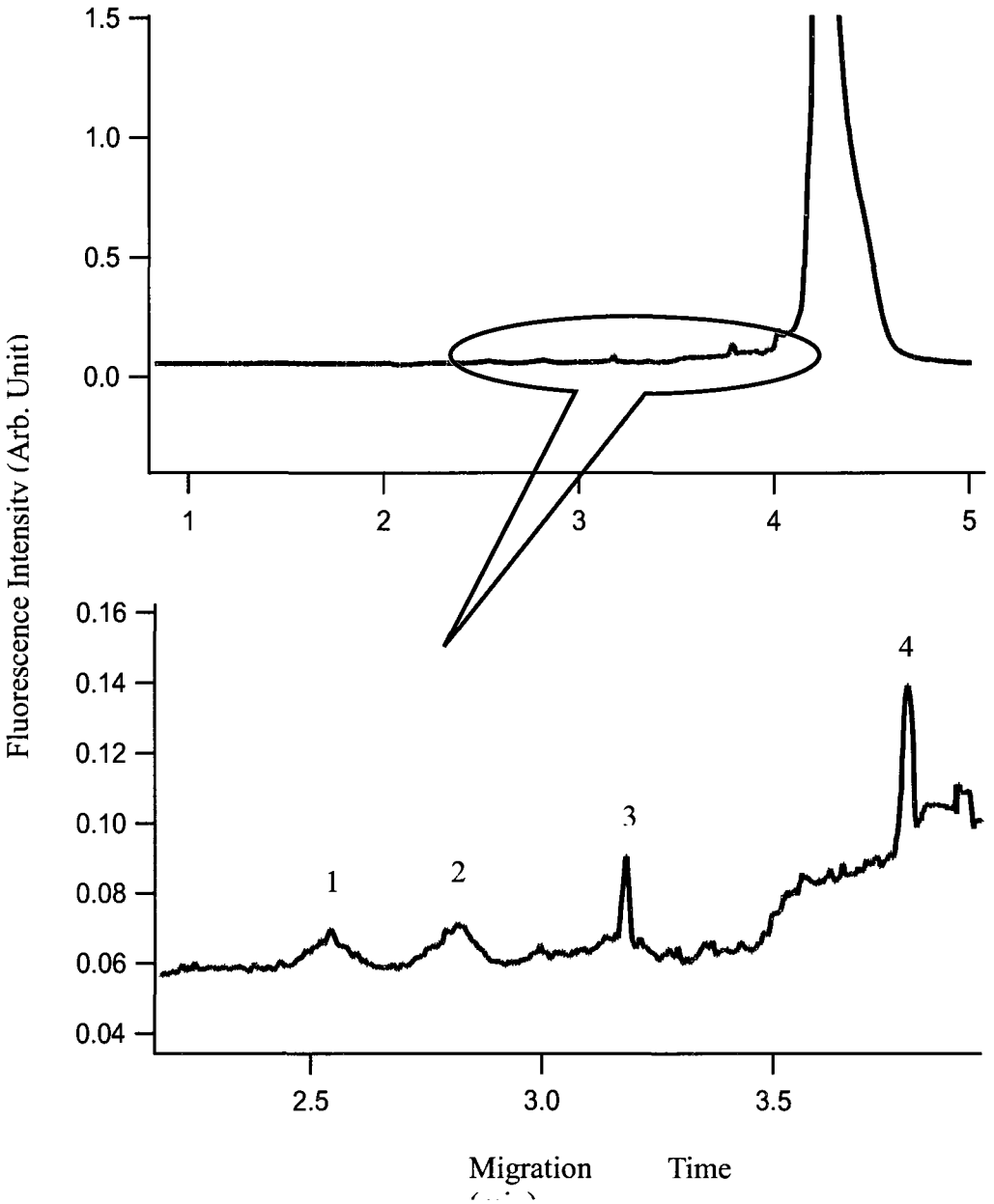

Figure 2.9. Electropherogram showing the detection of trace levels of proteins using tunable aptamer CE. Peaks 1-4 represent aptamer complexes of IgE (peak 1), HIV-RT (peak 2), thrombin (peak 3), and PDGF-BB (peak 4). The concentrations of four proteins were 250pM for IgE, 100 pM for HIV-RT and thrombin, and 50 pM for PDGF-BB.

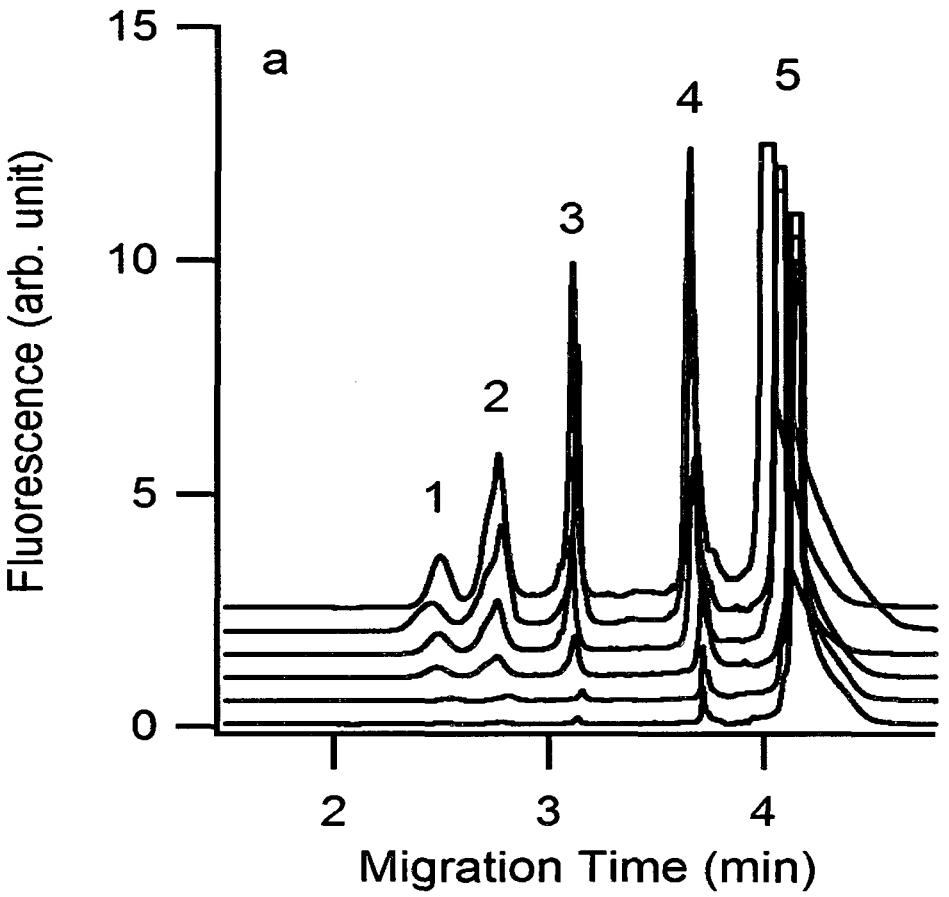

Figure 2.10a Electropherograms showing the analysis of four proteins in mixture solutions containing varying concentrations of proteins (0-100nM). Peaks 1-4 represent aptamer complexes of IgE (peak 1), HIV-RT (peak 2), thrombin (peak 3), and PDGF-BB (peak 4), and peak 5 represents a mixture of fluorescent aptamers for the four proteins.

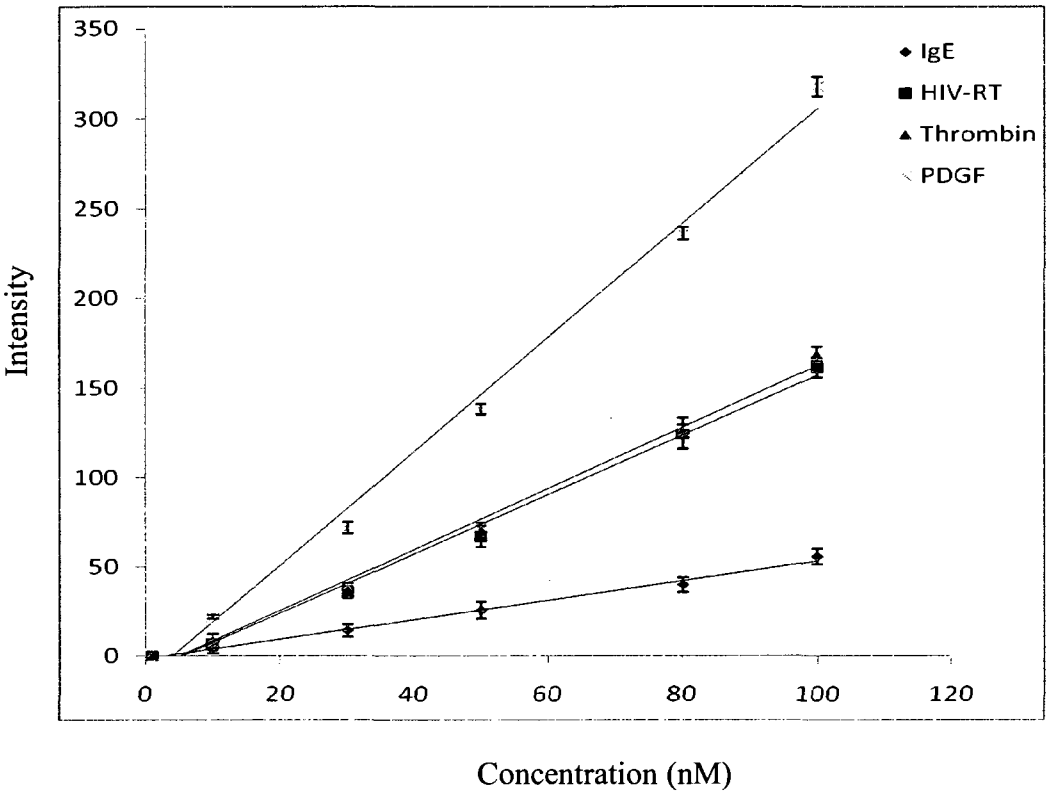

Figure 2.10b. Calibration curves constructed from mixture solutions containing varying concentrations of proteins (0-100nM)

2.4.4 Detection of proteins in dilute human serum sample

To demonstrate the applicability of this assay to sample analysis, the tunable aptamer CE was applied to the detection of the four proteins in a dilute human serum sample. The four proteins were spiked into human serum sample diluted 10 times with incubation buffer, and the concentrations of the proteins were determined in the spiked samples. **Figure 2.11** shows the electropherograms from

the analysis of four proteins in the dilute human serum samples. The interference from serum matrix was examined first by the analysis of the dilute human serum sample containing only fluorescently labeled aptamers. The analysis of the serum samples showed matrix interference on the quantification of HIV-RT. A peak was observed with a similar migration time to that of HIV-RT. This peak may result from the non-specific binding of some DNA-binding proteins in human serum to fluorescent aptamers. It was subsequently found that the addition of a non-specific and non-fluorescent 49-mer oligonucleotide with 10 times higher concentration than the total fluorescent aptamers could eliminate the interference, probably by reducing any non-specific binding of the serum proteins to the fluorescent aptamers. Finally, the detection of four proteins was achieved in dilute human serum by tunable aptamer CE. The analysis of the four proteins was complete in 6 min. Recoveries ranged from 92% to 113%.

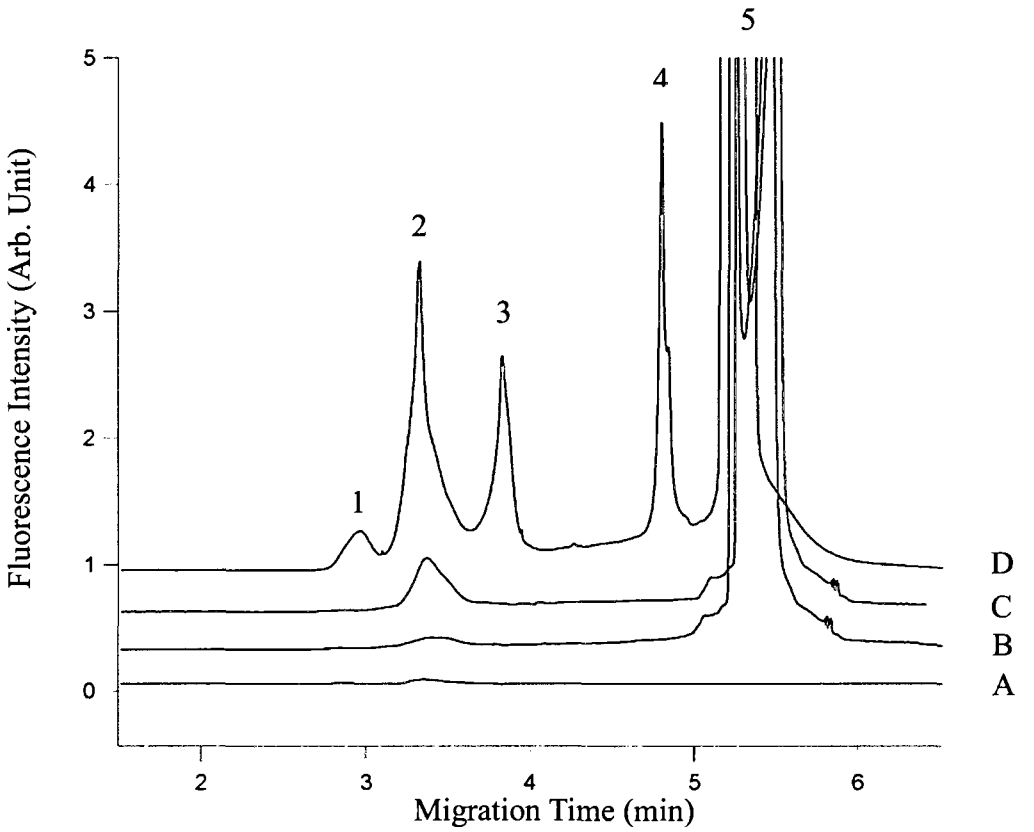

Figure 2.11. Electropherograms showing the analysis of four proteins in dilute human serum sample. Peaks 1-4 represent aptamer complexes of IgE (peak 1), HIV-RT (peak 2), thrombin (peak 3), and PDGF-BB (peak 4), and peak 5 represents a mixture of fluorescent aptamers for the four proteins. A corresponds to dilute human serum only; B corresponds to dilute human serum sample containing fluorescent aptamers and a non-specific and non-fluorescent 49-mer oligonucleotide; C corresponds to dilute human serum sample containing fluorescent aptamers; and D corresponds to dilute human serum sample containing four proteins, fluorescent aptamers and the non-specific and non-fluorescent 49-mer oligonucleotide.

2.5 Conclusions

A tunable aptamer CE assay has been developed that enables highly sensitive fluorescence detection of multiple proteins. The simultaneous determination of pM levels of four proteins was achieved in a single CE analysis. The multiplex capability and high sensitivity were achieved by introducing tunable aptamers as both charge modulators for electrophoretic separation and as fluorescent affinity probes for ultrasensitive fluorescence detection. The assay is not limited to the four proteins shown here, and the principle can be extended to the simultaneous analysis of other species to which aptamers can bind, including proteins, peptides, carbohydrates, and whole cells. The throughput of the assay can be further enhanced by using electrophoresis systems with multiple capillaries (22), or microfluidic devices with multiple channels. The assays for multiple proteins are potentially useful for biomarker development, clinical testing, and medical diagnostics.

2.6 References

1. I. German, D. D. Buchanan and R. T. Kennedy, *Anal. Chem.,* 1998, 95, 4540-4545.

2. V. Pavski and X. C. Le, *Anal. Chem.,* 2001, 73, 6070-6076.

3. M. Berezovski, R. Nutiu, Y. Li and S. N. Krylov, *Anal. Chem.*, 2003, 75, 1382-1386.

4. C.-C. Huang, Z. Cao, H.-T. Chang and W. Tan, *Anal. Chem.* 2004, 76, 6973-6981.

5. H. Zhang, X.-F. Li, and X. C. Le, *J. Am. Chem. Soc.* 2008, 130, 34-35.

6. Y. Li, L. Guo, F. Zhang, Z. Zhang, J. Tang and J. Xie. *Electrophoresis,* 2008, 29, 2570-2577.

7. A. J. Haes, B. C. Giordano and G. E. Collins, *Anal. Chem.,* 2006, 78, 3758-3764.

8. P. Yang, R. J. Whelan, Y. Mao, A. W.-M. Lee, C. Carter-Su and R. T. Kennedy, *Anal. Chem.*, 2007, 79, 1690-1695.

9. R. C. Tim, R. A. Kautz and B. L. Karger, *Electrophoresis*, 2000, 21, 220-226.

10. R. J. Meagher, J.-I. Won, L. C. McCormick, S. Nedelcu, M. M. Bertrand, J. L. Bertram, G. Drouin, A. E. Barron and G. W. Slater, *Electrophoresis*, 2005, 26, 331-350.

11. T. W. Wiegand, P. B Williams, S. C Dreskin, M. H. Jouvin, J. P. Kinet and D. Tasset,

J. Immunol. 1996, 157, 221-230.

12. D. M. Tasset, M. F. Kubik and W. Steiner, J. Mol. Biol. 1997, 272, 688-698.

13. L. S. Green, D. Jellinek, R. Jenison, A. Ostman, C. H. Heldin and N. Janjic, Biochemistry, 1996, 35, 14413-14424.

14. D. J. Schneider, J. Feignon, Z. Hostomsky and L. Gold, Biochemistry 1995, 34, 9599-9610.

15. Q. H. Wan and X. C. Le, *Anal. Chem.*, 2000, 72, 5583-5589.

16. H. Wang, M. Lu, M. Weinfeld and X. C. Le, *Anal. Chem.*, 2003, 75, 247-254.

17. H. Wang, M. Lu and X. C. Le, *Anal. Chem.*, 2005, 77, 4985-4990.

18. J. Gao, F. A. Gomze, R. Härter and G. M. Whitesides, *Proc. Natl. Acad. Sci. U.S.A.,* 1994, 91, 12027-12030.

19. J. Gao, M. Mammen and G. M. Whitesides, *Science,* 1996, 272, 535-537.

20. R. P. J. Sear, *Chem. Phys.*, 2003, 118, 5157-5161.

21. H. Wang, M. Lu, M. Weinfeld and X.C. Le, *Anal. Chem.*, 2003, 75, 247-254.

22. N. J. Dovichi and J. Z. Zhang, *Angew. Chem. Int. Ed.,* 2000, 39, 4463-4468.

23. D. Craig, E. A. Arriaga, P. Banks, Y. Zhang, A. Renborg, M. M. Palcic and N. J. Dovichi, *Anal. Biochem.,* 1995, 226, 147-153.

Chapter Three

Differentiation and Detection of PDGF Isomers and Their Receptors by Tunable Aptamer Capillary Electrophoresis

3.1 Introduction

PDGF was discovered as a major mitogen and chemoattractant in serum for mesenchymal-derived cells (1-3). PGDF is composed of two disulfide-linked polypeptide chains designated A and B (4). The native protein occurs as the homodimers AA or BB or the heterodimer AB. The dimeric isomers PDGF-AA, AB, and BB are differentially expressed in various cells and their biological functions are mediated through binding to two cell surface proteins, PDGF receptors α and β (5-7). Differences exist in isoform binding to each receptor. The receptor α binds to all three PDGF isomers, whereas the receptor β binds only to the PDGF-AB and PDGF-BB isomers with high affinity (8-10). It is essential to determine the composition of PDGF isomers and their receptors in order to understand their functions and their interactions. A variety of aptamer-based methods have been demonstrated for the determination of PDGF-AB and BB (11-15). However, all these methods allowed the determination of only the total amount of PDGF-AB and BB. They are not able to differentiate and detect PDGF-AB and BB separately in a mixture.

The objective of this chapter is to demonstrate the capability of the tunable aptamer CE for analysis of protein isomers or families of proteins. The PDGF-AB and BB were chosen as a model because aptamers for them are available. We take

advantage of the discovery that these aptamers bind only to PDGF B chain with high affinity (16). PDGF receptors α and β were also determined based on the interaction of isomers with their receptors.

3.2 Experimental

3.2.1 Reagents

Recombinant human PDGF-AA, PDGF-AB, PDGF-BB, PDGF receptor α, and PDGF receptor β were all obtained from R&D Systems (Minneapolis, MN) in lyophilized form, free from carrier protein. BSA and human serum were purchased from Sigma (Oakville, ON). PDGFs were reconstituted in 4 mM HCl containing 0.1% BSA to prepare a stock solution of 1 μM. The PDGF receptor stock solution at 5 μM was prepared by reconstitution of receptors in 1×PBS buffer containing 0.1% BSA. The stock solutions were stored at -20 °C when not in use. PDGF binding aptamers, 20t-4 (5'-AGG GCGCGTTCTTCGTGGTTACTTTTAGTCCCG-3') and 36t-4 (5'-CAGGCTACGGCACGTAGAGCATCACCATGATCCTG-3'), and a non-specific 49 mer oligonucleotide (5'-TGGTCTTGTGTGGCTGTGGCTATGTCTGATCTT AATCCACGAAGTCACC-3') were synthesized, and purified by Integrated DNA Technologies (Coralville, IA). The 6'-FAM label was attached directly to the 5' end of aptamers, and fluorescently labeled aptamers were purified by reversed-phase HPLC. The 10×TG was obtained from Bio-Rad Laboratories (Mississauga, ON). 1× TG buffer (25 mM Tris and 192 mM glycine, pH 8.3) was diluted with deionized water from 10×TG and then adjusted to desired pH by 1 M NaOH. All other reagents were commercially available analytical grade.

3.2.2 Capillary electrophoresis

A laboratory-built CE-LIF system was used in this work (17-19). The schematic of the CE-LIF system is shown in **Figure 2.2**. The separation was conducted by using 40 cm long uncoated fused silica capillaries (20-μm i.d., 150-μm o.d. Polymicro Technologies, Phoenix, AZ) at room temperature. Samples were electrokinetically injected into the capillary at a voltage of 18 kV for 5 s, and a running voltage of 18 kV (450 V/cm) was employed to drive separation. The running buffer used for all experiments was 1×TG adjusted to pH 8.5 by 1 M NaOH unless otherwise stated. Periodically, the capillaries were treated by running 0.02 M NaOH for 5 min, followed by water for 3min and running buffer for 5 min at 300–450V/cm. All CE data were analyzed using Igor Pro software (version 4.04, WaveMetrics, Lake Oswego, OR).

3.2.3 Formation of complexes

To place aptamers in their desired conformation, the 5 μM aptamer stock solution in 10 mM Tris·HCl (7.4) + 1 mM $MgCl_2$ was treated at 80 °C for 5 min followed by cooling slowly to room temperature before analysis. The sample incubation buffer was 10 mM Tris·HCl (7.4) containing 1 mM $MgCl_2$ and 0.2% BSA. To form complexes, the appropriate volumes of aptamer and protein stock solutions were mixed and diluted with incubation buffer to obtain the desired concentrations of aptamers and proteins. The final sample solution was 50 μL. Before injection, the sample solution was incubated at 37 °C for 20 min.

3.2.4 Serum sample preparation

A frozen serum sample was thawed in a water bath at 30 °C, and then kept

on ice. Prior to analysis, 0.5 mL of the serum sample was centrifuged at 10,000 rpm for 10 min to remove precipitate. The appropriate volumes of aptamer, non-specific DNA sequence, and protein stock solutions were mixed with 5 μL serum to obtain the desired concentration, and the incubation buffer was then added to produce a final volume of 50 μL. Samples were incubated and injected as indicated above.

3.3 Results and Discussion

3.3.1 Tunable aptamer capillary electrophoresis of protein isomers

In tunable aptamer CE, fluorescently labeled aptamers serve as charge modulators to modify the electrophoretic mobility of proteins, in addition to binding specifically to the target proteins that enables laser-induced fluorescence detection of proteins (20). Two aptamers, 20t-4, and 36t-4, have been isolated to bind to the PDGF B chain with much higher affinity than the A chain (11). The value of the dissociation constant (Kd) of aptamers to the B chain is around 10^{-10} M. In contrast, the Kd value of these two aptamers to the A chain is higher than 10^{-8} M. Therefore, only one aptamer molecule can be introduced to bind with a single PDGF-AB molecule, forming a 1:1 protein-aptamer complex, whereas one PDGF-BB molecule is capable of binding to two molecules of the aptamer, forming a 1:2 protein-aptamer complex. Although the two isomers have similar molecular weight (PDGF-AB, 27 kDa; PDGF-BB, 25 kDa) and pI value (pI 9.5-10.0), the formation of two types of complexes lead to the isomers carrying on different numbers of nucleotides. This difference further results in the difference in the electrophoretic mobility of two isomers, which allows us to achieve the

separation of these isomers by tunable aptamer CE.

3.3.2 Separation of PDGF isomers

Figure 3.1 presents electropherograms obtained from analysis of PDGF-AA, AB, and BB by using aptamers 20t-4 or 36t-4. As expected, neither 20t-4 nor 36t-4 produced the peak of the complex between aptamers and PDGF-AA (**Figure 3.1a**), because of the low binding affinity of aptamers to the A chain. An extra peak appeared prior to the aptamer peak, when 20t-4 was applied to the analysis of both PDGF-AB and BB (**Figure 3.1b and c**). This peak resulted from the formation of protein-aptamer complex. A similar result was obtained when 36t-4 was used for the detection of PDGF-AB and BB. Under the running buffer pH of ~8.5, the net charges of both PDGF-AB and BB were positive, because the pI of both isomers was clearly higher than the pH of the running buffer. The uncoated fused-silica capillary would not be suitable for direct analysis of these proteins due to the adsorption of proteins to the negatively charged capillary surface. The binding of aptamers to proteins makes complexes negatively charged, thereby eliminating the adsorption problem and focusing the protein-aptamer complexes into narrow zones.

In principle, PDGF-BB is able to bind to one or two aptamer molecules depending on the ratio of the protein-to-aptamer concentration present in the solution. However, initial experiments did not produce peak from the 1:1 protein-aptamer complex except for a small baseline shift before the peak from the 1:2 protein-aptamer complex, even when the concentration of the protein was higher than that of the aptamer in samples. These results suggest that probably the PDGF

B chain carries positive charges and it is responsible for basic properties of both PDGF-AB and BB, instead of the A chain. The presence of positive charges from unbound B chain in the 1:1 PDGF BB-aptamer complex probably leads to the adsorption of complex to the capillary surface. Therefore, the 1:1 PDGF BB-aptamer complex did not come off the column, and did not interfere with the detection of PDGF-AB.

The complex peaks with similar intensity were obtained under the same experimental conditions when 20t-4 was employed for analysis of PDGF-AB and BB. However, under the same conditions the use of 36t-4 produced a much smaller complex peak for analysis of PDGF-AB, and a little smaller complex peak for analysis of PDGF-BB. The possible reason is because 20t-4 and 36t-4 bind to the different sites on the surface of the PDGF B chain. The binding of 36t-4 to B chain may not cover efficiently all of the surface positive charges, and some amount of the complex is adsorbed on the capillary surface. Therefore, the use of 36t-4 resulted in smaller complex peaks for analysis of PDGF-AB and BB, although 20t-4 and 36t-4 have similar Kd to the PDGF B chain. This explanation is further supported by additional experiments shown later in section 3.3.4. Consequently, 20t-4 was chosen for separation of PDGF-AB and BB.

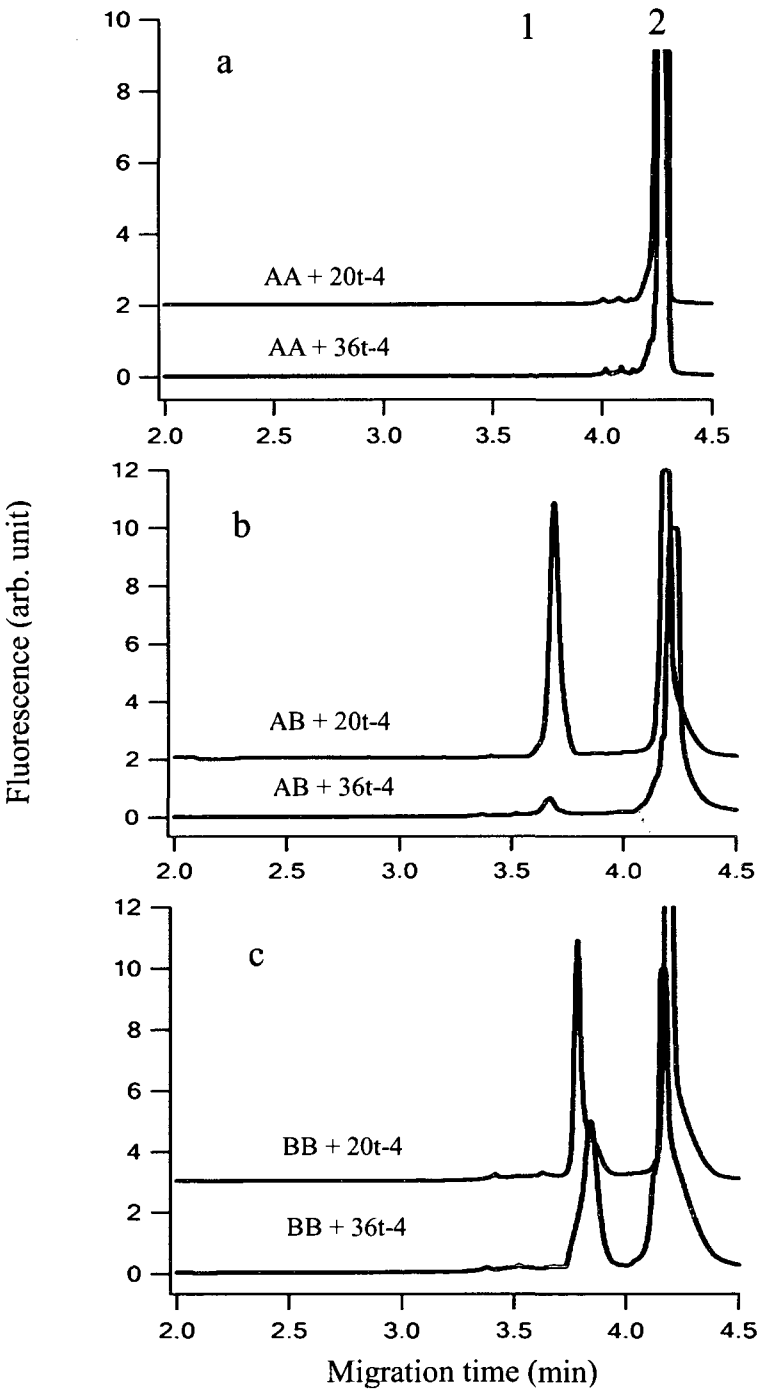

Figure 3.1. Electropherograms showing analysis of PDGF-AA (a), AB (b), and BB (c) using aptamer 20t-4 or 36t-4. The sample solutions contained 50 nM protein and 250 nM aptamer. Peak 1 is the complex of the aptamer and protein; and peak 2 is the unbound fluorescent aptamer.

The PDGF-AB bound to a single 20t-4 was resolved well from the PDGF-BB that was bound to two 20t-4 molecules as shown in **Figure 3.2**. PDGF-BB has smaller molecular weight and carries more positive charges than PDGF-AB under the pH of the running buffer, so free PDGF-BB presents faster mobility than PDGF-AB. However, upon binding to two aptamer molecules, the more negatively charged nucleotides made the PDGF-BB aptamer complex carry more negative charges than the PDGF-AB-aptamer complex, which resulted in the slower migration of PDGF-BB through the capillary than PDGF-AB.

The pH of running buffer plays critical roles in influencing the shapes, sizes, and charges of proteins and the formation of the protein-aptamer complex. The effect of running buffer pH on the separation of the PDGF-AB aptamer complex from the PDGF-BB-aptamer complex was studied. The results are shown in **Figure 3.3**. The best resolution and sharpest peaks were produced with pH of 8.5 and 8.3. At pH 9.0, the lower complex peaks resulted, showing the decrease of the stability of complexes at higher pH. At pH 7.5, the resolution was also good, but it also resulted in longer migration time and wider peak shape, because of the lower EOF and more interaction of proteins with the capillary wall when pH was decreased. The pH of 8.5 was finally chosen for the separation and detection of PDGF isomers.

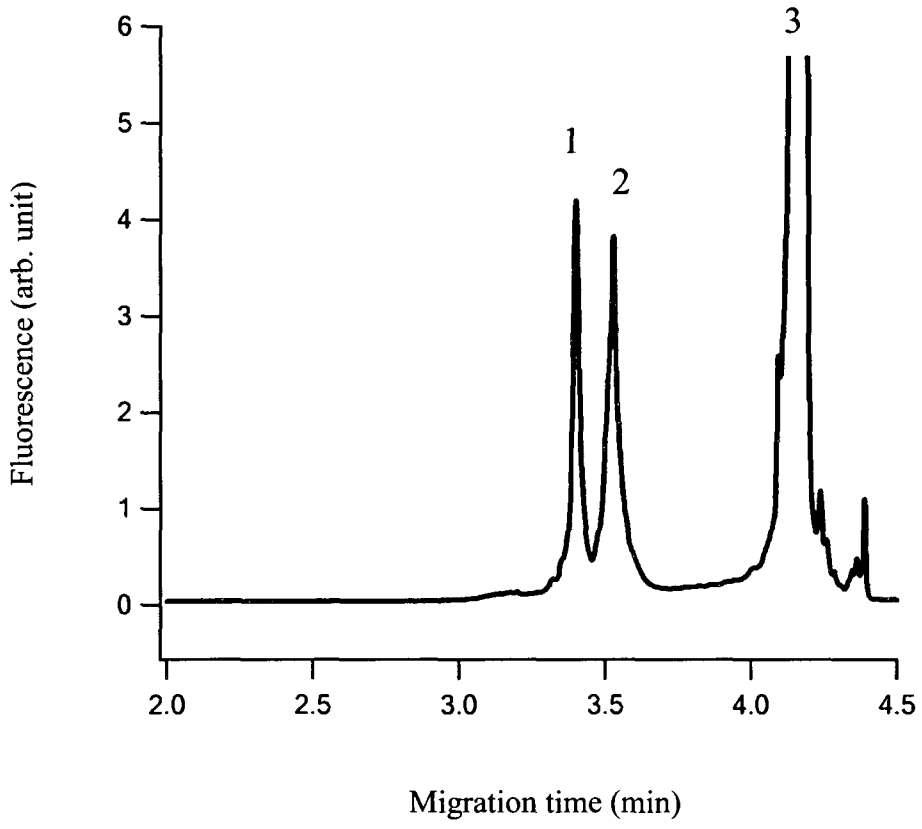

Figure 3.2. Separation of PDGF-AB from BB by tunable aptamer CE. The sample solution contained 25 nM PDGFs and 250 nM 20t-4. Peak 1 is the complex of the PDGF-AB with a single 20t-4 molecule; peak 2 is the complex of the PDGF-BB with two 20t-4 molecules; peak 3 is due to the unbound fluorescent aptamer.

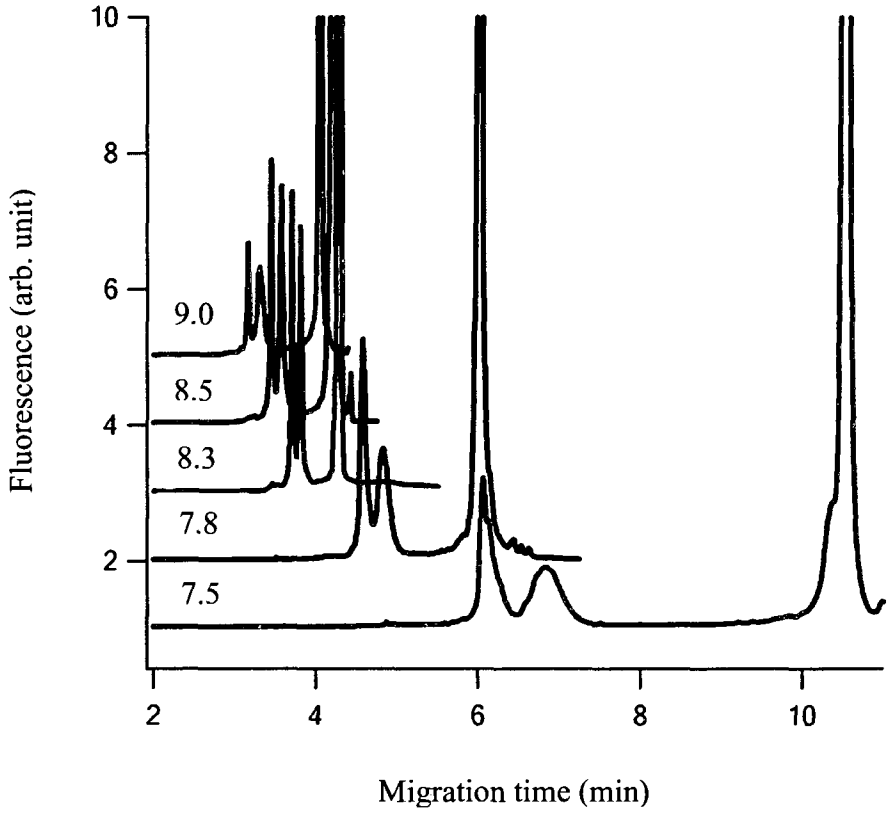

Figure 3.3. Effect of the pH of the running buffer on the separation of PDGF-AB from BB. The first peak of each electropherogram is the complex of the PDGF-AB with a single 20t-4 molecule; the second peak is the complex of the PDGF-AB with two 20t-4 molecules; the third one is due to the unbound fluorescent aptamer.

3.3.3 Determination of PDGF isomers

The presence of Mg^{2+} in the incubation buffer can usually enhance the aptamers to form their desired conformation, thereby improving the formation of protein-aptamer complexes. **Figure 3.4** shows the peak area variation of protein-aptamer complexes obtained from the analysis of solutions containing varying concentrations of Mg^{2+} and constant concentrations of the aptamer and protein. The peak area of complexes increased with the increase of Mg^{2+} concentration until reaching to a plateau at Mg^{2+} of 1 mM. 1 mM was chosen as the Mg^{2+} concentration in the incubation buffer to obtain the best sensitivity.

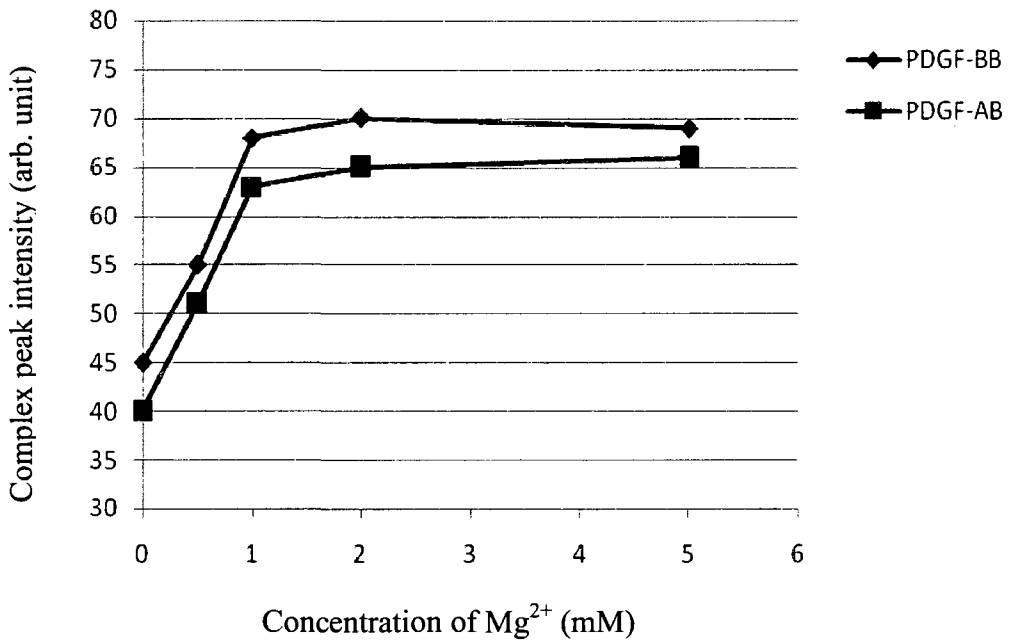

Figure 3.4. Effect of Mg2+ concentration on the formation of PDGF-aptamer complexes. Standard deviation: 1.32 -3.67.

Optimized separation and detection conditions were used to examine the dynamic range of analysis. **Figure 3.5** shows a series of electropherograms from the analysis of PDGF isomers in mixture solutions containing varying concentrations of proteins (0.5-50 nM) and 300 nM of 20t-4. Calibration curves were constructed using peak areas as a function of the protein concentration. Calibrations were linear for the determination of both PDGF-AB (r^2=0.998) and PDGF-BB (r^2=0.994). A linear dynamic range of two orders of magnitude (0.5-50nM) was obtained for both isomers, and this dynamic range could be extended to higher concentrations of proteins by using proportionally higher concentrations of the aptamers. The binding of fluorescent aptamers to non-fluorescent proteins makes proteins amenable for highly sensitive laser-induced fluorescence detection. Detection limits, defined as the concentration corresponding to a signal three times standard deviation of the background, were 50 pM for both PDGF-AB and PDGF-BB as shown in **Figure 3.6**.

The applicability of the assay to sample analysis was demonstrated by the determination of spiked proteins in a 10-fold diluted human serum sample. The human serum was diluted to decrease the ionic strength of sample and the potential interference from high abundant proteins in the serum. A non-specific and non-fluorescent 49-mer oligonucleotide was added into the sample to reduce any non-specific binding of the serum proteins to the fluorescent aptamer. No obvious interference was observed when spiked isomers were detected in a 10-fold diluted human serum samples as shown in **Figure 3.7**. Recoveries ranged from 96% to 115%.

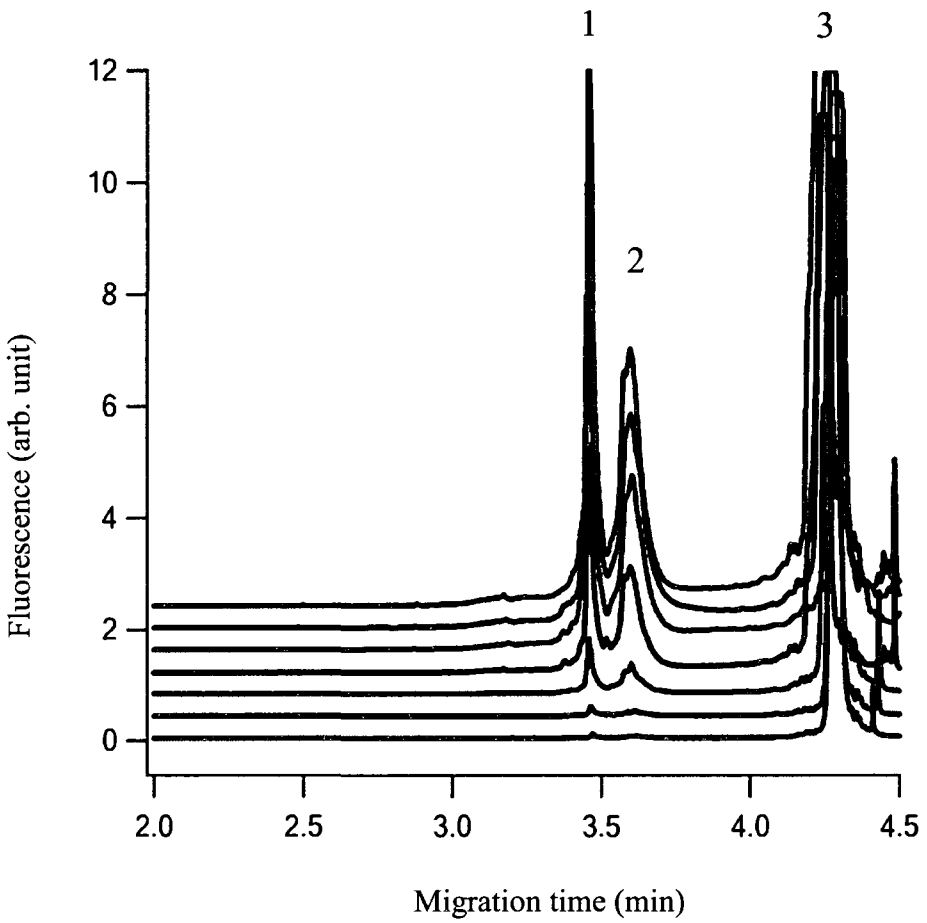

Figure 3.5. Electropherograms showing the analysis of PDGF-AB and BB. The concentrations of proteins are 0.5, 2, 5, 10, 30, 40, and 50 nM from the bottom traces to the top.

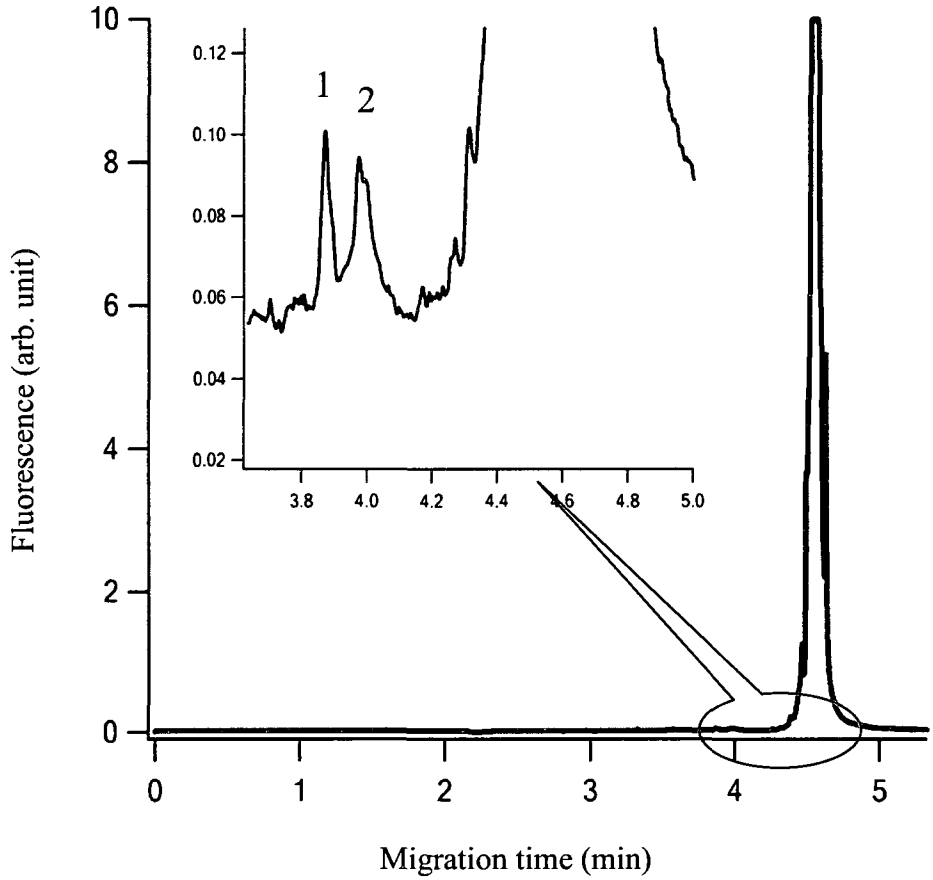

Figure 3.6. Electropherogram showing the detection limits of the method for the analysis of PDGF-AB and BB. Peak 1 is the complex of PDGF-AB with 20t-4; peak 2 is the complex of PDGF-BB with 20t-4; and peak 3 is due to the unbound fluorescent aptamer. The concentrations were 50 pM for both PDGF-AB and PDGF-BB, and 100nM fluorescently labelled aptamer 20t-4.

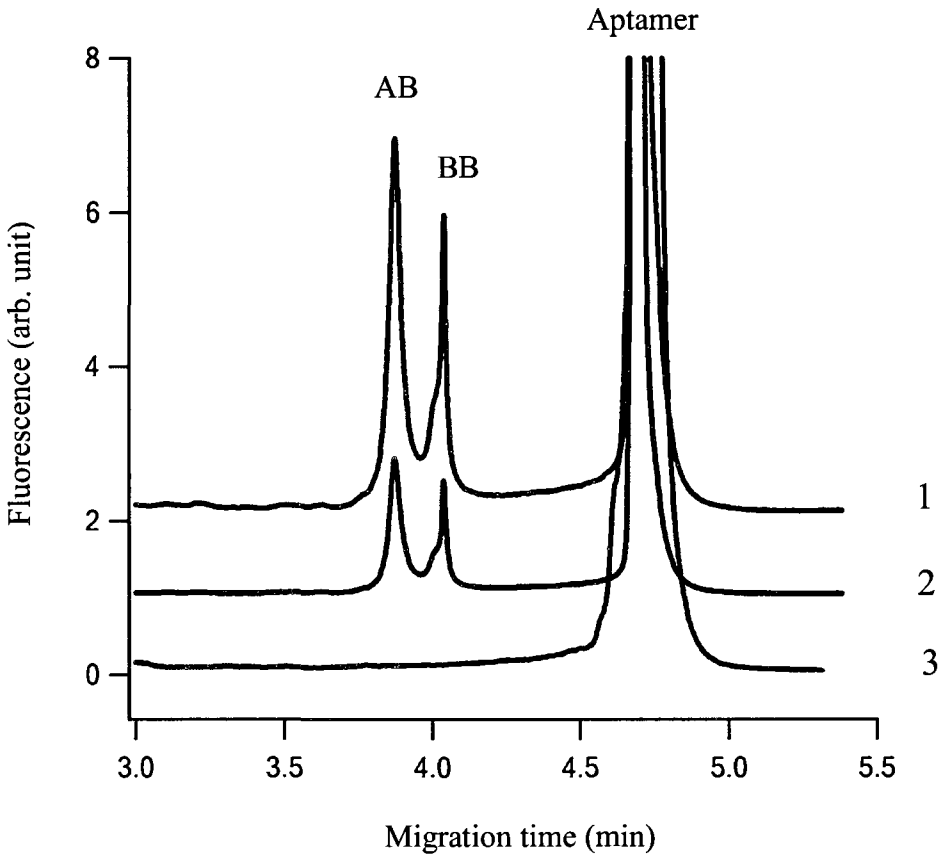

Figure 3.7. Electropherograms showing analysis of PDGF-AB and BB in the diluted serum. The concentration of PDGFs and aptmer is (1) 25 nM and 250 nM, (2) 10 nM and 250 nM, and (3) 0 nM and 250 nM, respectively.

3.3.4 Analysis of PDGF receptor α

PDGF receptor α binds to both PDGF A and B chains, while PDGF receptor β binds only to PDGF B chain. Having this information combined with the results from this chapter showing that aptamers 20t-4 and 36t-4 bind only to the PDGF B chain with high affinity (**Figure 3.1**), it is possible to develop assays for these receptors. Specifically, in the first approach, it is possible to apply PDGF-AB as a connector, bringing the receptor α and the fluorescent aptamer into a single complex molecule, if the two binding events are compatible. The formation of a (receptor α)-(PDGF-AB)-(aptamer) ternary complex represents the incorporation of the fluorescent aptamer as a probe, enabling the laser-induced fluorescence detection of receptor α (**Figure 3.8**).

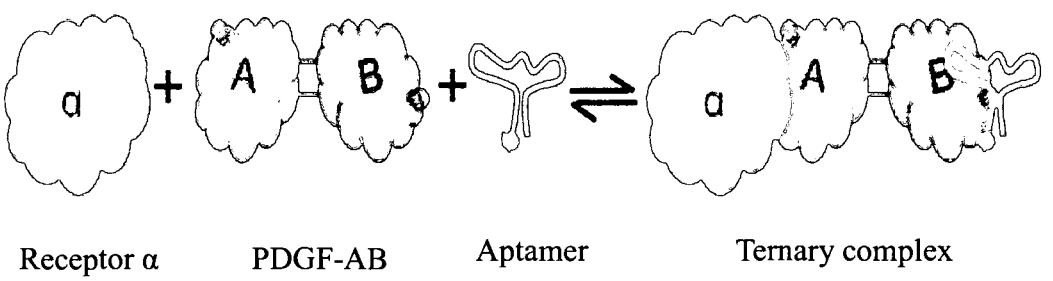

Figure 3.8. Schematic of formation of the (receptor α)-(PDGF-AB)-(aptamer) ternary complex

The ability of 20t-4 and 36t-4 to form the (receptor α)-(PDGF-AB)-(aptamer) complex was examined by incubating 20t-4 and 36t-4 separately with PDGF receptor α and PDGF-AB. The results are shown in **Figure 3.9**. A small peak was observed at the front of the peak of the PDGF-AB aptamer complex

when aptamer 20t-4 was used (**Figure 3.9 A**). In contrast, the use of 36t-4 led to a much larger ternary complex peak under the same experimental conditions (**Figure 3.9 B**). This peak resulted from the formation of the (receptor α)-(PDGF-AB)-(aptamer) complex. The binding of an additional large protein (MW of receptor α, 56 kDa) reduced the negative charge density of the PDGF-AB-aptamer complex, thereby bringing the (receptor α)-(PDGF-AB)-(aptamer) complex with a faster migration rate through the capillary. The difference in the peak intensity of the (receptor α)-(PDGF-AB)-(aptamer) complex is consistent with the previous suggestion that aptamers 20t-4 and 36t-4 bind to different sites of the PDGF B chain. The binding of aptamer 36t-4 probably covers one site of PDGF B chain and leaves other more positively charged sites exposed, which brings about the strong adsorption of (PDGF-AB)-(aptamer 36t-4) complex to the capillary wall. But the exposed sites on PDGF-AB provide enough space for the binding of receptor α to the PDGF A chain. On the other hand, the binding of aptamer 20t-4 to a different site of the PDGF B chain effectively blocks the surface positive charges, and avoids the adsorption of the (PDGF-AB)-(aptamer 20t-4) complex. However, the binding of aptamer 20t-4 to PDGF B chain hinders the binding of receptor α to the PDGF A chain. So aptamer 20t-4 has a stronger ability to inhibit the binding of receptor α to PDGF-AB. Based on the above results, aptamer 36t-4 was chosen as the probe for the analysis of receptor α.

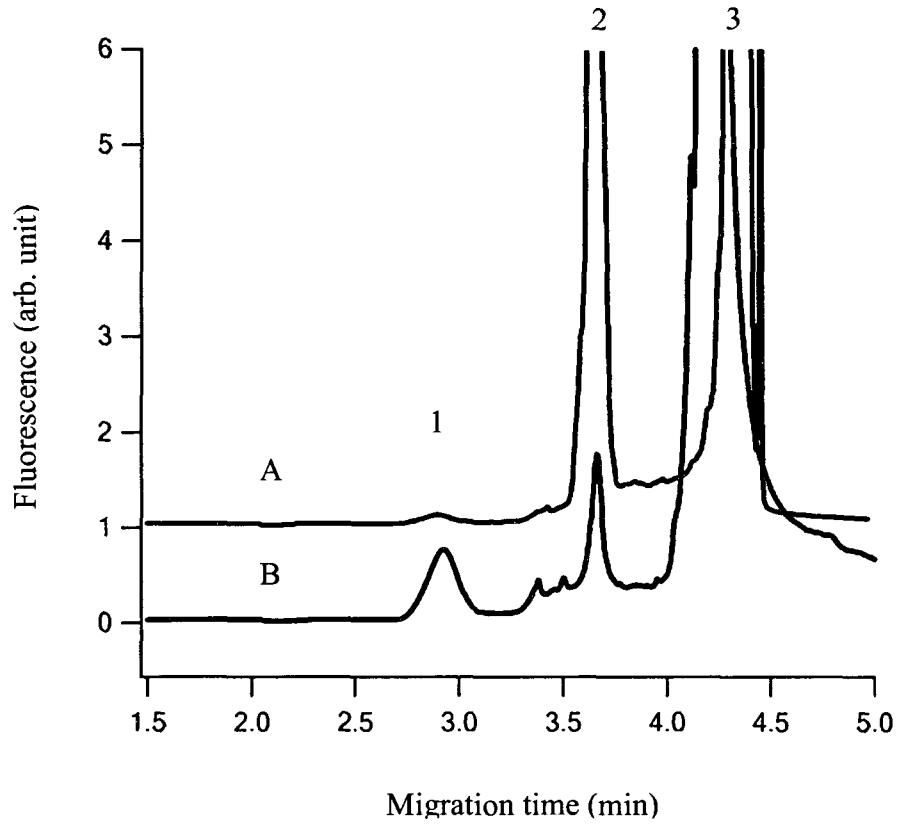

Figure 3.9. Electropherograms showing analysis of PDGF receptor α by using aptamer 20t-4 or 36t-4. Sample (A) contained 25nM receptor α, 100 nM PDGF-AB, and 500 nM 20t-4; sample (B) contained 25nM receptor α, 100 nM PDGF-AB, and 500 nM 36t-4. Peak 1 is the complex of receptor α, PDGF-AB and aptamer; peak 2 is the complex of PDGF-AB and aptamer; and peak 3 is due to the unbound fluorescent aptamer.

Experiments were conducted to compare the impact of three incubation modes (sequence) on the formation of the (receptor α)-(PDGF-AB)-(aptamer) complex. In the first experiment, the receptor α was first incubated with PDGF-AB for 10 min, followed by the addition of 36t-4 and another 10 min incubation. In the second experiment, the PDGF-AB was incubated with 36t-4 for 10 min, and then receptor α was added for the next 10 min incubation. In the last experiment, the three components were mixed at the same time and incubated for 20 min. The results indicated that all three conditions produced little difference in the formation of the (receptor α)-(PDGF-AB)-(aptamer) complex. So two binding events, the binding of receptor α to PDGF-AB and the binding of 36t-4 to PDGF-AB, are quite compatible and do not affect each other.

To achieve better sensitivity, a 5:1 ratio of fluorescent 36t-4 to PDGF-AB was used in the experiment to deplete the existence of unbound PDGF-AB, reducing the possible formation of (receptor α)-(PDGF-AB)-(aptamer) complex without the fluorescent aptamer. Under the optimum conditions, the method was able to detect at levels as low as 0.5 nM PDGF receptor α as shown in **Figure 3.10**. **Figure 3.11** shows a series of electropherograms from the analysis of PDGF receptor α in mixture solutions containing varying concentrations of receptor α and constant concentration of PDGF-AB and 36t-4 aptamer. A linear calibration curve was obtained for the determination of receptor α with an r^2 value of 0.989. A linear dynamic range from 1 to 50 nM was obtained, and this dynamic range could be extended to higher concentrations of protein by using proportionally higher concentrations of PDGF-AB and 36t-4. The spiked receptor α was also

successfully detected in 10-fold diluted serum as shown in **Figure 3.12**. The addition of the non-specific, non-fluorescent oligonucleotide eliminated the interference from the non-specific binding of serum proteins to the fluorescent aptamers.

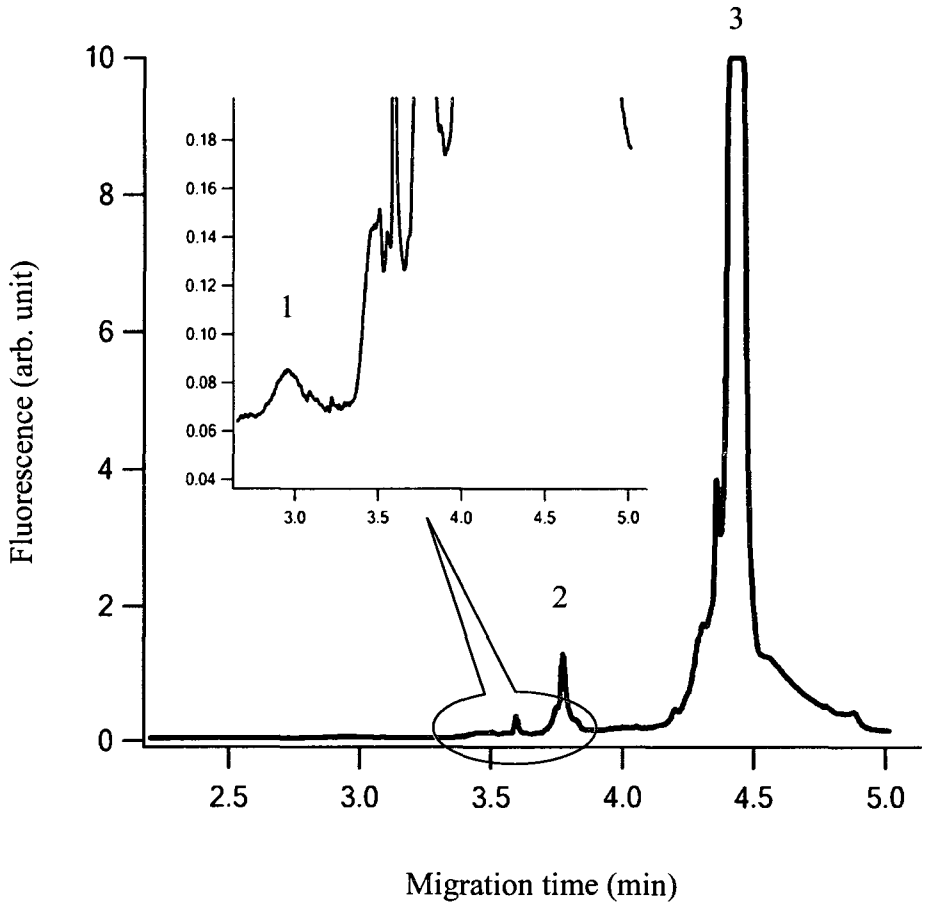

Figure 3.10. Electropherogram showing the detection of 0.5 nM PDGF receptor α

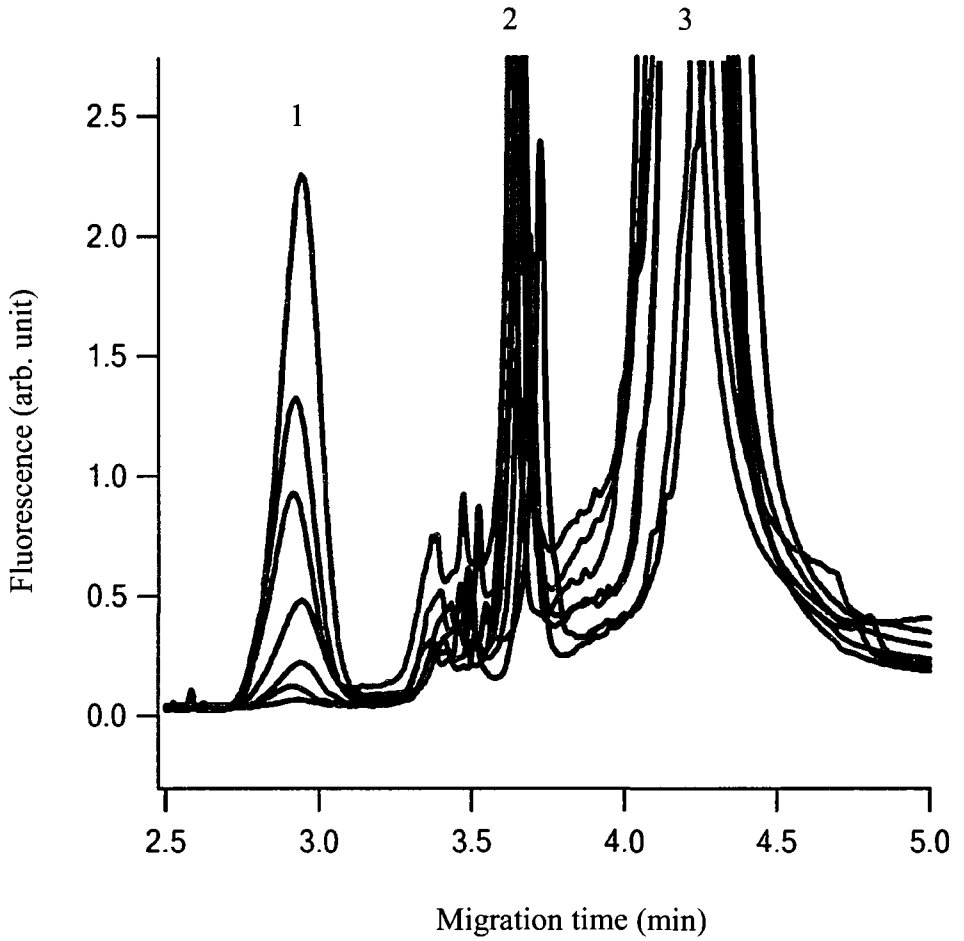

Figure 3.11. Electropherograms showing the analysis of PDGF receptor α. The concentrations of proteins are 1, 5, 10, 15, 25, 35, and 50 nM from the bottom traces to the top. Peak 1 is the complex of receptor α, PDGF-AB, and aptamer; peak 2 is the complex of PDGF-AB and aptamer; and peak 3 is due to the unbound fluorescent aptamer.

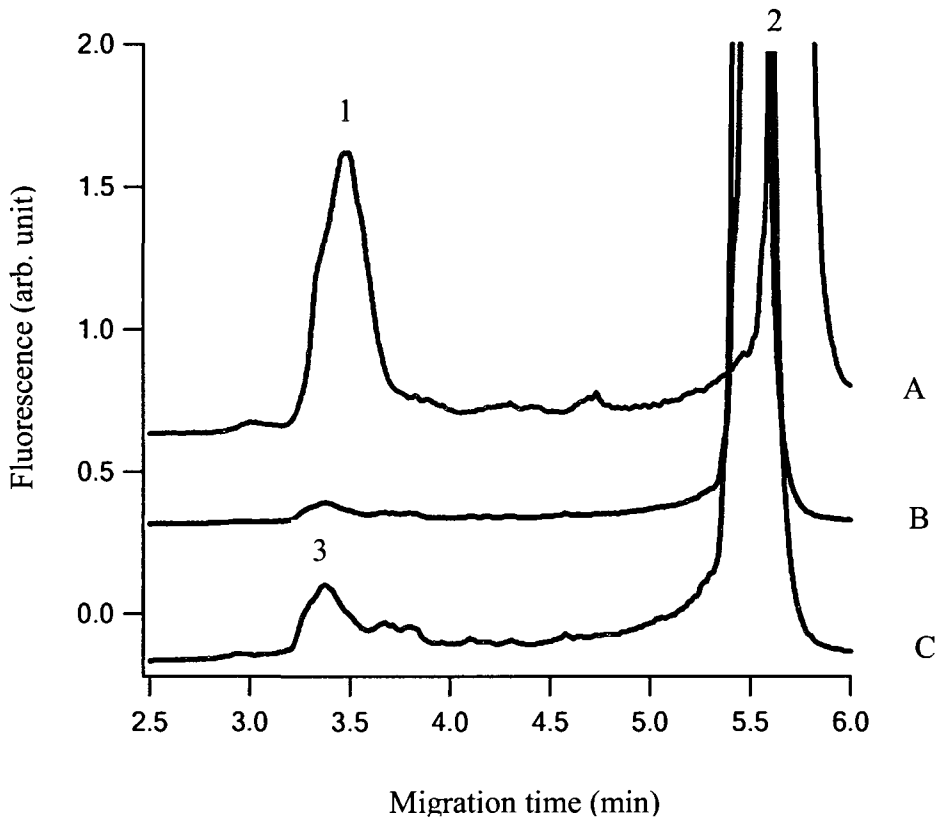

Figure 3.12. Electropherograms showing the analysis of PDGF receptor α in the diluted human serum sample. Sample A contained 30 nM receptor α, 100 nM PDGF-AB, 500 nM aptamer 36t-4, and 5 μM non-specific oligonucleotide; Sample B contained 100 nM PDGF-AB, and 500 nM 36t-4, and 5 μM non-specific oligonucleotide; Sample C contained 500 nM 36t-4. All three samples contained 10-fold diluted human serum. Peak 1 is the complex of receptor α, PDGF-AB, and aptamer; peak 2 is the unbound fluorescent aptamer; and peak 3 is due to non-specific binding of serum proteins to the fluorescent aptamers.

3.3.5 Competitive assay for PDGF receptor β

Since PDGF receptor β, 20t-4, and 36t-4 bind only to the PDGF B chain, two possible strategies were considered to detect PDGF receptor β. If the binding of PDGF receptor β and the aptamer to the PDGF B chain are compatible with each other, PDGF-BB could be used as a connector to bring the receptor β and fluorescent aptamer together, forming a (receptor β)-(PDGF-BB)-(aptamer) complex. Alternatively, the analysis of receptor β could be carried out in a competitive assay format based on the competition between the receptor β and a fluorescent aptamer in binding to the PDGF B chain.

The possibility of forming the (receptor β)-(PDGF-BB)-(aptamer) complex was first determined by mixing receptor β and PDGF-BB with aptamer 20t-4 or 36t-4. The electropherograms are shown in **Figure 3.13**. Except for the peaks from the PDGF-BB aptamer complex and unbound aptamer, no ternary complex peak could be attributed to the binding of receptor β, PDGF-BB, and the aptamer when either 20t-4 or 36t-4 was used, which agreed with the reported results that these aptamers can inhibit efficiently the binding of PDGF-BB to receptors (11, 21).

A competitive assay format was tested, and PDGF-AB and BB were compared as the competitive binding target for analysis of receptor β in the competitive format. The results are shown in **Figure 3.14**. The use of PDGF-BB leads to a better sensitivity than AB, which suggests that the binding of the second aptamer to PDGF-BB is weaker than that of the first aptamer. This is not surprising because the presence of negative charges from the first aptamer repels

the binding of the second aptamer. So PDGF-BB and 20t-4 were chosen for the analysis of receptor β.

The concentration of the aptamer and PDGF-BB is critical to the analysis of receptor β. Too high a concentration produces an overly large PDGF-BB aptamer complex peak, and measuring the small change in peak area produced by the low concentration of receptor β is difficult, damaging the sensitivity of the assay. However, too low a concentration would narrow the dynamic range of the analysis. The optimized concentrations of the aptamer and PDGF-BB were 10 nM and 5 nM, respectively. A detection limit of 3 nM was obtained for analysis of receptor β under the optimized conditions. A linear calibration curve was obtained for the determination of receptor with an r^2 value of 0.986 as shown in **Figure 3.15**. A linear dynamic range from 5 to 200 nM was determined.

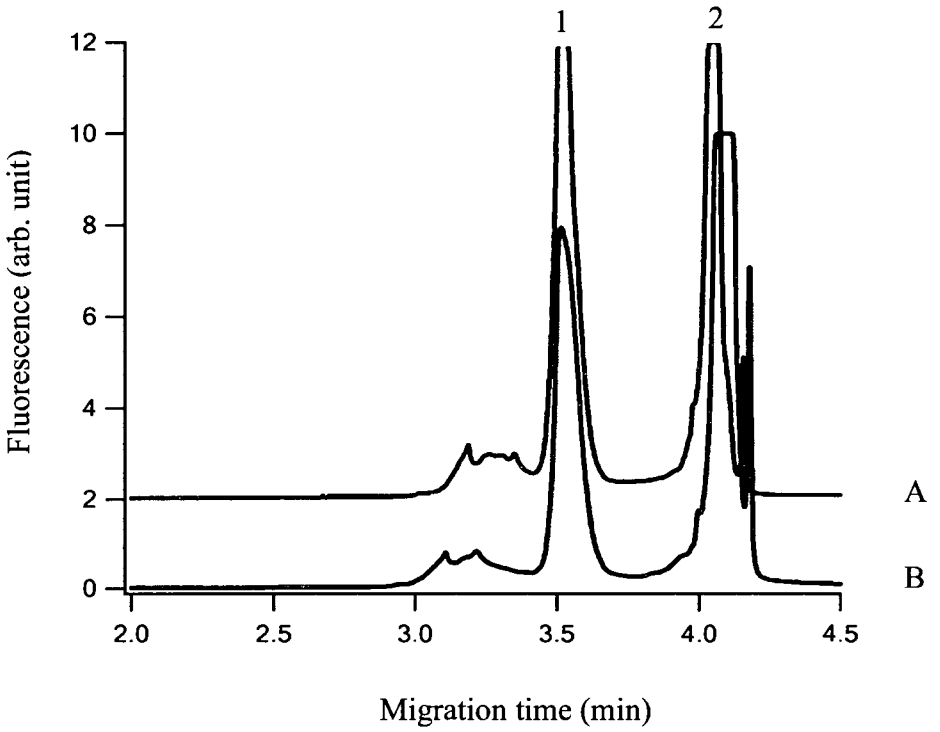

Figure 3.13. Electropherograms showing the analysis of PDGF receptor β using PDGF-BB and aptamer 20t-4 or 36t-4 in a noncompetitive format. Sample A contained 25 nM receptor β, 100 nM PDGF-BB, and 500 nM 20t-4; Sample B contained 25 nM receptor β, 100 nM PDGF-BB, and 500 nM 36t-4. Peak 1 is the complex of PDGF-BB and the aptamer; peak 2 is due to the unbound fluorescent aptamer.

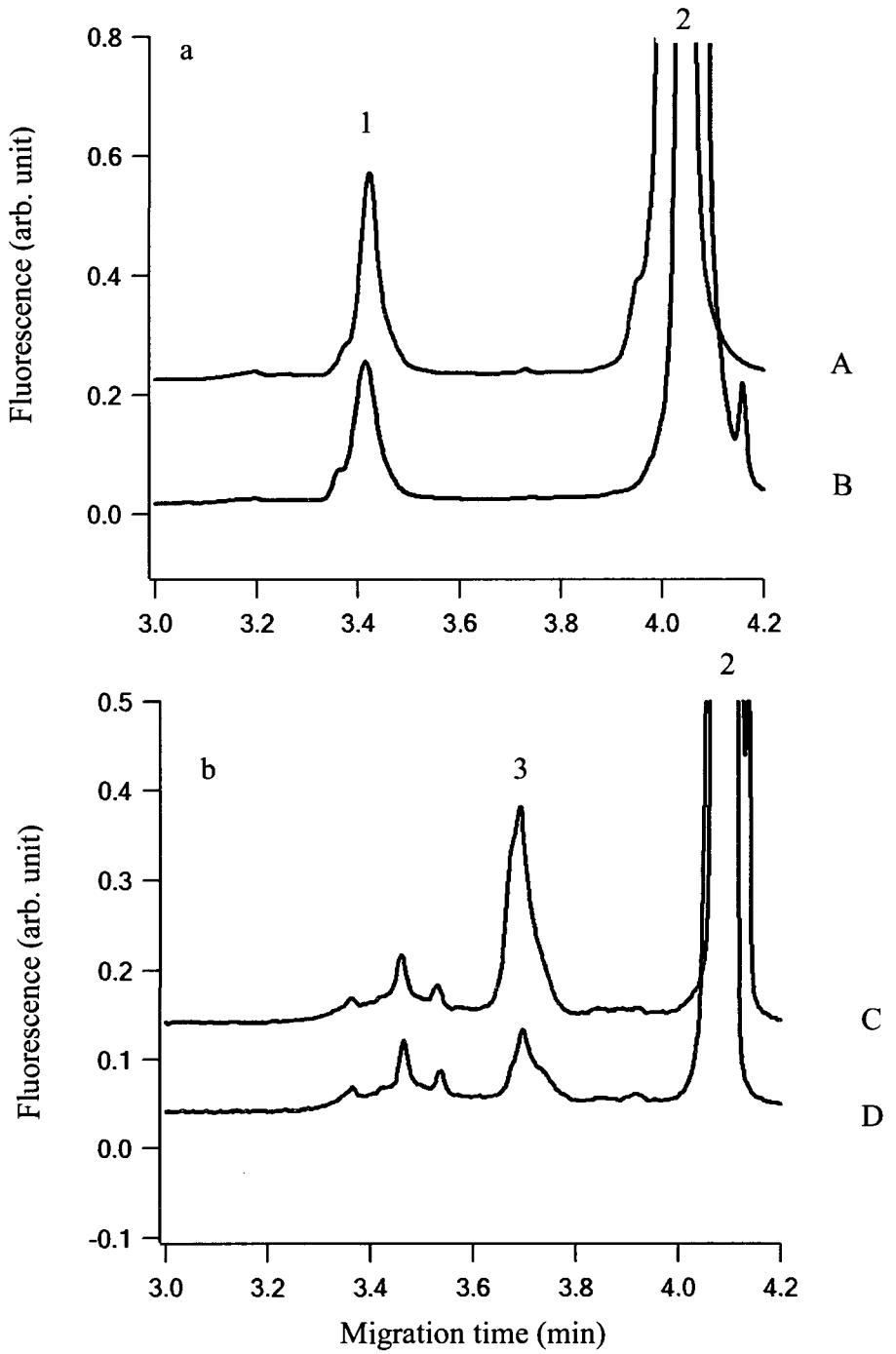

Figure 3.14. Electropherograms showing analysis of PDGF receptor β by using PDGF AB and 20t-4 (a) or using PDGF BB and 20t-4 (b). Sample A contained 5 nM PDGF-AB and 10 nM 20t-4; sample B contained 100 nM receptor β, 5 nM PDGF-AB and 10 nM 20t-4; sample C contained 5 nM PDGF-BB and 10 nM 20t-4; sample D contained 100 nM receptor β, 5 nM PDGF-BB and 10 nM 20t-4. Peak 1 is the complex of PDGF-AB and aptamer; peak 2 is due to the unbound fluorescent aptamer; peak 3 is the complex of PDGF-BB and aptamer

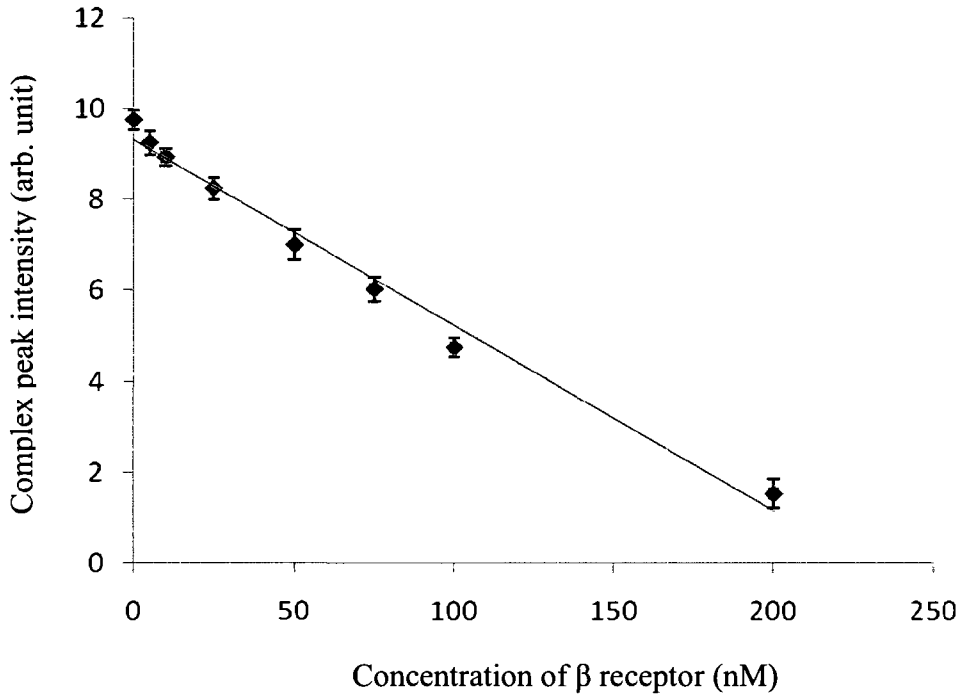

Figure 3.15. Calibration curve constructed by using samples containing 5nM PDGF-BB and 10nM 20t-4 with various concentrations of receptor β

3.4 Conclusions

The differentiation and detection of PDGF-AB and PDGF-BB isomers have been achieved by the tunable aptamer CE. Using an aptamer that binds to the B chain but not the A chain of PDGF, the electrophoretic mobilities of the PDGF isomers were tweaked for their separation. PDGF-AB bound to a single aptamer was resolved well from PDGF-BB bound to two aptamer molecules. Simultaneous determination of pM levels of two isomers was accomplished in a single analysis. To our knowledge, this is the first demonstration of separation and

determination of these PDGF isomers in a mixture by using an aptamer as a probe.

PDGF-AB has been employed as a connector to bring the receptor α and the fluorescent aptamer into a single complex molecule. The formation of a (receptor α)-(PDGF-AB)-(aptamer) complex represents the incorporation of the fluorescent aptamer as probe, enabling detection of the receptor α in a noncompetitive affinity assay. The method was able to detect as low as 0.5 nM of receptor α. Furthermore, by conducting a competitive assay, the determination of receptor β was demonstrated based on competition between the receptor β and a fluorescent aptamer in binding to the PDGF B chain. The detection limit of 5 nM was obtained for determination of receptor β.

Two aptamers, 20t-4 and 36t-4, showed different performances in analysis of PDGF isomers and their receptors. The differences in both the formation of the PDGF-AB aptamer complex and the formation of (receptor α)-(PDGF-AB)-(aptamer) complex indicate that 20t-4 and 36t-4 bind to different sites of the PDGF B chain. Aptamer 20t-4 has a stronger ability to inhibit the binding of receptor α to PDGF -AB. The methods developed in this study provide another potential approach to determine the impact of aptamers on the inhibition of the binding of PDGF isomers to their receptors.

The assay is not limited to the PDGF isomers shown here, and the principle can be extended to separation and detection of other protein isomers or a family of proteins to which aptamers can bind. The throughput of the assay can be further enhanced by using electrophoresis systems with multiple capillaries (22) or microfluidic devices with multiple channels.

3.5 References

(1) R. Ross, J. Glomset, B. Kariya and L. Harker, *Proc. Natl. Acad. Sci. U.S.A.*, 1974, 71, 1207-1210.

(2) N. Kohler and A. Lipton, *Exp. Cell Res.*, 1974, 87, 297-301.

(3) G. R. Grotendorst, H. E. Seppä, H. K. Kleinman and G. R. Martin, *Proc. Natl. Acad. Sci. U.S.A.*, 1981, 78, 3669-3672.

(4) C. H. Heldin, *EMBO J.*, 1992, 11, 4251-4259.

(5) Y. Yarden, J. A. Escobedo, W. –J. Kuang, T. L. Yang-Feng, T. O. Daniel, P. M. Tremble, E. Y. Chen, M. E. Ando, R. N. Harkins, U. Francke, V. A. Fried, A. Ullrich and L. T. Williams, *Nature,* 1986, 323, 226-232.

(6) T. Matsui, M. Heidaran, T. Miki, N. Popescu, W. La Rochelle, M. Kraus, J. Pierce and S. Aaronson, *Science*, 1989, 243, 800-804.

(7) L. Claesson-Welsh, A. Eriksson, B. Westermark and C. H. Heldin, *Proc. Natl. Acad. Sci. U S A.*, 1989, 86, 4917-4921.

(8) C.H. Heldin, G. Bäckström, A. Ostman, A. Hammacher, L. Rönnstrand, K. Rubin, M. Nistér and B. Westermark, *EMBO J.*, 1988, 7, 1387-1393.

(9) C. H. Heldin, A. Ernlund, C. Rorsman and L. Rönnstrand, *J. Biol. Chem.*, 1989, 264, 8905-8912.

(10) R. A. Seifert, C. E. Hart, P. E. Phillips, J. W. Forstrom. R. Ross, M. J. Murray and D. F. Bowen-Pope, *J. Biol. Chem.*, 1989, 264, 8771-8778.

(11) C. C. Huang, Y. F. Huang, Z. Cao, W. Tan and H. T. Chang, *Anal. Chem.*, 2005, 77, 5735-5741.

(12) C. Zhou, Y. Jiang, S. Hou, B. Ma, X. Fang and M. Li, *Anal. Bioanal. Chem.,* 2006, 384, 1175-1180.

(13) R. Y. Lai, K. W. Plaxco and A. J. Heeger, *Anal. Chem.,* 2007, 79, 229-233.

(14) L. Yang, C. W. Fung, E. J. Cho and A. D. Ellington, *Anal. Chem.* 2007, 79, 3320-3329.

(15) Y. Y. Li, C. Zhang, B. S. Li, L. F. Zhao, X. B. Li, W. J. Yang and S. Q. Xu, *Clin. Chem.,* 2007, 53, 1061-1066.

(16) L. S. Green, D. Jellinek, R. Jenison, A. Ostman, C. H. Heldin and N. Janjic, *Biochemistry,* 1996, 35, 14413-14424.

(17) Q. H. Wan and X. C. Le, *Anal. Chem.*, 2000, 72, 5583-5589.

(18) H. Wang, M. Lu, M. Weinfeld and X. C. Le, *Anal. Chem.*, 2003, 75, 247-254.

(19) H. Wang, M. Lu and X. C. Le, *Anal. Chem.*, 2005, 77, 4985-4990.

(20) H. Zhang, X.-F. Li, and X. C. Le, *J. Am. Chem. Soc.,* 2008, 130, 34-35.

(21) J. Floege, T. Ostendorf, U. Janssen, M. Burg, H. H. Radeke, C. Vargeese, S. C. Gill, L. S. Green and N. Janjić, *Am. J. Pathol.,* 1999, 154, 169-179.

(22) N. J. Dovichi and J. Z. Zhang, *Angew. Chem. Int. Ed.,* 2000, 39, 4463-4468.

Chapter Four*

Ultrasensitive Detection of Proteins by Amplification of Affinity Aptamers

4.1 Introduction

Determination of low-abundance proteins is essential for characterizing proteomes and studying their biochemical functions. To improve the sensitivity and specificity of protein detection, the proximity-dependent DNA-ligation assays (1-4), immuno-PCR, (5-7) and nanoparticle-based bio-barcode technique (7-13) have been developed, albeit each has its own advantages and drawbacks.

Although nucleic acids can be amplified by PCR to improve the sensitivity, there is no comparable technique to chemically amplify proteins. The primary objective of this chapter is to develop a novel technology that enables the detection of proteins with high sensitivity, by taking advantage of PCR technology for DNA amplification. The main approach is the integration of affinity aptamer recognition, CE separation, and PCR amplification. **Figure 4.1** shows the concept and process of the aptamer amplification assay. First, an aptamer is introduced to bind to a target protein, forming a protein-aptamer complex. The protein-aptamer complex is then separated from the unbound aptamer using CE. The fractions containing only the protein-aptamer complex are collected. The bound aptamer is then dissociated from the complex, and then amplified by PCR. The amplification of the aptamer to which the protein binds dramatically improves the sensitivity of

* A portion of this chapter has been published in H. Zhang, Z. Wang, X.-F. Li and X. C. Le, *Angew. Chem. Int. Ed.*, 2006, 45, 1576-1580.

the detection of proteins. Since this affinity aptamer PCR technique fulfills the ultrasensitive protein detection through PCR amplification of the aptamer bound to the protein, it is termed an affinity aptamer amplification assay. To demonstrate the proof of principle, HIV-RT was chosen as the initial target protein because of the importance of this protein in the life cycle of the HIV virus.

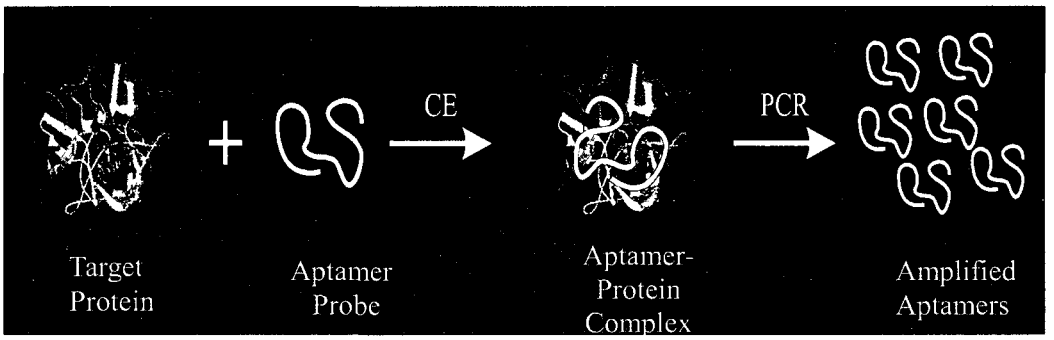

Figure 4.1. Concept and process of the affinity aptamer amplification assay

4.2 Experimental

4.2.1 Reagents

HIV-RT was obtained from Worthington Biochemical (Lakewood, NJ). RT26 (5'-ATCCGCCTGATTAGCGATACTTACGTGAGCGTGCTGTCCCCT AAAGGTGATACGTCACTTGAGCAAAATCACCTGCAGGGG-3'), both unlabeled and labeled with 5'-FAM, were synthesized at the University Core DNA Services, University of Calgary. Both the forward primer (5-CCGCCTGATTAGCGATACTT-3') and the reverse primer (5'-TGCAGGTGATTTTGCTCAAG-3') were obtained from Integrated DNA

Technologies (Corarville, IA). Platinum Pfx DNA polymerase and Platinum Taq DNA polymerase (both from Invitrogen, Burlington, ON) were tested initially, and Platinum Taq DNA polymerase was chosen for all the subsequent PCR experiments. Tris-borate-EDTA (TBE) buffer solution (89 mM Tris base, 89 mM boric acid, and 2 mM EDTA, pH 8.0) was prepared in autoclaved and deionized water by dissolving appropriate amounts of the reagent-grade materials. 1×TG buffer solution (25 mM Tris and 192 mm glycine, pH 8.3) was diluted with autoclaved, deionized water from10×TG buffer that was obtained from Bio-Rad Laboratories (Mississauga, ON).

As a negative control, a non-specific DNA oligonucleotide with sequence 5'-ATCCGCCTGATTAGCGATACTTGTAGACTGGAGACGAATGCGCATAC GAGTCGAACGCTTGAGCAAAATCACCTGCAGGGG-'3 was obtained from Integrated DNA Technologies (Corarville, IA). It has the same size and primer regions (underlined) as aptamer RT26, but the middle 35-nt sequence is random and is different from that of aptamer RT26.

4.2.2 Capillary electrophoresis with laser-induced fluorescence detection.

Figure 2.2 shows the schematic of CE-LIF system used in this work (14-16). Electrophoresis was carried out at room temperature with a voltage of 15 kV (electric field 375 V/cm) with TG buffer solution as the running buffer. Samples were injected electrokinetically for 3 s at 15 kV. Following each CE run, the capillary was washed sequentially with TG buffer solution (10 min), water (5 min), and 1×TG buffer solution (5 min). Aptamers and proteins of desired concentrations were mixed in TBE buffer solution (60 μL) in 200 μL

microcentrifuge vials. The vials were vortexed for 20 s and put on ice for 5 min prior to analysis by CE.

4.2.3 Fraction collection, PCR amplification and gel electrophoresis

Fractions from the outlet of the capillary were collected into separate 200 μL vials, each containing 1×TG buffer (15 μL). Fractions were collected for 30 s intervals of CE separation (initially 15 s collections were also used). Between fractions, the CE voltage was temporarily stopped to allow changes of new vials for collection of the subsequent fractions. From the initial CE-LIF analysis of an incubation solution that contained fluorescently labeled aptamer (10 nM) and HIV-1 RT (1 nM), the protein-aptamer complex (3-3.5 min) and the unbound aptamer (4-5 min) were detected by LIF. However, further decreased concentrations of the aptamer and protein could not be detected even by the most sensitive LIF technique. Therefore, the fractions had to be collected without LIF monitoring. Fraction collection intervals of 15 s and 30 s were initially compared. Although 15 s fractions provided a better resolution of separation, the 30 s fractions provided a more reproducible collection of sufficient amounts for the subsequent PCR. Thus, fractions at 30 s intervals were collected and analyzed.

A fraction collected from CE was mixed with 10×PCR buffer solution (5 μL; minus Mg), dNTP mixture (1 μL, 10 mM), $MgCl_2$ (1.5 μL, 50 mM), primer mix (1.5 μL, 10 μM), and 0.2 μL Platinum Taq DNA polymerase, in 50 μL autoclaved, distilled water. The mixture was initially heated to 94 °C for 3 min. The subsequent temperature cycling program included 94 °C for 30 s, 55 °C for 30 s, and 72 °C for 30 s, and finally 10 min extension at 72 °C. PCR programs of

25, 40, and 50 cycles were compared, and the PCR program with 50 cycles was chosen to maximize the products. At a lower number of cycles (25 cycles) no primer dimer was seen; at 50 cycles, however, the band was distinctly observed. A positive control (2 μL 10–13 M aptamer RT26) and a negative control (15 μL autoclaved, distilled water) were included with each set of PCR experiments.

The PCR products were separated by using gel electrophoresis on 8% polyacrylamide gels. The electric field was 8 V/cm and the running buffer solution was TBE. The gel was stained by submerging it in ethidium bromide (0.5 μg/mL) for 5–10 min. The bands were visualized on a Syngene (Cambridge, UK) UV illuminator and the intensity was integrated using Adobe Photoshop and Polaroid PhotoMaxPro. The DNA marker was a 10 bp DNA ladder consisting of 33 repeats of 10 bp plus a fragment at 1668 bp. The 100 bp band is approximately 2-3 times stronger than other ladder bands to provide internal orientation.

4.2.4 Sequencing of PCR amplified aptamer

The PCR products were sequenced at the Molecular Biology Facility in the Department of Biological Sciences, University of Alberta. A solution containing aptamer RT26 (0.1 nM) and HIV-1 RTase protein (150 fM) was separated by CE and the fraction at t=3-3.5 min, which contained the protein-aptamer complex, was collected and amplified using PCR as described above. This PCR product was purified by QIAGEN MinElute PCR Purification Kit (Mississauga, ON) and diluted to 200 μL with autoclaved deionized water, from which 5 μL was used for each of ten replicate PCR reactions. These ten PCR reactions were each carried out under the same conditions as described above, with the exception that 12

cycles were used. The PCR products were pooled, purified by a Qiagen MinElute PCR Purification Kit, and concentrated by ethanol precipitation. Sequencing from both the forward primer and the reverse primer directions was performed.

4.3 Results and Discussion

4.3.1 Amplification of aptamer for HIV-RT

To achieve the ultrasensitive protein detection in this study, the aptamer is required to play two roles: to recognize the target protein and serve as the template of subsequent PCR amplification. The former role requires the aptamer used to possess high binding affinity for the protein, whereas the latter requires that the aptamer be long enough to contain the primer regions for PCR amplification. A high-affinity DNA aptamer (RT 26, Kd = 1 nM) for HIV-RT had been previously chosen using the SELEX process. RT 26 is a relatively long aptamer containing 81 nt. A pair of primers 20 nt each was designed to allow the production of a 75-nt amplified aptamer. To determine minute amounts of HIV-RT, the PCR amplification is required to enable detection of very low numbers of the aptamer. To ensure that low number of aptamer molecules can be amplified by PCR and analyzed by gel electrophoresis, three PCR experiments with different amplification cycles were carried out to amplify the serially diluted aptamer solutions that contained 6000, 600, and 60 aptamer molecules (**Figure 4.2**). The amplification of 25 cycles was not sufficient to produce enough DNA from 60-6000 aptamer molecules to result in an observable band corresponding to the amplified aptamer. Although amplification of 40 cycles resulted in a clear band for each aptamer solution, the stronger bands were obtained under amplification

of 50 cycles. Therefore, amplification of 50 cycles was used in PCR experiments for protein detection. The detection limit of the aptamer was further determined by amplification of a series of serially diluted aptamer solution that contained 6000, 600, 60, and 6 aptamer molecules (**Figure 4.3**). Through PCR, six aptamer molecules were amplified and detected, whereas in the duplicate blanks, no aptamer was detected.

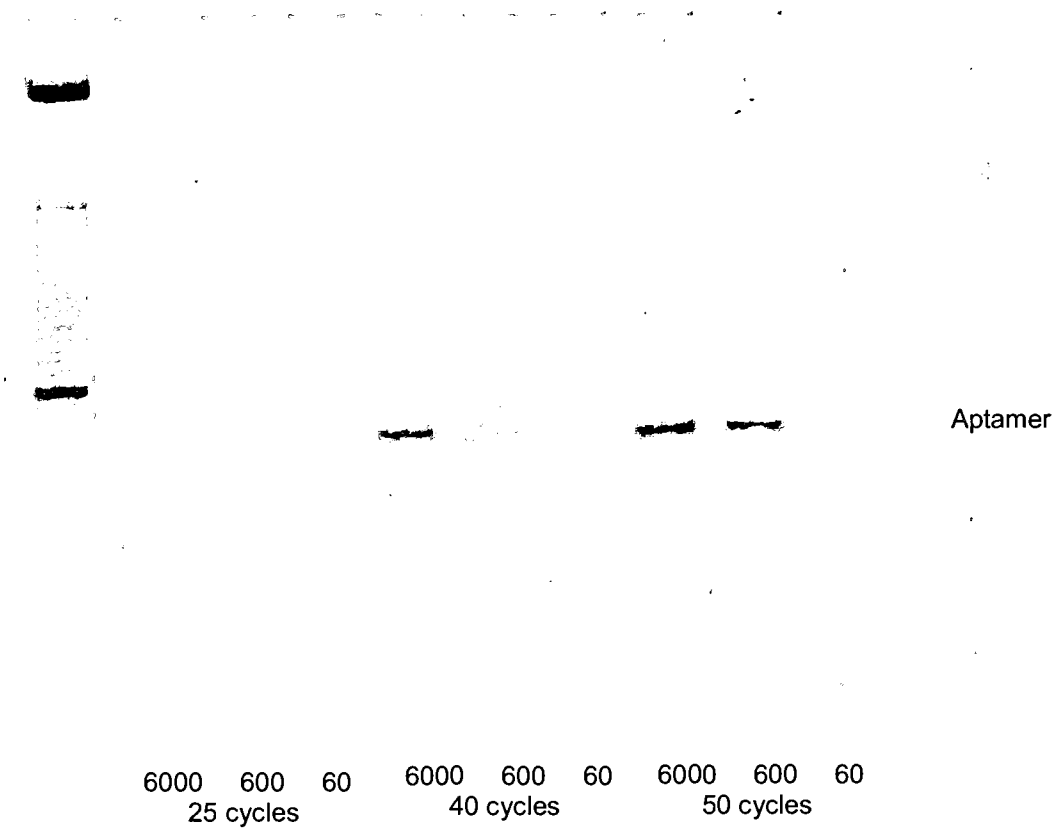

Figure 4.2. PCR with different amplification cycles and gel electrophoresis showing amplification of serially diluted aptamer solutions, containing 6000, 600, and 60 aptamer molecules

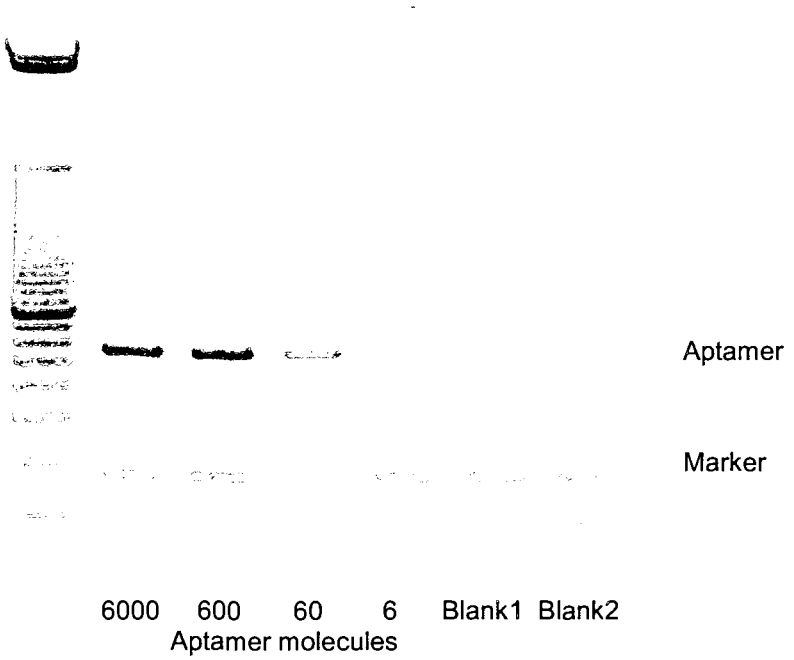

Figure 4.3. PCR and gel electrophoresis showing amplification of serially diluted aptamer solutions, containing 6000, 600, 60, and 6 aptamer molecules. Duplicate blanks were carried out in parallel.

4.3.2 Separation of the protein-aptamer complex from the unbound aptamer

In addition to the extreme sensitivity of the PCR technique for detection of aptamers, the powerful separation ability of CE is another critical factor that contributes to the accomplishment of the detection of trace amounts by the affinity aptamer amplification assay. If the protein-aptamer complex could be completely separated from the unbound aptamer by using CE, it would be possible to collect the fractions containing only the protein-aptamer complex. Thus, background signal from unbound aptamer could be avoided, thereby enabling ultrasensitive protein detection. The separation of the protein-aptamer complex from the unbound aptamer was initially studied by analysis of a sample solution containing HIV-RT and fluorescently labeled RT-26 at a concentration that could be detected by CE-LIF. **Figure 4.4** shows the electropherograms of the analysis. In an open capillary and under free-zone electrophoresis conditions, the electrophoretic mobility of the analyte was proportional to its charge-to-mass ratio. At the running buffer pH of 8.3, the aptamers are highly negatively charged due to the phosphate group in the nucleotides, while the charge on the HIV-RT was nearly neutral because the pI of HIV-RT is at approximately pH 8 (17). When HIV-RT bound with the negatively charged DNA aptamers at pH 8–9, the complex formed was larger and its charge-to-mass ratio was lower than that of the unbound aptamer. This resulted in the protein-aptamer complex migrating first leaving the excess unbound aptamer behind. From the CE-LIF analysis of two incubation solutions, one containing 10 nM aptamer and 1 nM HIV-RT, and the other containing 120

nM aptamer and 30 nM HIV-RT, the first peaks at 3-3.5 min are due to the migration of the protein-aptamer complexes, and the peaks at 4-5 min represented the migration of the unbound aptamer. Therefore, the protein-aptamer complex (3-3.5 min) and the unbound aptamer (4-5 min) were well separated and detected by CE-LIF. To ensure that the protein-bound and free aptamers are collected separately for subsequent analysis, collection intervals of fractions were determined at 0-2, 2-2.5, 2.5-3, 3-3.5, 3.5-4, and 4-5 min.

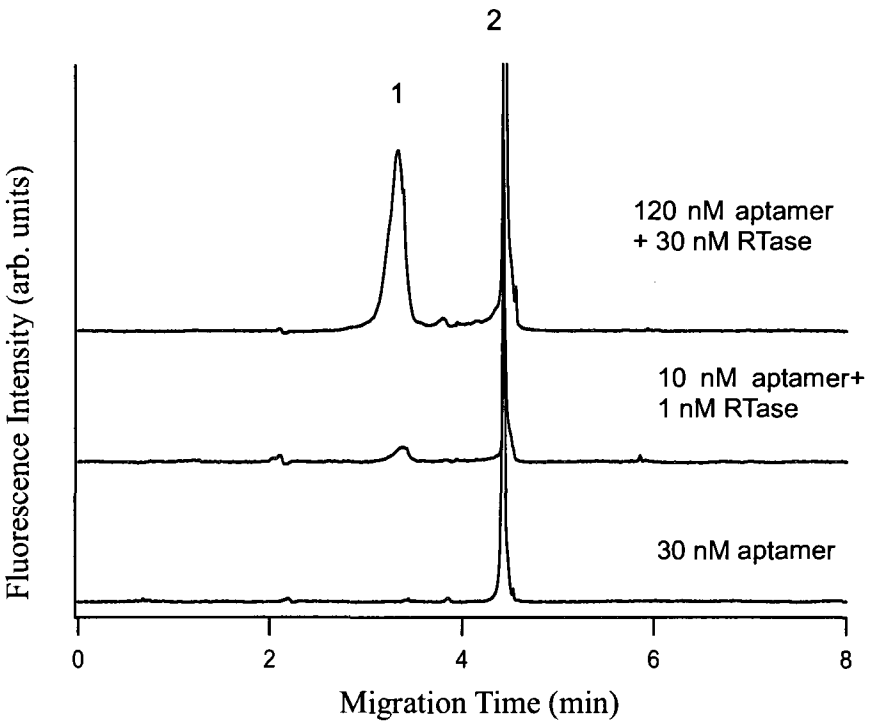

Figure 4.4. Electropherograms showing separation of the protein-aptamer complex from the unbound aptamer. Peak 1 corresponds to protein-aptamer complex and peak 2 corresponds to the unbound fluorescent aptamer.

4.3.3 Detection of HIV- RT by affinity aptamer amplification assay

To analyze trace levels of HIV-RT protein in a sample, the sample was incubated with aptamer RT 26 (0.1 nM), and an aliquot (10 nL) of the incubation solution was subjected to CE separation. Fractions at 0-2, 2-2.5, 2.5-3, 3-3.5, 3.5-4, and 4-5 min were collected. Each fraction was subjected to PCR amplification and gel electrophoresis analysis. **Figure 4.5** shows the gel electrophoresis of the PCR products of the collected CE fractions from the analysis of HIV-RT (**Figure 4.5a**) and control (**Figure 4.5b**). The fractions collected before 3 min did not contain any aptamer or protein-aptamer complex. In the fraction at t=3-3.5 min, a strong band corresponding to the amplified aptamer is present in the sample but not in the control. This represented the protein-aptamer complex only. The fraction at t=3.5-4 min contained a mixture of the protein-aptamer complex and the unbound aptamer. The fraction at t=4-5 min contained the excess amount of the unbound aptamer (0.1 nM). As expected, the unbound aptamer was present in both the sample and the control. Both the negative (-ve) and positive (+ve) controls of the aptamer showed the expected results. The band at 40 base pairs (bp; primer dimer) served as a marker along with the DNA-ladder marker (the far left lane, 10 bp DNA ladder with 100 bp band 2-3 times darker than other bands). The CE migration behavior of the protein-aptamer complex and the unbound aptamer, as shown from the collected fractions, was consistent with that observed previously with CE separation and LIF detection of the fluorescently labeled aptamer and its complexes.

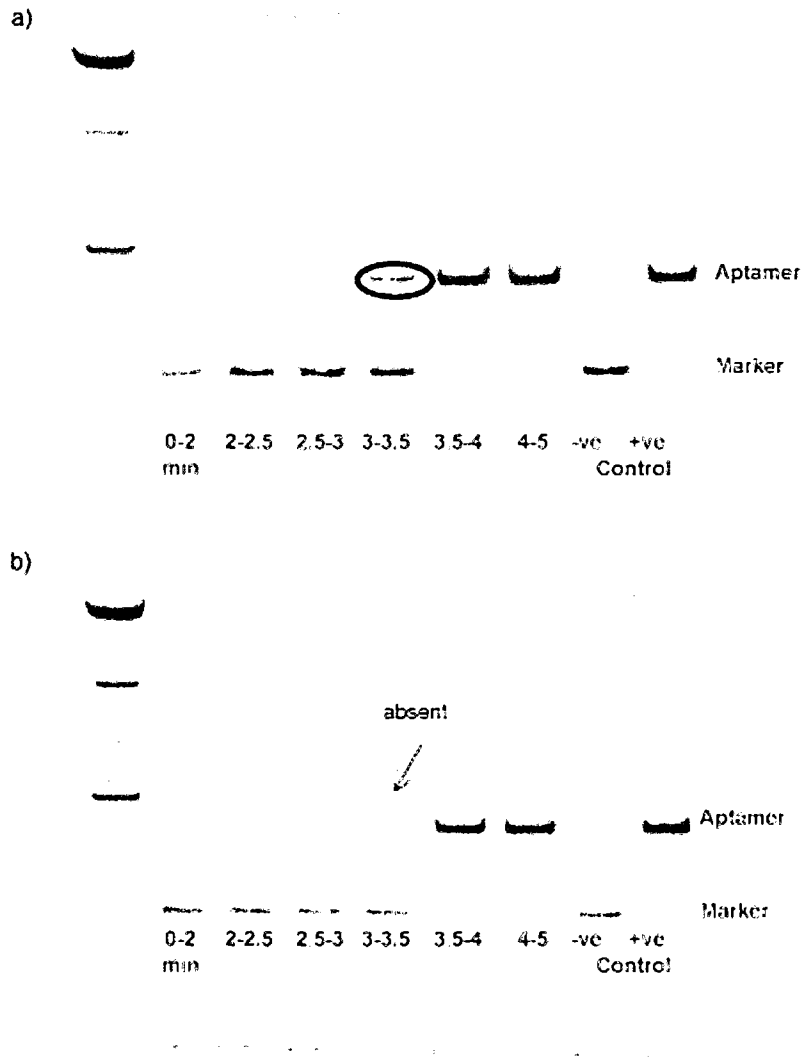

Figure 4.5. Gel electrophoresis of the PCR products of the collected CE fractions from the analysis of HIV-RT (a) and control (b). The sample solution contained 0.1 nM RT 26 and 150 fM HIV-RT; blank solution contained 0.1 nM RT 26.

To achieve reproducible detection of trace levels of proteins, each component of the experiments has been optimized, including the aptamer affinity complex formation (aptamer concentrations and incubation conditions), CE separation and fraction collection, and PCR amplification. Varying concentrations of aptamer RT26 (10^{-3}, 10^{-2}, 0.1, and 0.5 nM) were initially tested and the concentration of 0.1 nM was chosen because it was sufficient to bind with low levels of protein and its unbound fraction was readily separated from its protein complex by CE. The optimum incubation conditions are incubation of the aptamer (0.1 nM) with the sample in TBE (60 μL) buffer solution on ice for 5 min. An aliquot of approximately 10 nL was injected into CE for analysis. Reproducibility was assessed through repeated analysis of HIV-RT (150 fM) in five consecutive experiments. Under the optimum conditions, consistent results were obtained from the five replicate analyses of HIV-1 RT (150 fM).

4.3.4 Detection limit and calibration

Detection limit of the affinity aptamer amplification assay for HIV-RT was determined by analyzing the sample containing the lowest amount of HIV-RT that was able to yield a visible band corresponding to the protein-aptamer complex. **Figure 4.6** shows the representative PCR products from the CE analysis of an approximate 10 nL (10^{-8} L) aliquot, which contained HIV-RT (3×10^{-14} M) and aptamer RT26 (10^{-10} M). A band from the aptamer bound to the HIV-RT is also clearly visible here, but is absent in the control. The products resulted from approximately 3×10^{-22} mole (or 180 molecules) of HIV-RT protein. Among these 180 molecules, 16 of them were bound with the aptamer RT26. The ability to

detect as few as 180 protein molecules represents a major technological advance that will be particularly useful for proteomics research and medical diagnostics.

In the equilibrium-mixture solution that contained HIV-RT (3×10^{-14} M) and aptamer RT26 (10^{-10} M), the concentration of the aptamer complex of HIV-RT was approximately 3×10^{-15} M (based on a Kd value of 1 nM). With an injection volume of 10^{-8} L, approximately 18 molecules (3×10^{-23} mole) of the protein-aptamer complex were injected into the electrophoretic capillary. Taking into account the possible loss of the protein-aptamer complex owing to dissociation and adsorption, the number of the protein-aptamer complex molecules collected could be fewer than 18.

Although quantitation of HIV-RT by the affinity aptamer amplification assay is limited because of the general PCR technique used that is unable to provide accurate quantitation information for aptamer detection, the calibration curve for HIV-RT was constructed by analysis of a series of solutions containing 0.1 nM RT26 and various concentrations of HIV-RT (**Figure 4.7**). When the concentration of the aptamer (10^{-10} M) was not in large excess over that of the protein ($1.5\text{x}10^{-11}$ M), two complexes corresponding to 1:1 (2.5-3 min) and 1:2 (3-3.5 min) stoichiometries were observed (**Figure 4.7 b**). When the aptamer was in large excess over the protein (**Figure 4.7c, d and e**), which is the case for the detection of ultratrace proteins, a single complex was detected, corresponding to the binding of a protein to two aptamer molecules (1:2). The calibration curve was plotted by using intensity of complex bands as the function of concentration of HIV-RT. A calibration curve (r^2=0.98) was obtained with trace levels of HIV- RT

(0, 3×10^{-14}, 1.5×10^{-13}, 1.5×10^{-12}, and 1.5×10^{-11} M).

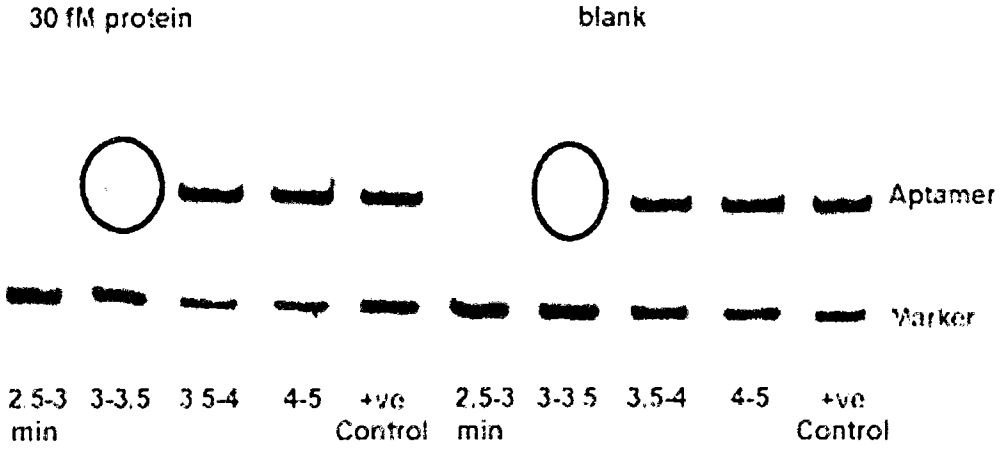

Figure 4.6. PCR and gel electrophoresis of fractions collected from the CE analysis of an approximately 10 nL mixture that contained aptamer (0.1 nM) and either protein (30 fM; 3×10^{-14} M) or blank

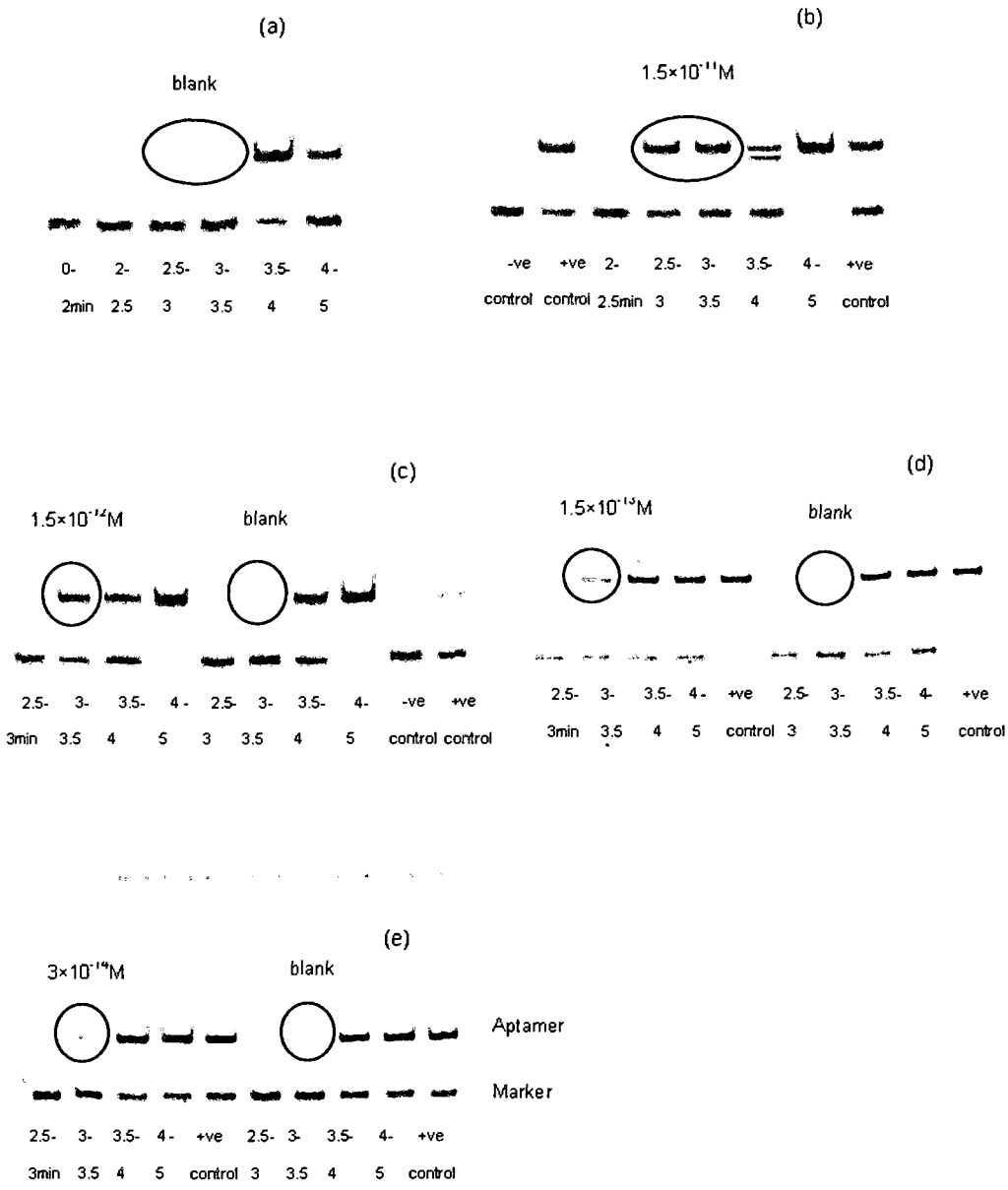

Figure 4.7. PCR and gel electrophoresis of fractions collected from CE analysis of mixtures containing 0.1 nM aptamer and varying concentrations of HIV-RT protein ($1.5x10^{-11}$, $1.5x10^{-12}$, $1.5x10^{-13}$, and $3x10^{-14}$ M) or blank

4.3.5 Specificity of the assay for detection of HIV-RT

To determine the specificity of the method, parallel experiments were conducted with human IgG and RNase H reverse transcriptase in place of HIV-RT (**Figure 4.8 and Figure 4.9**). No extra band corresponding to the protein-aptamer complex was observed in the sample compared to the results of the blank. The results showed that these proteins did not bind to the specific aptamer for HIV-RT or interfere with the detection of the target HIV-RT.

To determine that the detected PCR product was the expected aptamer, the PCR product was sequenced that was amplified from the collected protein-aptamer complex. Duplicate sequencing from both the forward and reverse primer directions confirmed that the sequence of the middle 35 nucleotides of the PCR product (excluding the two primer sequences) was identical to that of the aptamer.

To further demonstrate the specificity of the assay, a control experiment was performed using a DNA molecule that was the same size as the aptamer. The DNA molecule had the same primer binding sites for PCR but had a scrambled sequence in the middle. This non-specific oligonucleotide (0.1 nM) was incubated with HIV-RT protein (1.5×10^{-12} M) and the mixture was subjected to CE separation. Analysis of the PCR products from the collected CE fractions showed the absence of a protein-DNA complex (**Figure 4.10**). This is compared with the strong signals observed when the specific aptamer was used under the same conditions (**Figure 4.5a**). These results further support the validity of the affinity aptamer for the analysis of specific proteins.

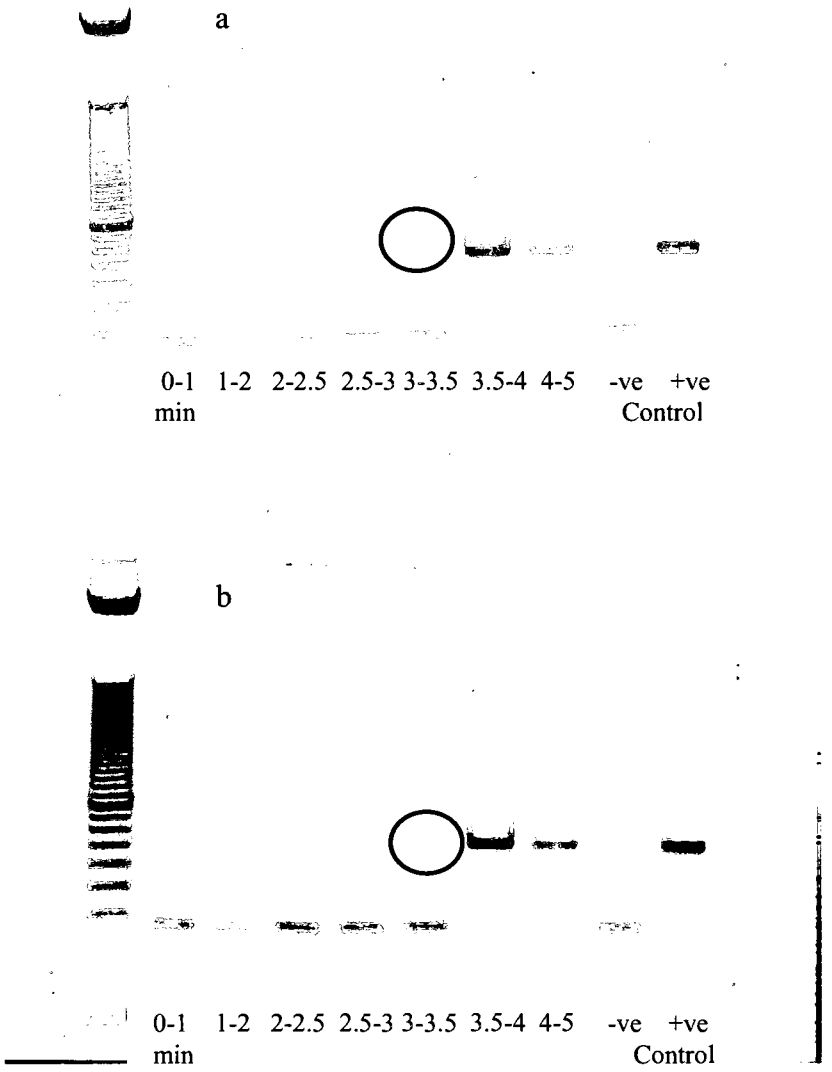

Figure 4.8. Control experiments show the absence of the protein-aptamer complex when human IgG was substituted for HIV-RT. (a) PCR and gel electrophoresis analysis of fractions collected from the CE analysis of a mixture that contained RT 26 (0.1 nM) and human IgG (10 nM), and (b) parallel control that did not contain human IgG.

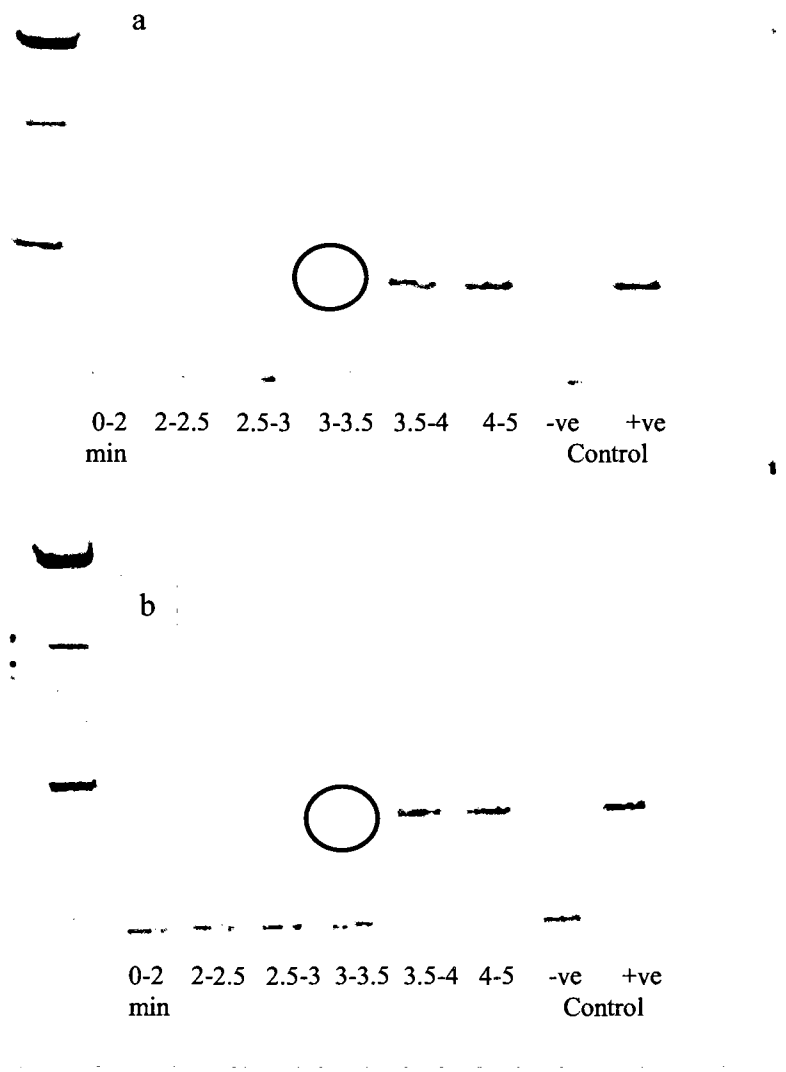

Figure 4.9. Control experiments show the absence of the protein-aptamer complex when RNase H reverse transcriptase was substituted for HIV-RT. (a) PCR and gel electrophoresis analysis of fractions collected from the CE analysis of a mixture that contained RT 26 (0.1 nM) and RNase H reverse transcriptase (10 nM), and (b) parallel control that did not contain RNase H reverse transcriptase.

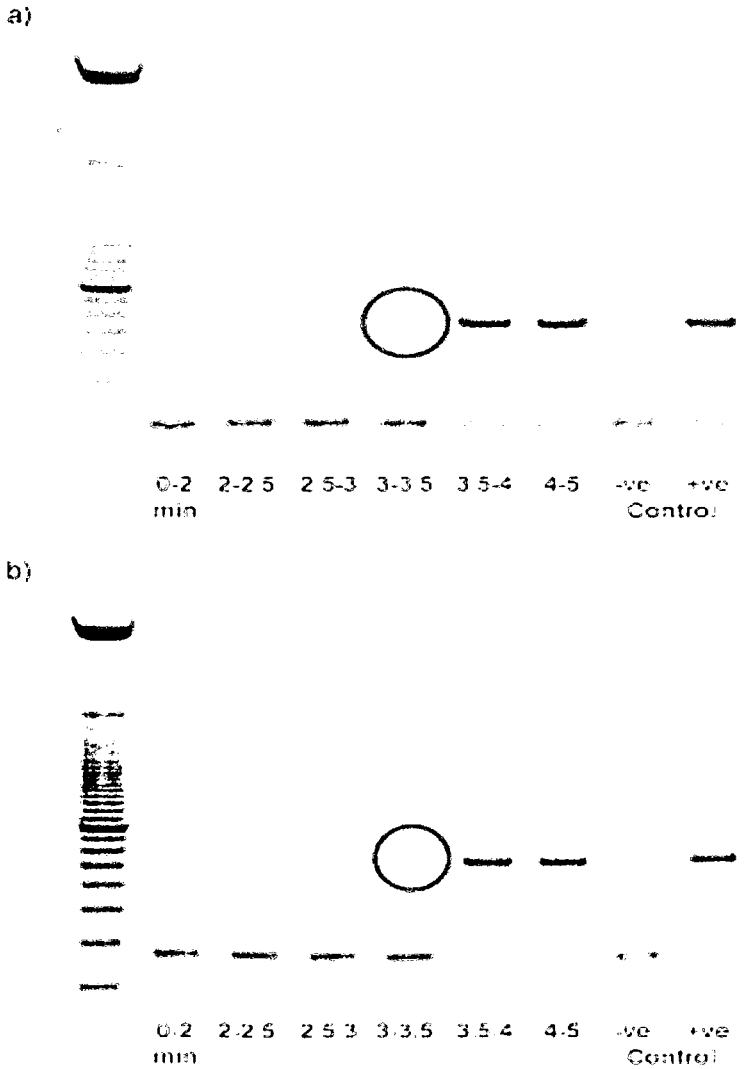

Figure 4.10. Control experiments show the absence of the protein-aptamer complex when a non-specific DNA oligonucelotide was substituted for the specific aptamer. (a) PCR and gel electrophoresis analysis of fractions collected from the CE analysis of a mixture that contained non-specific DNA oligonucelotides (0.1 nM) and HIV-RT protein (1.5 pM), and (b) parallel control that did not contain the HIV-RT protein.

4.4 Conclusions

An affinity aptamer amplification assay was developed. Through PCR amplification of the aptamer dissociated from the protein-aptamer complex, the assay enables ultrasensitive detection of the protein. As few as 180 HIV-RT molecules were detected by this assay. This sensitivity represents an improvement of several orders of magnitude greater than that of other available methods of protein detection.

The previously reported immuno-PCR assay and nanoparticle-based barcode technique require the use of specific antibodies for the targeting of proteins and thus are limited by the availability and specificity of the antibodies. The proximity-dependent DNA-ligation assay requires the ligation of two proximal probes that bind to a target protein in order to give rise to an amplifiable DNA sequence; thus it is useful mainly for the detection of targets that have two proximal binding probes. The affinity aptamer amplification assay described herein requires only a single aptamer for each target molecule of interest, and the CE separation provides additional specificity. It is possible to scale this assay through the separation of multiple protein-aptamer complexes in a single capillary. The affinity aptamer amplification assay can also be multiplexed by using CE systems with multiple capillaries, such as those used for genome sequencing (18), to further improve the throughput of multiple-target analysis.

Potential applications of the affinity aptamer amplification assay include detection of low-abundance proteins for proteomics research and medical diagnostics, studies of molecular interactions, and biosensing. Aptamers for a

wide variety of molecular targets can be selected from a random nucleic acid library of 10^{13-15} different sequences (19-21). Therefore, the principle of the aptamer-affinity PCR technique is not limited to the detection of proteins, and it can be applied to the analysis of any other molecular targets that can bind to aptamers.

4.5 References

1. S. Fredriksson, M. Gullberg, J. Jarvius, C. Olsson, K. Pietras, S. M. Gustafsdottir, A. Ostman and U. Landergren, *Nat. Biotechnol.,* 2002, 20, 473-477.

2. M. Gullberg, S. M. Gustafsdottir, E. Schallmeiner, J. Jarvius, M. Bjarnegard, C. Betsholtz, U. Landegren and S. Fredriksson, *Proc. Natl. Acad. Sci. U. S. A.,* 2004, 101, 8420-8424.

3. E. Schallmeiner, E. Oksanen, O. Ericsson, L. Spångberg, S. Eriksson, U. Stenman, K. Pettersson and U. Landegren, *Nat. Methods,* 2007, 4, 135-137.

4. S. Fredriksson, W. Dixon, H. Ji, A. C. Koong, M. Mindrinos and R. W. Davis, *Nat. Methods,* 2007, 4, 327-329.

5. T. Sano, C. L. Smith and C. R. Cantor, *Science,* 1992, 258, 120-122.

6. C. M. Niemeyer, M. Adler and R. Wacker, *Trends Biotechnol.,* 2005, 23, 208-216.

7. M. Adler, R. Wacker and C. M. Niemeyer, *Analyst*, 2008 133, 702-718.

8. J. M. Nam, C. S. Thaxton and C. A. Mirkin, *Science*, 2003, 301, 1884-1886.

9. D. G. Georganopoulou, L. Chang, J.-M. Nam, C. S. Thaxton, E. J. Mufson, W. L. Klein and C. A. Mirkin, *Proc. Natl. Acad. Sci. U. S. A.,* 2005, 102, 2273-2276.

10. J. M. Nam, A. R. Wise and J. T. Groves, *Anal. Chem.,* 2005, 77, 6985-6988.

11. B. K. Oh, J. M. Nam, S. W. Lee and C. A. Mirkin, *Small,* 2006, 2, 103-108.

12. Y. P. Bao, T. F. Wei, P. A. Lefebvre, H. An, L. He, G. T. Kunkel and U. R. Muller, *Anal. Chem.,* 2006, 78, 2055–2059.

13. K. A. Shaikh, K. S. Ryu, E. D. Goluch, J.-M. Nam, J. Liu, C. S. Thaxton, T. N. Chiesl, A. E. Barron, Y. Lu, C. A. Mirkin and C. Liu, *Proc. Natl. Acad. Sci. U. S. A.,* 2005, 102, 9745–9750.

14. Q. H. Wan and X. C. Le, *Anal. Chem.,* 2000, 72, 5583-5589.

15. V. Pavski and X.C. Le, *Anal. Chem.,* 2001, 73, 6070-6076.

16. H. Wang, M. Lu and X. C. Le, *Anal. Chem.,* 2005, 77, 4985-4990.

17. R. Bhikhabhai, T. Joelson, T. Unge, B. Strandberg, T. Carlsson and S. Lövgren, *J. Chromatogr.,* 1992, 604, 157–170.

18. N. J. Dovichi and J. Z. Zhang, *Angew. Chem. Int. Ed.,* 2000, 39, 4463-4468.

19. S. E. Osborn and A. D. Ellington, *Chem. Rev.,* 1997, 97, 349-370.

20. S. D. Jayasena, *Clin. Chem.,* 1999, 45, 1628-1650.

21. C. L. A. Hamula, J. W. Guthrie, H. Zhang, X.-F. Li, and X. C. Le, *Trends Anal. Chem.,* 2006, 25, 681-691.

Chapter Five

Multiple Protein Detection by the Affinity Aptamer Amplification Assay

5.1 Introduction

Having established the affinity aptamer amplification assay for detection of HIV-RT (1), it was proposed to further develop this technique as a generalized approach for multiple protein detection. Separation using a typical free zone CE is based on differences in the charge-to-mass ratio of the analytes (2). Because charge-to-mass ratios of aptamers are approximately constant, various aptamers migrate through the capillary at a similar mobility. The binding of protein to aptamer alters the charge-to-mass ratio of the aptamer, resulting in different mobilities of the protein-aptamer complexes from unbound aptamers. Since aptamers are highly negatively charged, the protein-aptamer complexes generally migrate faster than unbound aptamers through the capillary. It is possible to determine a boundary between protein-aptamer complexes and the unbound aptamers. The fractions before the boundary are collected, which contain only protein-aptamer complexes, but not unbound aptamers. Then the bound aptamers in the complexes are released from proteins and subjected to PCR amplification. The detection of amplified aptamers represents the detection of the corresponding protein targets. Different pairs of primers can be designed to amplify the specific aptamers for each of the proteins. Therefore, the multiple protein targets can be detected simultaneously. In this study, IgE, HIV-RT, and thrombin were chosen

as initial targets to demonstrate the proof of principle. Real-time PCR was used to achieve quantitation of the protein-bound aptamers.

5.2 Experimental

5.2.1 Reagents

Human IgE, HIV-RT, and thrombin were obtained from Athens Research & Technology (Athens, GA), Worthington Biochemical (Lakewood, NJ), and Haematologic Technologies (Essex Junction, VT), respectively. Aptamers for human IgE, HIV-RT, and thrombin were synthesized, and purified by Integrated DNA Technologies (Corarlville, IA). The 6'-FAM label was directly attached to the 5' end of aptamers, and fluorescently labeled aptamers were purified by reversed-phase HPLC. **Table 5.1** lists the sequences of aptamers and their corresponding primers. The 10×TG was obtained from Bio-Rad Laboratories (Mississauga, ON). The 1× TG buffer (25 mM Tris and 192 mM glycine, pH 8.3) was diluted with deionized water from 10×TG. All other reagents were commercially available analytical grade.

Table 5. 1. Sequences of aptamers and their corresponding primers

Proteins	Corresponding aptamers (5'— 3')	Primers (5'— 3')
IgE	AGGGGCACGTTTATCCGTCCCTCC TAGTGGCGTGCCCCTGTCTGACTG TCTCG	CGTTTATCCGTCCCTC CGAGACAGTCAGAC AG
HIV-RT	ATCCGCCTGATTAGCGATACTTAC GTGAGCGTGCTGTCCCCTAAAGG TGATACGTCACTTGAGCAAAATCA CCTGCAGGGG	CCGCCTGATTAGCGA TACTT TGCAGGTGATTTTGC TCAAG
Thrombin	CAGTCCGTGGTAGGGCAGGTTGG GGTGACTTCGTGGAA	GTGGTAGGGCAGGTT CCACGAAGTCACCC

5.2.2 Capillary electrophoresis with laser-induced fluorescence detection

A laboratory-built CE-LIF system was used in this work (3-5). The schematic of the CE-LIF system was shown in chapter 2, **Figure 2.2**. Uncoated fused-silica capillaries (50 μm inner diameter, 150 μm outer diameter, 50 cm in length; Polymicro Technologies, Phoenix, AZ) were used for CE separation. Electrophoresis was carried out at room temperature with a voltage of 15 kV (300 V/cm) using 1×TG buffer solution as the running buffer. Samples were electrokinetically injected into the capillary at a voltage of 15 kV for 5 s. Following each CE run, the capillary was washed sequentially with 1×TG buffer solution (10 min), water (5 min) and 1×TG buffer solution (10 min). All CE data were analyzed using Igor Pro software (version 4.04, WaveMetrics, Lake Oswego, OR).

5.2.3 Formation of complexes

In order to place aptamers in their desired conformation, the 1 μM aptamer stock solution in 10 mM Tris·HCl (7.4) + 1 mM $MgCl_2$ was treated first by heating to 80 °C for 5 min followed by cooling slowly to room temperature. The sample incubation buffer was 10 mM Tris·HCl (7.4) containing 1 mM $MgCl_2$ and 0.05% BSA. To form complexes, the appropriate volumes of protein stock solutions were mixed with 5 μL aptamer solution containing 5 nM of each aptamer and 50 nM of fluorescein. Incubation buffer was then used to make the final incubation solution 50 μL. Fluorescein was added to the mixture and was used as an indicator to determine fraction collection intervals. Before injection, sample solutions were incubated at room temperature for 20 min.

5.2.4 Fraction collection

Fractions from the outlet of the capillary were collected into separate 200 μL microcentrifuge vials, each containing 10 μL 1×TG buffer. Between fractions, the CE voltage was temporarily stopped to allow changes of new vials for collection of the subsequent fractions. The fraction collection intervals were determined based on the electropherogram from the initial analysis of an incubation solution by CE-LIF. This incubation solution contained 20 nM of each protein and 100 nM of their corresponding aptamers. Fluorescein (10 nM) was used to indicate the boundary between complexes and unbound aptamers. To help establish the time interval for the fraction collection, on-column fluorescence detection by LIF was first used to monitor the migration of protein-aptamer complexes, fluorescein, and unbound aptamers with a detection window at 43 cm

of capillary from inlet. Under the free zone CE conditions used in this study, fluorescein migrated between the protein-aptamer complexes and the unbound aptamers. Therefore, fluorescein was added to the sample and it was monitored by LIF to guide the fraction collection for the analysis of trace amount of proteins. Even though the concentration of the protein-aptamer complex was too low to be detectable by LIF, monitoring of fluorecein by LIF provided a reference to ensure that only the fraction before the appearance of fluorescein was collected accounting for the protein-aptamer complexes.

5.2.5 Real-time PCR amplification

An aliquot (2 μL) of each fraction was then transferred into three real-time PCR reaction tubes (Applied Biosystems, Foster City, CA). After the addition of the reagents for amplification, the final 20 μL reaction solution contained 0.25 μM of each primer (forward and reverse) corresponding to their amplified aptamers, ROX reference dye, and 10 μL SYBR Green^{ER} qPCR Supermix Universal (Invitrogen, Burlington, ON). The reactions were then transferred into a real-time PCR instrument (ABI 7500 Fast Real-Time PCR System). The PCR program consisted of 50 °C for 2 min, 95 °C for 10 min followed by 50 cycles of 95 °C for 15 s, 53 °C for 30 s, and 60 °C for 30 s.

5.2.6 Preparation of cell lysate

1.5 mL of medium containing approximately 2×10^6 Vero 76 monkey kidney cells was spun at 10,000 g for 3 min. After being washed three times with cold 1× PBS, the pellet was resuspended in 250 μL ice-cold lysis buffer containing 50 mM Tris pH 7.4, 150 mM NaCl, 1% Triton X-100, 1% NP-40,

0.1% SDS, and 0.5 mM PMSF. The lysate was spun at 15,000g for 10 min at 4 °C. The supernatant was carefully transferred into another tube and diluted 10-fold with incubation buffer. When not analyzed immediately, the cell lysate was stored at 4 °C.

5.3 Results and Discussion

The success of the affinity aptamer amplification assay for multiple proteins depends on three main processes: tunable aptamer CE for separation of protein-aptamer complexes from the unbound aptamers; efficient collection of fractions containing only the protein-aptamer complexes; and real-time PCR amplification and fluorescent detection of the collected protein-bound aptamers. Each of these steps were carefully evaluated and optimized to achieve the best detection limit and minimum background interference.

5.3.1 Design of aptamers and primers for real-time PCR

In the affinity aptamer amplification assay, aptamers play two important roles: to specifically bind to their target proteins, and to serve as the templates for subsequent PCR amplification. To design suitable primers for real-time PCR, some aptamers used for multiple protein analysis need to be extended. However, the length of aptamers has a direct effect on the separation of protein-aptamer complexes from unbound aptamers (6). The binding of longer aptamers to proteins yields smaller differences in the electrophoretic mobility between the protein-aptamer complexes and the unbound aptamers. To achieve a satisfactory separation of protein-aptamer complexes from the unbound aptamers, long aptamers were avoided. However, the use of short aptamers makes it difficult to

adopt a fluorescent reporter probe (e.g. Taqman). Consequently, SYBR green, a DNA binding dye, which intercalates to all double-stranded DNA was employed in real-time PCR.

When using the DNA binding dye to measure the amount of PCR product at each cycle, the accuracy of real-time PCR is readily affected by non-specific PCR products, such as primer dimers. To examine the specificity of the primers designed for amplification of their aptamers, three conventional PCR experiments were conducted to amplify each aptamer in the presence of the other two aptamers. **Figure 5.1** shows the results from analysis of PCR products using polyacrylamide gel electrophoresis. Except for the bands corresponding to the amplified aptamers, no other bands from non-specific PCR products were observed. Therefore, these designed primers are specific for each of the aptamers. They can be used to amplify the corresponding aptamers in a mixture without interference from each other.

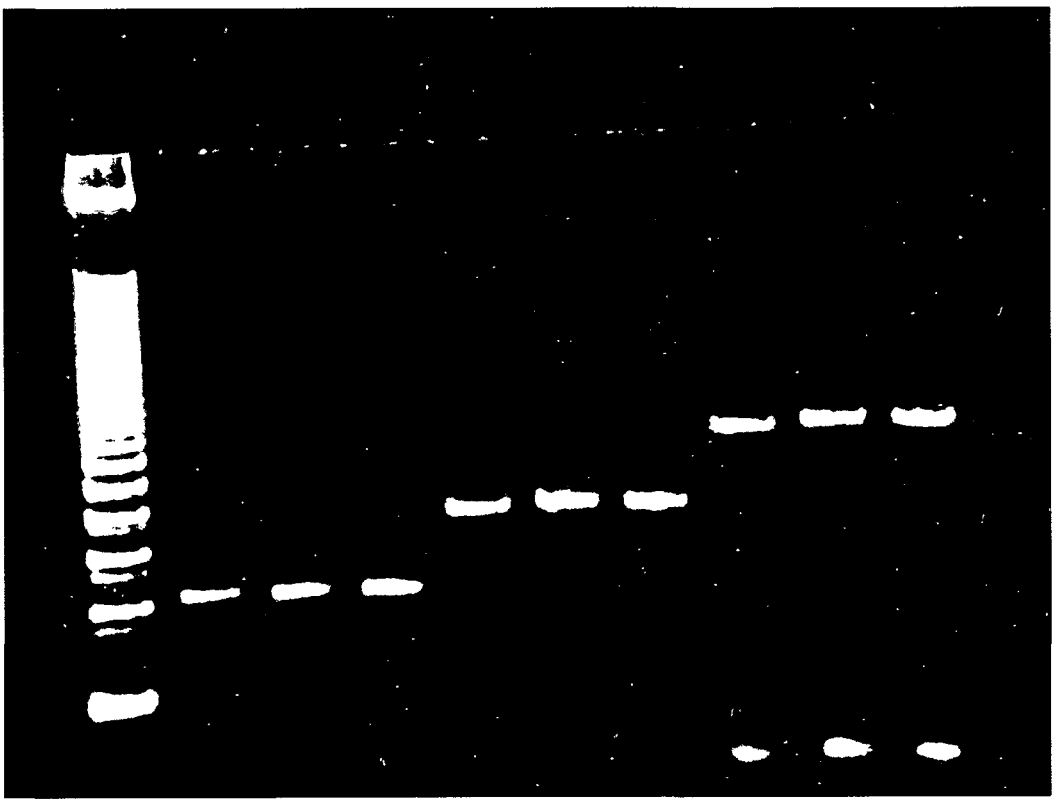

Figure 5.1. PCR and gel electrophoresis of aptamers for thrombin, IgE, and HIV-RT. Triplicate 5 μL 1×TG solutions containing 200 aptamer molecules were amplified for 50 cycles by conventional PCR for each aptamer. A 10bp DNA ladder with an 100 bp band brighter than other bands was used to indicate the length of amplified aptamers. They were 30 nt (for thrombin), 46nt (for IgE), and 75nt (for HIV-RT).

5.3.2 Optimization of real-time PCR conditions

Having demonstrated the specificity of PCR amplification for three aptamers, the real-time PCR conditions were optimized further for quantitation of these aptamers. The optimum conditions for the best signal-to-background were summarized in section **5.2.5**. To determine the sensitivity of real-time PCR for the detection of three aptamers, a series of diluted solutions containing varying concentrations of aptamers were analyzed. The results are shown in **Figure 5.2**. A detection limit, defined as the concentration corresponding to a signal three times standard deviation of the background, was 1×10^{-17} M obtained for all three aptamers. This detection limit represents the ability of optimized real time PCR to detect as few as 6 aptamer molecules in 1 μL. Calibrations were linear for the determination of IgE binding aptamer (r^2 = 0.996), HIV-RT binding aptamer (r^2 = 0.991), and thrombin binding aptamer (r^2 = 0.992). A linear dynamic range of 4 orders of magnitude (1×10^{-17} M to 1×10^{-14} M) was obtained for all three aptamers. Therefore, the optimized real-time PCR offered the high sensitivity needed for the subsequent development of protein detection by using the affinity aptamer amplification assay.

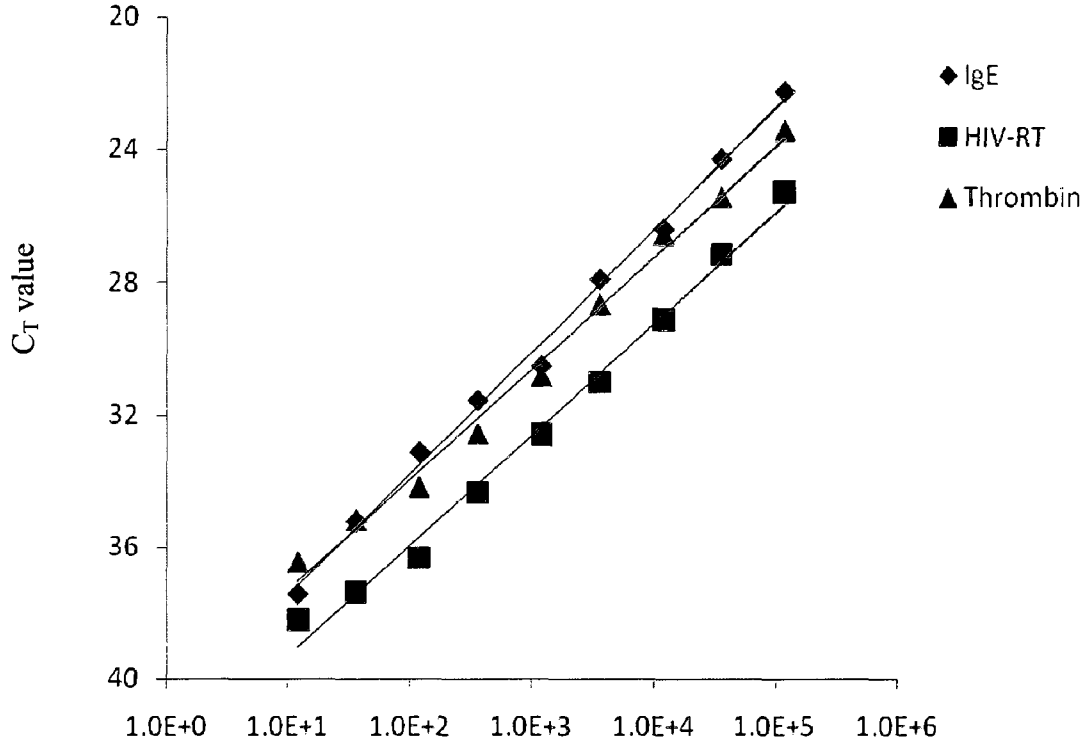

Figure 5.2. Detection of IgE, HIV-RT, and thrombin binding aptamers by real-time PCR. A series of diluted solutions of 2 μL each containing 12, 36, 120, 360, 1200, 3600, 12000, 36000, and 120000 molecules of each aptamers were amplified and detected by real-time PCR. C_T is threshold cycle. Standard deviation: 0.24 -0.86.

5.3.3 Fraction collection and real time PCR amplification

To determine the time intervals for fraction collection, the separation of the protein-aptamer complexes from unbound aptamers was initially studied by analysis of an incubation solution containing aptamers and proteins at a concentration that could be detected by CE-LIF. **Figure 5.3** shows the electropherograms of this analysis. Three aptamers migrated through the capillary at a similar mobility, thereby presenting a single unbound aptamer peak (peak 4), while three corresponding protein-aptamer complexes migrated through the capillary faster than unbound aptamers, producing the complex peaks with shorter migration times (peaks 1-3). All protein-aptamer complexes were well resolved from unbound aptamers. Because fluorescein presented a peak between the unbound aptamers and the protein-aptamer complexes, it was used as an indicator (peak IS) for determination of the boundary between aptamers and complexes.

One molecule of HIV-RT is capable of binding to two aptamer molecules, so two complexes with one or two aptamers were observed in the electropherogram (peaks 2 and 2'). Although the peak from the complex of HIV-RT with two aptamers overlapped with the peak from the thrombin-aptamer complex, this does not present a problem for their quantification, as discussed later. The use of specific primers for amplification of each aptamers enables the discrimination of the different aptamer-protein complexes. For this reason, the various protein-aptamer complexes do not need to be separated from one another. A critical requirement is to separate the unbound aptamers from all the protein-aptamer complexes. This is a unique advantage of the affinity aptamer

amplification assay for multiple protein analysis. Unlike tunable aptamer CE, the capability of the affinity aptamer amplification assay for multiple protein analysis is not limited by the separation ability of CE.

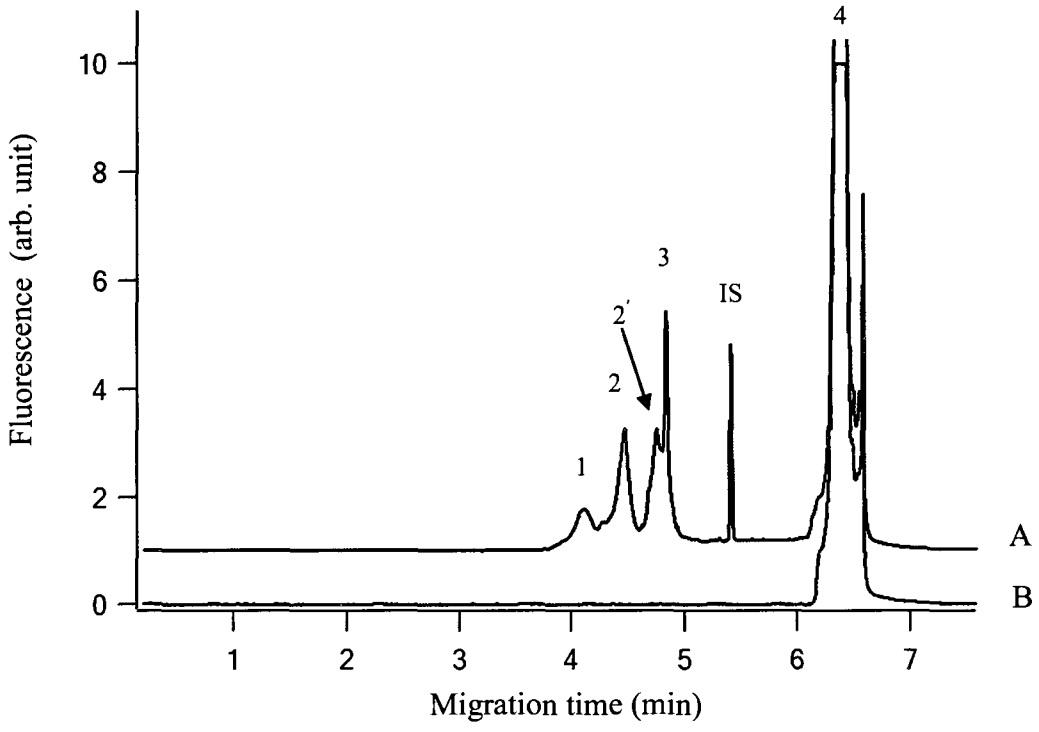

Figure 5.3. Electropherograms showing separation of the protein-aptamer complexes from the unbound aptamers by CE. Aptamers were fluorescently labeled and detected by LIF. Electropherogram A corresponds to analysis of the solution containing 20 nM IgE, HIV-RT, thrombin, and 100 nM each of their aptamers. Electropherogram B corresponds to analysis of the solution containing 100 nM each of three aptamers. Peak 1 is the complex of IgE and aptamer; peak 2 is the complex of HIV-RT with a single aptamer molecule; peak 2' is the complex of HIV-RT with two aptamer molecules; peak 3 is the complex of the thrombin and aptamer; and peak 4 is due to the unbound aptamers. Fluorescein (10 nM) was used as internal standard (IS).

In order to achieve the best detection limit for multiple protein analysis, the fraction designated as the protein-aptamer complexes should have no or minimum unbound aptamers. Any interfusion of unbound aptamers into the fraction of the protein-aptamer complexes could lead to an increase in the background, thereby affecting the detection limit of the assay. Two parameters, the resolution of complexes from unbound aptamers and the peak shape and width of the aptamers, are critical to reproducible collection of the protein-aptamer complex fraction. A narrow zone of the unbound aptamers and the efficient resolution of the protein-aptamer complexes from unbound aptamer zone would facilitate the collection of the fraction containing only protein-aptamer complexes. Although the electropherogram from CE-LIF indicated that the interval between the end of the last complex peak and the beginning of the unbound aptamer peak was approximately one minute (**Figure 5.3**), this interval might be smaller if sample matrix affects the separation. In addition, because real-time PCR has a much higher sensitivity for detection of aptamers, trace amounts of the unbound aptamers would give high background even if they are not detectable by LIF. Fortunately, the protein-aptamer complexes migrate faster than the unbound aptamers. Therefore, in principle, the collection of the protein-aptamer complex fraction would have little contamination from the unbound aptamers. However, diffusions of the unbound aptamer toward the protein-aptamer complex zone would affect the integrity of collecting only the protein-aptamer complexes. Therefore, it is necessary to reduce diffusion of aptamers by minimizing the separation time and the initial concentration of the unbound aptamers. Using

aptamer for IgE as an example, the aptamer collected at the various migration time intervals was determined using real-time PCR detection. The initial solutions containing 0.1, 0.5, 2.5, or 5 nM aptamer for IgE were separated by CE, and the fractions were collected at 0-2, 2-3, 3-4, 4-5, 5-5.5, 5.5-6, and 6-9 min. Each fraction was subjected to real-time PCR amplification and detection. The results are shown in **Figure 5.4**. Although the profiles are similar when different concentrations of the aptamer were used, the amount of the aptamer that was diffused into the 4-5 min fraction interval increases with the initial concentration of the aptamer. The diffused aptamer into the 4-5 min fraction would represent background for measuring the protein-aptamer complexes. The lowest background resulted from the aptamer concentration of 0.1 nM. However 0.5 nM aptamer was chosen as a compromise for the relatively lower background and a sufficient concentration to favor the formation of protein-aptamer complexes.

Building on the optimization of time intervals for fraction collection and the concentration of aptamers, the affinity aptamer amplification assay was applied to analysis of 1 pM IgE, HIV-RT, and thrombin in a solution. The concentration of aptamers was 0.5 nM, both in the sample solution and the blank. The results are shown in **Figure 5.5**. Except for that at 4-5min fraction, there is no obvious difference in the number of aptamer molecules between fractions of the sample and blank at each time interval. The increase of number of aptamer molecules for the fraction at 4-5min represents the presence of protein-aptamer complexes in this fraction. The CE migration behavior of protein-aptamer complexes and unbound aptamers is consistent regardless whether LIF (**Figure**

5.3) or real- time PCR (**Figure 5.5**) is used for detection. These results demonstrate that the three proteins at 1 pM concentration can be successfully detected in a single analysis by the affinity aptamer amplification assay.

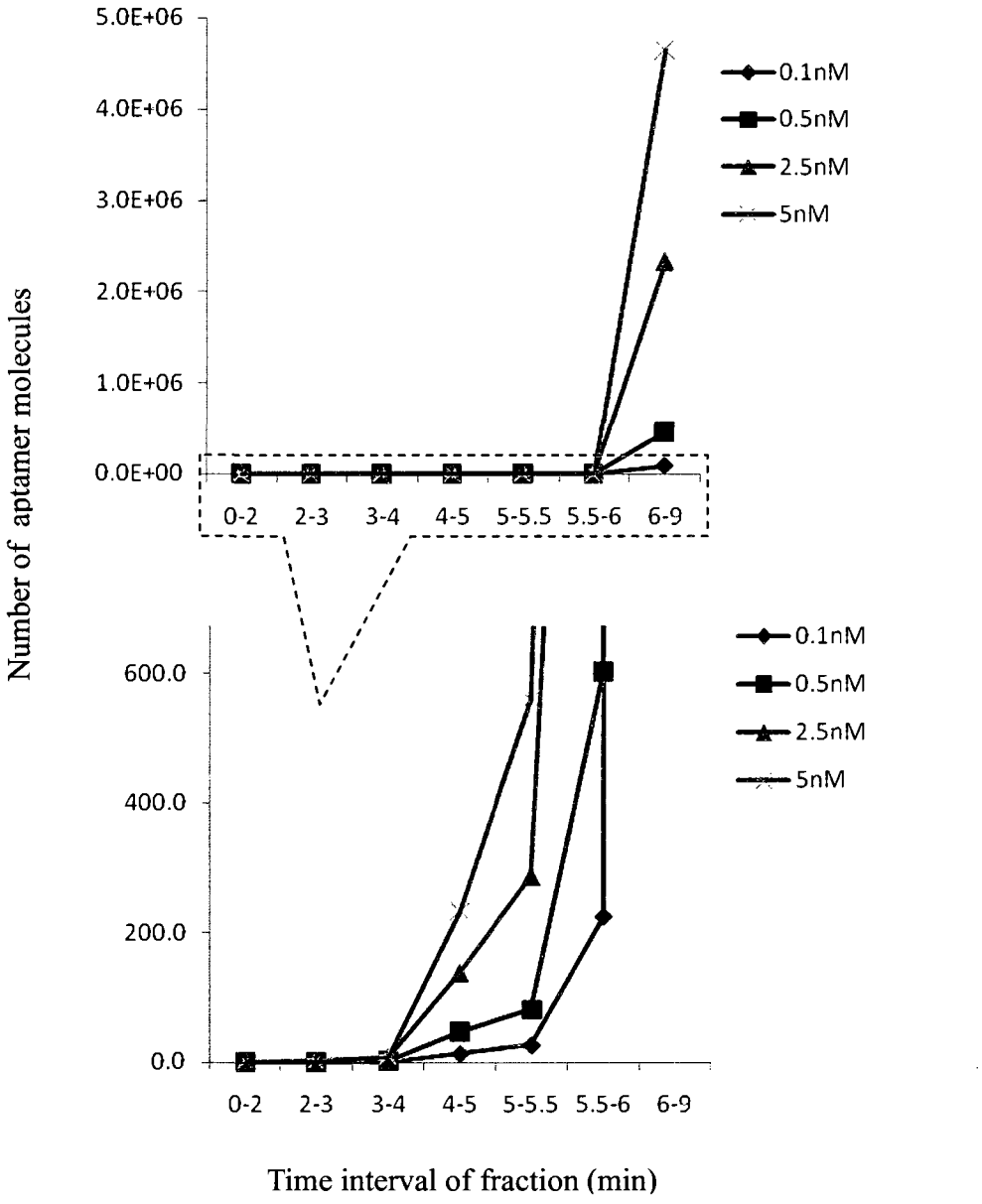

Figure 5.4. Results of real-time PCR analysis of CE fractions collected from CE separation of 0.1-5nM aptamer for IgE. Analyzed solutions contained 0.1 nM, 0.5 nM, 2.5 nM, and 5 nM aptamer for IgE. The number of aptamer molecules in each fraction was calculated from a standard calibration curve generated from real-time PCR analysis of diluted aptamer solutions.

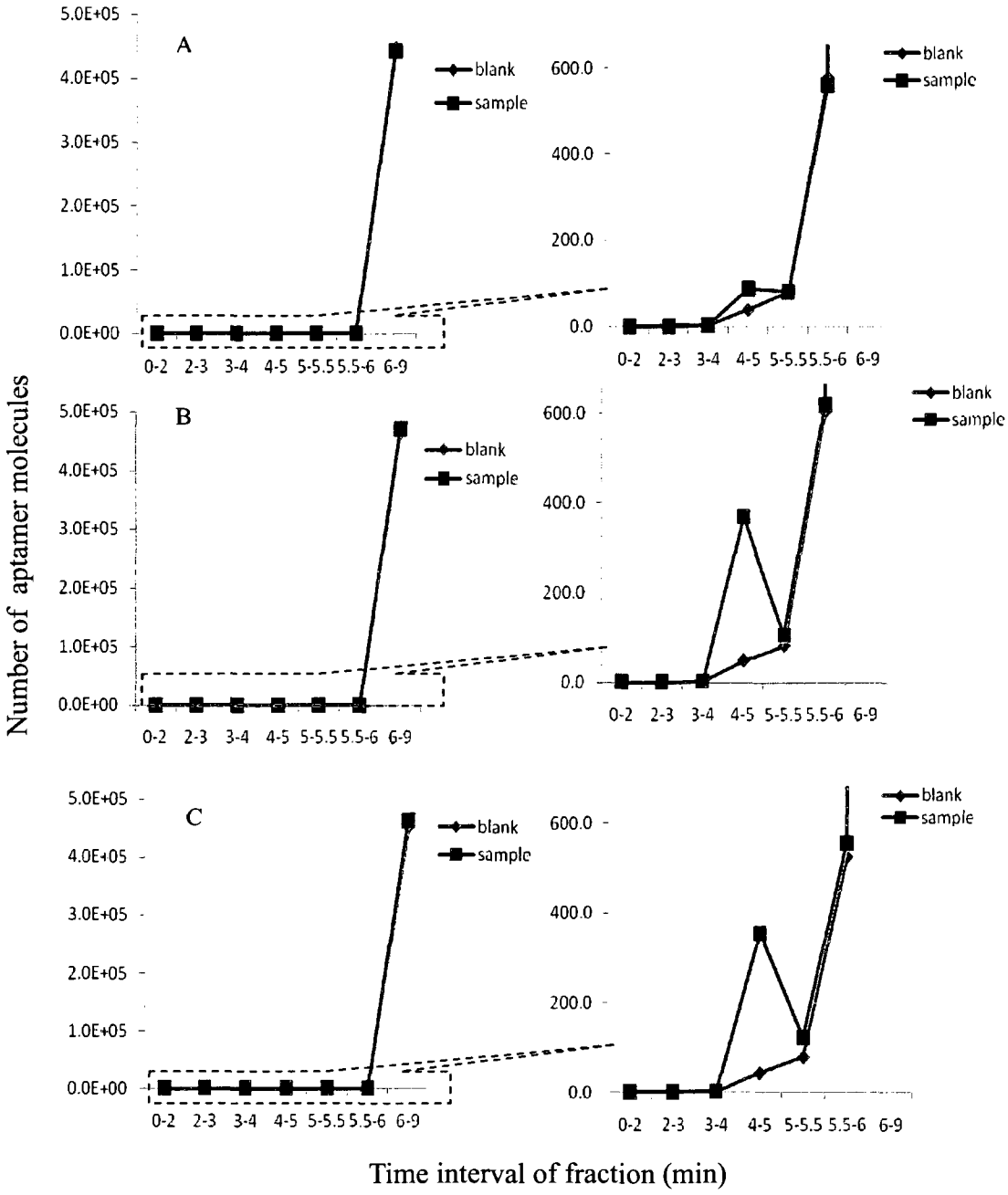

Figure 5.5. Detection of IgE, HIV-RT, and thrombin by the affinity aptamer amplification assay. A is the results of detection of 1 pM IgE; B is the results of detection of 1 pM HIV-RT; and C is the results of detection of 1 pM thrombin. The right-hand figures are expanded regions from the figures shown on the left.

5.3.4 Quantitation of proteins

Based on the results of the fraction collection optimization, only three time intervals, 0-3, 3-t_b, and t_b-9min, were used for the fraction collection in the subsequent experiments of quantitation of proteins. The migration time of internal standard fluorescein (t_b) was used as an indicator of the boundary between the protein-aptamer complexes and the unbound aptamers. Two major reasons contributed to the decision for collection of only three fractions from each separation. Firstly, the decrease of collected fraction numbers reduces the separation and collection time. When changing collection vials, the electrophoretic voltage is stopped, and diffusion between the analyte zones inside the capillary may take place. By reducing the number of fractions and the number of stopping times, the diffusion is reduced. Secondly, the smaller fraction number simplifies the fraction collection and real-time PCR procedures.

Although results from both CE-LIF (**Figure 5.3**) and the CE/real-time PCR (**Figure 5.5**) have established the appropriate time interval (4-5min) for the collection of the protein-aptamer complex, further quality control was built in to ensure the consistent and reproducible collection of fractions. Fluorescein was added to the sample as an internal standard and it was detected by on-column LIF. This interval marker helps to identify any variation in the migration time between separations. If the migration time changes, the collection interval could be adjusted accordingly. The collection of the fraction containing the protein-aptamer complexes was terminated when fluorescein was detected migrating through the on-column detection window of the capillary.

The three fractions of each separation play different roles in analysis. The first fraction was used to determine any residue of unbound aptamers carried over from the previous separation. The results of analysis could be accepted only if the the background from the first fraction was similar to that of the negative control after real-time PCR analysis. The second fraction which contained protein-aptamer complexes was used to determine the amount of proteins in the solutions. The real-time PCR results of the third fraction could provide the information on reproducibility of the experiment (e.g. injection and incubation) because this fraction contains the unbound aptamers.

After the optimization of the CE separation and fraction collection, the assay was applied to the analysis of solutions containing varying concentrations of IgE, HIV-RT, and thrombin and their corresponding aptamers. A linear dynamic range of three orders of magnitude was obtained for all three proteins (**Figure 5.6**). The detection limits of 5×10^{-13} M, 1×10^{-13} M, and 1×10^{-13} M, defined as the concentration equivalent to three times the standard deviation of background level, were obtained for the analysis of IgE, HIV-RT, and thrombin, respectively.

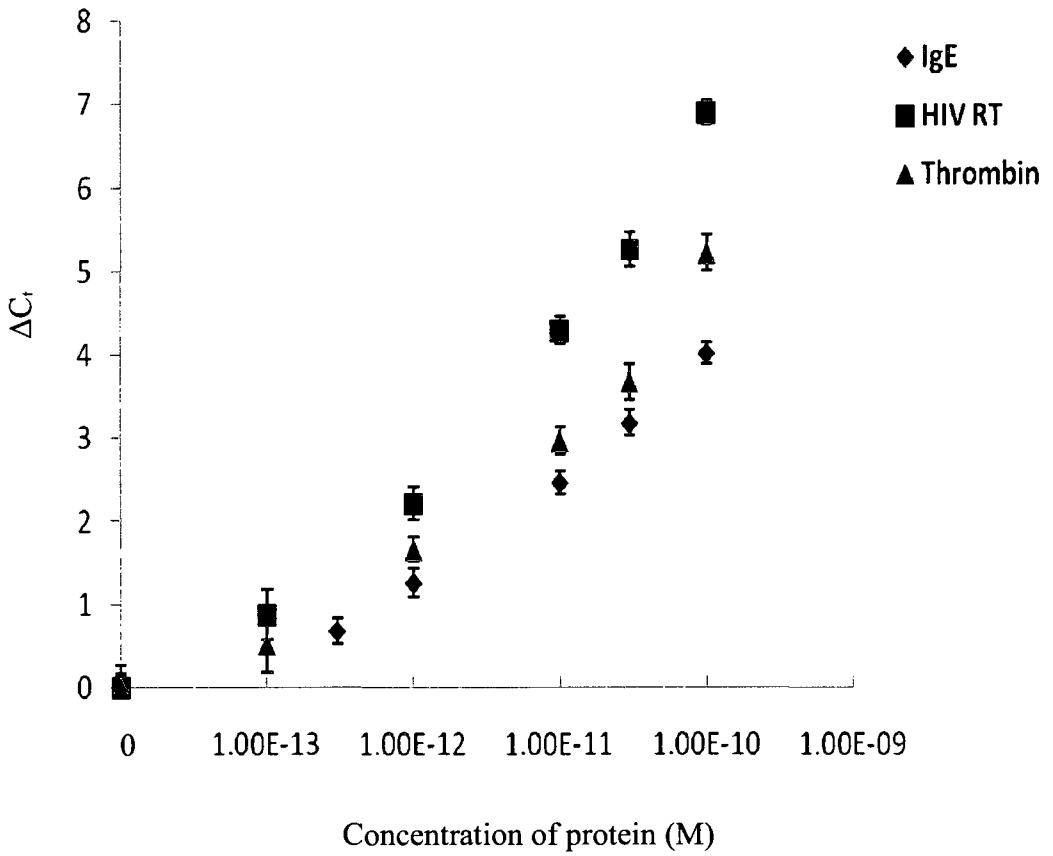

Figure 5.6. Determination of IgE, HIV-RT, and thrombin using affinity CE followed by real-time PCR. The sample solutions contain various concentrations of the three proteins and 0.5 nM each of three aptamers. ΔC_t is C_t of blank minus C_t of each sample.

5.3.5 Selectivity of assay

To determine the selectivity of the assay for IgE, HIV-RT, and thrombin, experiments were carried out with some possible interfering proteins in place of IgE, HIV-RT, and thrombin. Experiments were performed in which 0.5 nM of three aptamers were incubated with either 1 pM of IgE, HIV-RT and thrombin or 10 nM of interfering proteins, including BSA, human serum albumin (HSA), IgG, myoglobin and transferrin. The results are shown in **Figure 5.7**. ΔC values of the interfering proteins are negligible when compared to those of IgE, HIV-RT, and thrombin, which suggested that these proteins, present at 10,000–fold excess over that of the target proteins, did not bind to the specific aptamers for IgE, HIV-RT, and thrombin, and did not interfere with the detection of the three target proteins.

The ability of the method to detect three target proteins in complex sample matrix was further demonstrated by spiking them in the monkey kidney cell lysate. **Figure 5.8** shows the results of analyses of cell lysate samples spiked with varying concentrations of IgE, HIV-RT, and thrombin. The experiments for analyses of three proteins in the complex sample matrix presented similar dynamic ranges and detection limits to those in which proteins were analyzed in the incubation buffer (**Figure 5.6**).

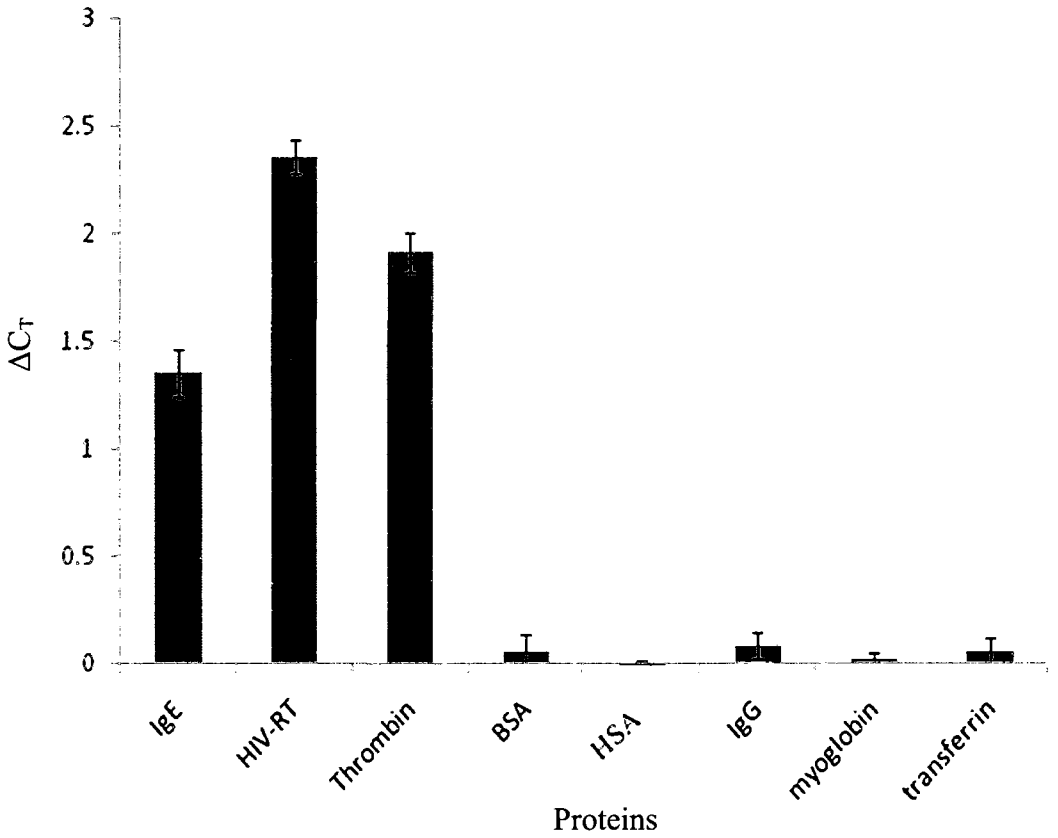

Figure 5.7. Selectivity of the assay for analysis of IgE, HIV-RT, and thrombin. Samples contained 0.5 nM of three aptamers and either 1 pM IgE, HIV-RT, and thrombin, or 10 nM BSA, HSA, IgG, myoglobin, and transferrin. Each sample was analyzed by affinity CE followed by real-time PCR.

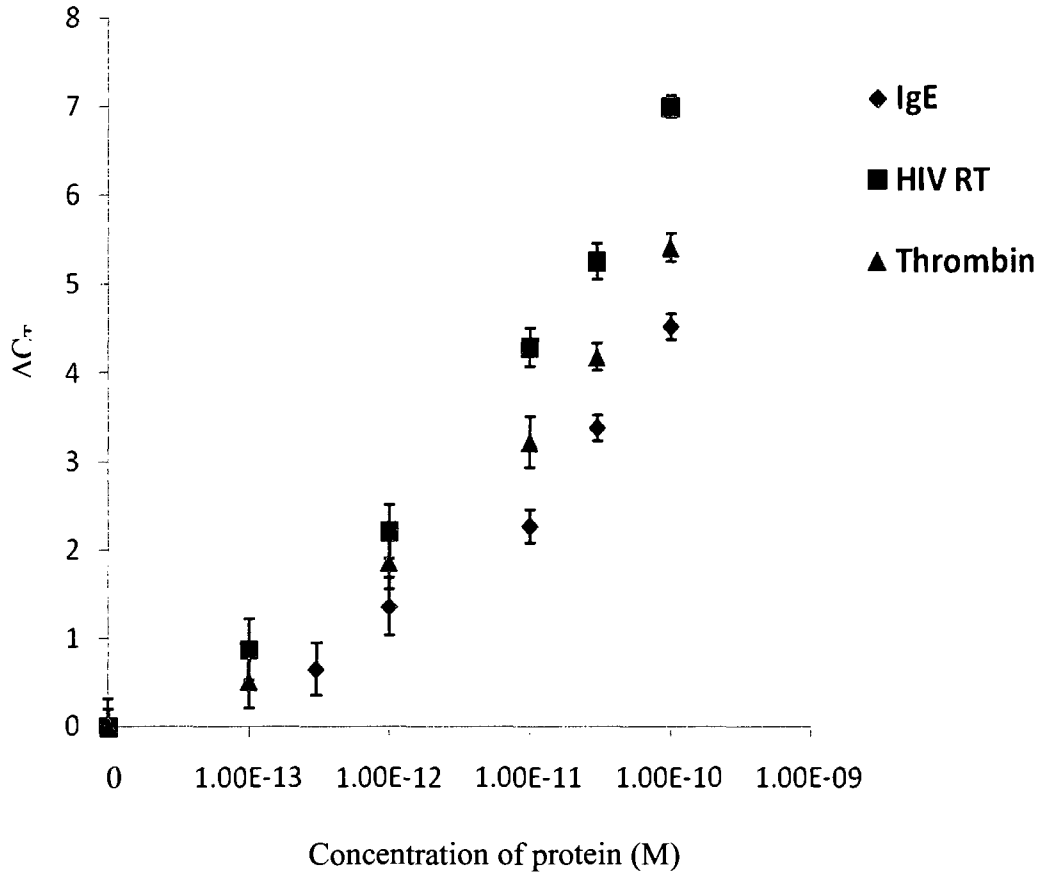

Figure 5.8. Determination of IgE, HIV-RT, and thrombin in cell lysate. Cell lysate samples contained various concentrations of IgE, HIV-RT, thrombin and 0.5 nM each of three aptamers.

5.4 Conclusions

The affinity aptamer amplification assay is able to quantify multiple target proteins in a single CE operation. The method takes advantage of the powerful separation ability of CE and the extreme sensitivity of PCR for nucleic acid

detection. Aptamer complexes with IgE, HIV-RT, and thrombin were well resolved from unbound aptamers. The fractions containing only complexes were collected and subjected to subsequent real-time PCR. Simultaneous determination of fM levels of three target proteins has been achieved, which represents an improvement of three orders of magnitude greater than other available aptamer-based methods involving CE (4, 6, 7-11). The substitution of conventional PCR with real-time PCR offered the affinity aptamer amplification assay with higher precision in quantitation and wider dynamic range.

In the multiplexed affinity aptamer amplification assay, aptamers serve both as affinity molecules for target protein recognition and as the templates for real-time PCR. Because the binding of specific aptamers encodes proteins with different nucleotide sequences, specific primers could be designed to associate with each individual protein, enabling the simultaneous detection of multiple proteins. Therefore, the key to achieve multiple protein analysis is to separate the protein-aptamer complexes from the unbound aptamers. The separation of protein-aptamer complexes from each other is not required. The advantage of not having to separate the individual protein-aptamer complexes from one another renders the method with great potential for multiple analysis capability. It is anticipated that the number of protein targets could be further expanded as long as stable protein-aptamer complexes could be formed and separated from their unbound aptamers.

5.5 References

1. H. Zhang, Z. Wang, X.-F. Li and X. C. Le, *Angew. Chem. Int. Ed.,* 2006, 45, 1576-1580.

2. J. P. Landers, *Handbook of Capillary Electrophoresis,* CRC press LLC, 1997.

3. Q. H. Wan and X. C. Le, *Anal. Chem.*, 2000, 72, 5583-5589.

4. V. Pavski and X. C. Le, *Anal. Chem.*, 2001, 73, 6070-6076.

5. H. Wang, M. Lu and X. C. Le, *Anal. Chem.,* 2005, 77, 4985-4990.

6. H. Zhang, X.-F. Li and X. C. Le, *J. Am. Chem. Soc.,* 2008, 130, 34-35.

7. I. German, D. D. Buchanan and R. T. Kennedy, *Anal. Chem.,* 1998, 4540-4545.

8. M. Berezovski, R. Nutiu, Y. Li and S. N. Krylov, *Anal. Chem.,* 2003, 75, 1382-1386.

9. C.-C. Huang, Z. Cao, H. –T. Chang and W. Tang, *Anal. Chem.,* 2004, 76, 6973-6981.

10. Y. Li, L. Guo, F. Zhang, Z. Zhang, J. Tang and J. Xie. *Electrophoresis*, 2008, 29, 2570-2577.

11. A. J. Haes, B. C. Giordano and G. E. Collins, *Anal. Chem.*, 2006, 78, 3758-3764.

Chapter Six

Binding-Induced Hairpin Assay and Its Application to Protein Analysis

6.1 Introduction

Nucleotides carrying hairpin structures have been found naturally present in cells. Studies have suggested hairpin structures may play an important regulatory role in gene expression and cellular metabolism (1, 2). In addition, DNA hairpins exhibit many advantages as hybridization probes. The thermodynamic studies have demonstrated that DNA hairpin probes show significantly higher specificity than the corresponding linear probes (3, 4). DNA hairpin probes can generally distinguish targets that are different from one another by as little as a single nucleotide substitution. The enhanced specificity is due to their constrained secondary structures. Molecular beacons are hairpin-shaped DNA molecules possessing a fluorophore at the end of one stem arm and a quencher at the end of the other arm (5-7). In the absence of targets, stem places the fluorophore and the quencher in close proximity so that the fluorophore is unable to fluoresce, and the molecular beacons are dark. When they encounter the target nucleic acids, the hybridization of molecular beacons to their targets detaches the hybrid formed by the arm sequences, thereby causing the fluorophore and quencher to come apart from each other. As a result, the fluorescence is restored and used as a signal for the detection of specific nucleic acids. DNA

hairpins have been widely applied to detection, amplification, and manipulation of nucleic acids (8-10). However, the potential of hairpin structures has seldom been explored for other macromolecule analysis because of lack of similar hairpin structure changes produced by hybridization.

Utilizing the unique properties of hairpin structures, this chapter describes a new principle for construction of probes that can be used for analysis of proteins and other macromolecules in homogeneous solutions (**Figure 6.1**). Techniques involving hairpin structures, such as molecular beacons, usually start with probes possessing hairpin structures and end with conformation change of hairpin structures upon hybridization of target nucleic acids. In contrast, the probes in this study were designed to be present free in the absence of targets, and to form hairpin structures only upon binding to target molecules. A pair of probes, Probe-F and Probe-R, were prepared through the conjugation of oligonucleotides (oligos) to affinity ligands. These probes were designed in such a way that when the affinity ligands bind to the target molecule, the oligos provide the complementary stem sequences at their free ends (**step 1**). In the absence of targets, the probes are present separately. The length of stem sequences is designed to be short enough so that the free oligos are unable to hybridize together under the temperature of the analysis. When both probes bind to a single target molecule, the target molecule serves as a connector, bringing the two probes into a single complex molecule (**step 2**). The stem sequences of the oligos in the single complex molecule then hybridize with each other, forming a hairpin structure. Because this hairpin structure is induced upon the binding of probes to the target

protein, it is termed as binding-induced hairpin. Unlike the traditional nucleotide hairpins, the binding-induced hairpin is a complex structure. The hairpin loop consists of the target molecule, the two affinity ligands, and the conjugated nucleotide sequences on the affinity ligands. The hybrid of the two free ends of the oligos forms the hairpin stem. The free end of probe-F was extended by an additional nucleotide sequence, forming another nucleotide hairpin structure at its end (**step 3**). The stem places two ends close to each other, both complementary to the other arm, allowing the ends to be joined by enzymatic DNA ligation (**step 4**). The occurrence of enzymatic DNA ligation corresponds to the binding of target molecules and formation of binding-induced hairpin structures, whereas the free ends of unbound probes stay separate. Therefore, the detection of targets can be carried out by detection of ligation-produced oligo in homogeneous solutions. Methods for detection of nucleic acids, such as real-time PCR, could be employed to provide the detection with ultrasensitivity.

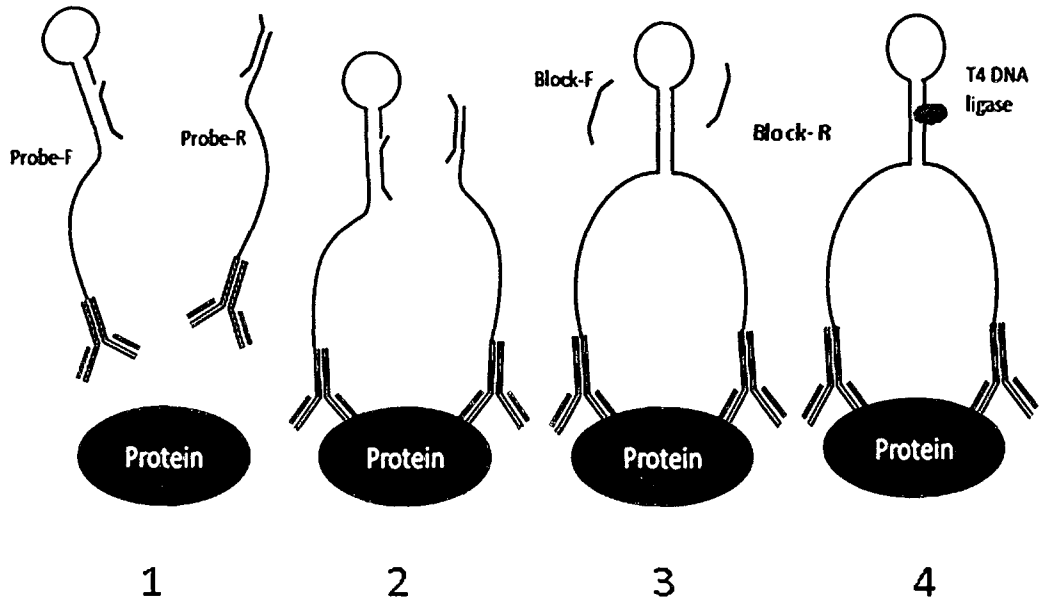

Figure 6.1. Principle of binding-induced hairpin assay. (1). A pair of probes, Probe-F and Probe-R, are designed with stem sequence at their free ends. A pair of nucleotides, Block-F and Block-R, are used to block the free ends of probes, reducing background hybridization of probes. (2) In the presence of target molecules, both probes bind to a single target molecule, placing the two probes into a single complex molecule. (3) The free ends of probes hybridize with each other, inducing a hairpin structure. (4) The formation of the hairpin structure assembles the free ends of Probe-R and Probe-F that contain another hairpin at its free end. The enzymatic DNA ligation results in a specific, amplifiable DNA sequence.

6.2 Experimental

6.2.1 Reagents

PDGF-AA, PDGF-AB, PDGF-BB, and biotinylated polyclonal anti-prostate specific antigen (PSA) antibody were obtained from R&D System (Minneapolis, MN). Streptavidin, PSA, BSA, goat serum, and biotin were obtained from Sigma-Aldrich (Oakville, ON). SYBR GreenER qPCR Supermix Universal was obtained from Invitrogen Canada (Burlington, ON). PDGF-BB binding aptamer (5'-/Biotin/TTTTTTTTTTTACTCAGGGCACTGCAAGCAATT GTGGTCCCAATGGGCTGAGTAT-3') was synthesized by Integrated DNA Technologies (Corarville, IA). It was labeled at the 5' end with a biotin group and purified by reversed-phase HPLC. **Table 6.1** lists the oligos used in this study. These oligos are all synthesized, labeled, and purified by Integrated DNA Technologies. The oligo of Probe-F was attached with a biotin group at the 5' end, and oligos of Probe-R were labeled with a phosphate group at the 5' end and a biotin group at the 3' end. The stem sequences are underlined in the oligos of Probe-F and Probe-R. The stem sequence of the oligo of Probe-R5, 6, 7, and 8 contains 5, 6, 7, and 8 complementary bases, respectively. Block-R6 was used in the assay when probe-R was constructed from oligos of Probe-R6, while Block-R7 was used when Probe-R was constructed from oligos of Probe-R7. Underlined sequences of Block-F and R are complementary to the corresponding sequences of the oligos of Probe-F and R, respectively. The 1× Phosphate buffered saline (PBS) (137 mM NaCl, 10 mM phosphate, 2.7 mM KCl, pH 7.4) was diluted with deionized water from 10×PBS buffer (from Fisher Scientific, Nepean, ON). All

other reagents were commercially available analytical grade.

6.2.1 Preparation of binding-induced hairpin probes

Since the 5' end of oligos of Probe-F and and 3' end of oligos of Probe-R were labeled with biotin, oligos of Probe-F and Probe-R were directly used as probes (Strep-Probe-F and Strep-Probe-R) for streptavidin analysis. Probes named as PDGF-Probe-F or PDFG-Probe-R for PDGF-BB analysis were prepared by incorporation of the oligos of Probe-F or Probe-R into the biotinylated aptamer through streptavidin biotin interaction. 100 μL 200 nM oligo of Probe-F or R and 100 μL 200 nM streptavidin, diluted in 1×PBS, were first mixed and incubated at 37 °C for 1 h. 100 μL the above solution was then added to 100 μL 100 nM biotinylated aptamer diluted in 1×PBS. The mixture was incubated at 37 °C for another 1 h forming PDGF-Probe F or R. The PDGF-Probe F or R solution was then diluted to 10 nM in 1×PBS buffer containing 1% BSA and 10 mM biotin, and stored at 4 °C. The preparation of probes (PSA-Probe-F and PSA-Probe-R) for analysis of PSA was a similar process to that of probes for analysis of PDGF-BB, except that the solutions were incubated at room temperature for 1 h instead of at 37 °C, and biotinylated polyclonal anti-PSA antibody (R&D System) replaced the biotinylated aptamer.

Table 6.1. Summary of oligonucleotides (oligos) used in this study

Oligos	Sequences (5'→ 3')
Oligo of Probe-F	ACTGTGTCTCGTCGTTGGTGTTTTGTTTTGTTTTAG GCTGGTCGCTTTGTTTTGCGAC
Oligo of Probe-R5	CAGCCCTTTGTTTGTTTTGTTTTTTTTGATGGAGCA GGTGTCAGATC
Oligo of Probe-R6	CAGCCTTTTTGTTTGTTTTGTTTTTTTTGATGGAGC AGGTGTCAGATC
Oligo of Probe-R7	CAGCCTATTTTGTTTGTTTTGTTTTTTTTGATGGAG CAGGTGTCAGATC
Oligo of Probe-R8	CAGCCTAATTTTGTTTGTTTTGTTTTTTTTGATGGA GCAGGTGTCAGATC
Block-F-1	TTTGCCTAAAATTT
Block-F-2	TTTGCCTAAAACTTT
Block-F-3	TTTGCCTAAAACATTT
Block-F-4	TTTGCCTAAAACAATTT
Block-F-5	TTTGCCTAAAACAAATTT
Block-R6-1	TTTAAAGGCTGTTT
Block-R6-2	TTTAAAAGGCTGTTT
Block-R6-3	TTTAAAAAGGCTGTTT
Block-R6-4	TTTCAAAAAGGCTGTTT
Block-R7-1	TTTAATAGGCTGTTT
Block-R7-2	TTTAAATAGGCTGTTT
Block-R7-3	TTTAAAATAGGCTGTTT
Block-R7-4	TTTCAAAATAGGCTGTTT

6.2.2 Analysis of streptavidin, PDGF-BB, and PSA

The procedures for analysis of three proteins are similar and are thereby described together. Unless otherwise indicated, a 50 μL 1×PBS (with 1 mM $MgCl_2$ for PDGF-BB) solution, containing 100 pM Probe-F and Probe-R, 100 nM Block-F and Block-R, and desired amount of proteins, was incubated at 37 °C for 30 min and then at room temperature for another 10 min. An aliquot (2 μL) of the above solution was then transferred into a real-time PCR reaction tube (Applied Biosystems (ABI), Foster City, CA). After addition of the reagents for ligation and amplification, the final 20 μL reaction solution contained 100 μM ATP, 0.4 Unit T4 DNA ligase (Invitrogen), 0.1 μM primers (forward and reverse), ROX reference dye, and 10 μL SYBR GreenER qPCR Supermix Universal (Invitrogen, Burlington, ON). After 10 min ligation reaction at room temperature, the reaction vials were transferred into a real-time PCR instrument (ABI 7500 Fast Real-Time PCR System). The PCR program consisted of 50 °C for 2 min, 95 °C for 6 min, followed by 50 cycles of 95 °C for 15 s, 60 °C for 60 s.

6.2.3 Cell lysate and serum sample preparation

1.5 mL of medium containing approximately 2×10^6 Vero 76 monkey kidney cells was spun at 10,000 g for 3min. After being washed three times with cold 1× PBS, the pellet was resuspended in 250 μL ice-cold lysis buffer containing 50 mM Tris (pH 7.4), 150 mM NaCl, 1% Triton X-100, 1% NP-40, 0.1% SDS and 0.5mM PMSF. The lysate were spun at 15,000g for 10 min at 4 °C. The supernatant was carefully transferred into another tube and diluted two-fold by 1× PBS containing 2 mM $MgCl_2$. When not analyzed immediately, the cell

lysate was stored at 4 °C.

The frozen serum was thawed in a water bath at 30 °C, and then kept on ice. Prior to analysis, 0.5 mL serum was centrifuged at 10,000 rpm for 10 min to remove solid particles. The appropriate volumes of PSA stock solutions were mixed with 2.0 μL serum to obtain the desired concentration, and 1×PBS was then used to produce a final volume of 50 μL.

6.3 Results

6.3.1 Design and construction of binding-induced hairpin probes

A pair of probes, Probe-F and Probe-R, were constructed in this experiment. Both probes were ligand-DNA conjugates. Ligands in probes can be small or macromolecules that are able to bind to the single target molecule. The ligands used in this study included biotin for detection of streptavidin, aptamers for PDGF-BB, and antibodies for PSA.

Oligos were conjugated to the ligands by different approaches. The 5' end of oligos was attached to ligands in Probe-F, while the 3' end of oligos was attached to ligands for Probe-R. In the first example of detecting streptavidin, biotin was covalently linked to the ends of oligos. In the case of detecting PSA, antibody for PSA was first biotinylated, and then the biotionylated oligos were conjugated to the antibody by using streptavidin as a connector. Likewise, in the experiments of detecting PDGF, the aptamer for PDGF was first biotinylated, and then the biotionylated oligos were conjugated to the aptamer by using streptavidin as a connector. Although aptamers can be extended directly with additional oligo bases, the approach using biotin-streptavidin chemistry offers two advantages.

The streptavidin not only works as a connector, it also serves as a spacer that could potentially reduce the effect of extended oligos on the favorable secondary conformation of the aptamer. The use of two shorter oligos makes their synthesis easier than having to preparing for a longer oligo.

The oligo in Probe-F was designed to possess a hairpin structure at its free end. This hairpin structure was created with strong stability, providing one side of the strand for subsequent DNA ligation. A piece of stem sequence was placed next to the hairpin structure. This sequence was used to hybridize the other stem sequence at the free end of the oligo in Probe-R when the binding-induced hairpin was induced by the binding to the target molecule. In order to facilitate the DNA ligation, a phosphate group was attached to the free end of the oligo in Probe-R.

The principle of using binding-induced hairpin assay for protein analysis may be expressed in the following equations. Equation 1 describes the process of inducing a hairpin structure through the binding of two probes to the target molecule:

$$\text{Probe-F} + \text{Probe-R} + \text{T} \overset{K_1}{\Leftrightarrow} \text{Probe-F-T-Probe-R}_{open} \overset{K_2}{\Leftrightarrow} \text{Probe-F-T-Probe-R}_{close} \quad (1)$$

Where T is the target molecule; $\text{Probe-F-T-Probe-R}_{open}$ is the complex of Probe-F, Probe-R, and target in the form of random coil; $\text{Probe-F-T-Probe-R}_{close}$ is the complex of Probe-F, Probe-R, and target in the form of hairpin structure; and K_1 and K_2 are equilibrium constants.

In the absence of target, Probe-F may also hybridize to Probe-R, producing background.

$$\text{Probe-F} + \text{Probe-R} \overset{K_3}{\Leftrightarrow} \text{Probe-F·Probe-R} \qquad (2)$$

Where Probe-F·Probe-R is the background (target-independent) hybrid of Probe-F and Probe-R.

While Probe-F·T·Probe-R_{close} is the desired complex that yields the subsequent signal for target detection, Probe-F·Probe-R produces background interfering with the detection. The signal to background ratio of the method can be expressed as follows:

$$\text{Signal}/\text{Background} = \frac{[\text{Probe-F·T·probe-R}_{close}]}{[\text{Probe-F·Probe-R}]} = \frac{K_1 K_2 [T]}{K_3} \qquad (3)$$

The value of K_1 is mainly dependent on the binding affinity of probes to the targets. The probes with higher binding affinity lead to higher sensitivity of analysis. K_2 and K_3 depend mainly upon the length and G-C content of the stem sequence for forming hairpin stems. Therefore, we can rationally design the stem sequence to produce the best signal to background ratio.

The initial concentrations of Probe-F and-R affect the value of [T], thereby producing an impact on the sensitivity of the method. In this study, we optimized the above parameters to achieve highly sensitive detection. To improve the sensitivity further, we applied the blocking oligonucletides to reduce the background (target independent) hybridization between Probe-F and Probe-R. One pair of blocking oligonucleotides Block-F and Block-R were designed to be complementary to part or whole of the stem sequence in Probe-F and Probe-R.

6.3.2 Analysis of streptavidin

To demonstrate the proof of principle, we chose the streptavidin as the

initial target protein because of its extraordinarily strong affinity for biotin (K_d = 10^{-15} M). The use of biotin-DNA conjugates as probes provided one of the strongest known non-covalent interactions, simplifying the impact of the binding affinity of probes on the sensitivity of the method. Therefore, we could focus on optimizing other important parameters, such as the length and G-C content of the stem sequence, the concentration of probes, the length of blocking oligonucleotides, and the ligation time.

The length and G-C content of the stem sequence were designed to achieve the largest K_2/K_3 value. That is, to obtain the highest sensitivity, the probes used should produce the lowest level of background hybridization on the basis of yielding enough percentage of probe target complex in hairpin structure. The ΔT_m, the difference in melting temperature between the hairpin structure and the hybrid formed from separate probes, is an important reference parameter in design of the arm sequence for the binding-induced hairpin. We used Oligoanalyzer 3.1 from IDT to estimate the T_m of hairpins with a loop containing 100-140 thymidines and the corresponding hybrids from separate nucleotides, and obtained a 5-base sequence as the starting stem sequence. Four pairs of probes containing this 5-stem base or 1-3 additional A-T base pairs were used for analysis of 10^{-13} M streptavidin. The results are shown in **Figure 6.2**. In order to easily compare the results under different conditions, the ΔC_t was applied as the cycle threshold with the largest value subtracting the value of the cycle threshold at each point. Therefore, the $\Delta\Delta C_t$ between sample and blank is the signal intensity of the analysis. The background or independent hybridization was

increased with the increase of number of complementary bases. The probes with six complementary bases resulted in the largest differences between the sample and the blank when analyzed by real-time PCR. The use of the probe sequence F1 and R6 (Table 6.1) to construct Strep-Probe-F1 and Strep-Probe-R6 probes resulted in best sensitivity for streptavidin analysis.

Using Strep-Probe-F1 and Strep-Probe-R6 as probes, a pair of blocking oligonucleotides was applied to further decrease the background produced by independent hybridization in solution. Block-R hybridized the part containing the whole arm sequence at the free end of Probe R, whereas Block-F, hybridizing the Probe F, was designed to cover the sequence containing the arm sequence with two bases left at the 3' end to avoid the occurrence of hybridization between Block R and F. **Figure 6.3** shows the analysis of 10^{-13} M streptavidin using pairs of blocking oligoncleotides with different numbers of complementary bases. The longer blocking oligonucleotide led to lower background. The pair of Block-F-4 and Block-R6-4 resulted in the largest differences in threshold cycles between the sample and the blank.

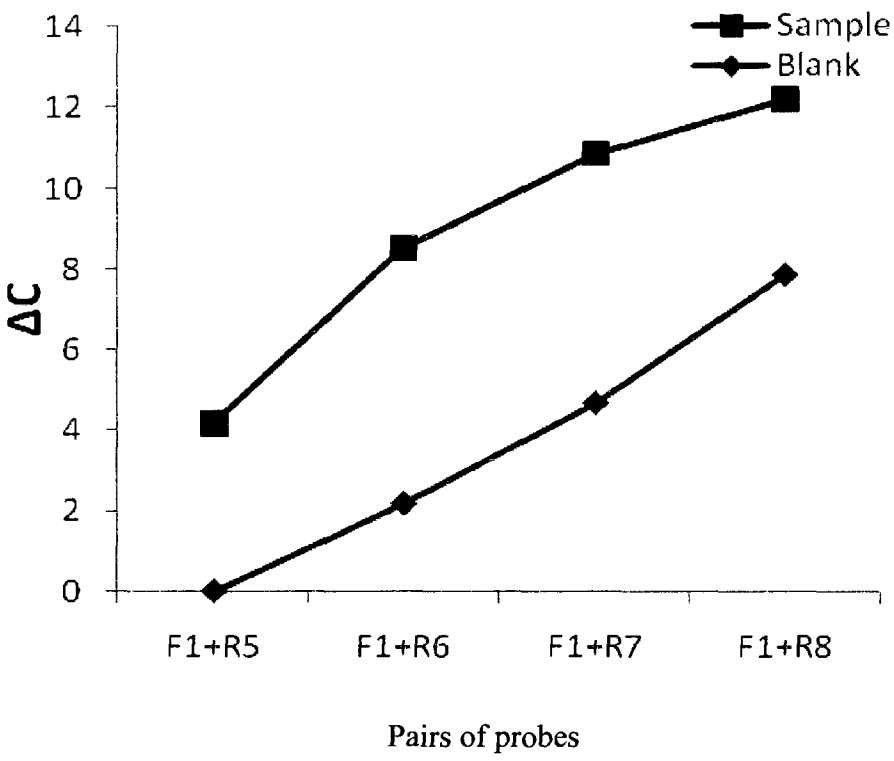

Figure 6.2. Effect of the length and G-C content of stem sequence on signal and background in hairpin-induced hairpin assay. F1 represents Strep-Probe-F1. R5, R6, R7, and R correspond to Strep-Probe-R5, R6, R7, and R8. The sequences of F1, R5, F6, R7, and R8 are shown in Table 6.1. Standard deviation: 0.23 -0.71.

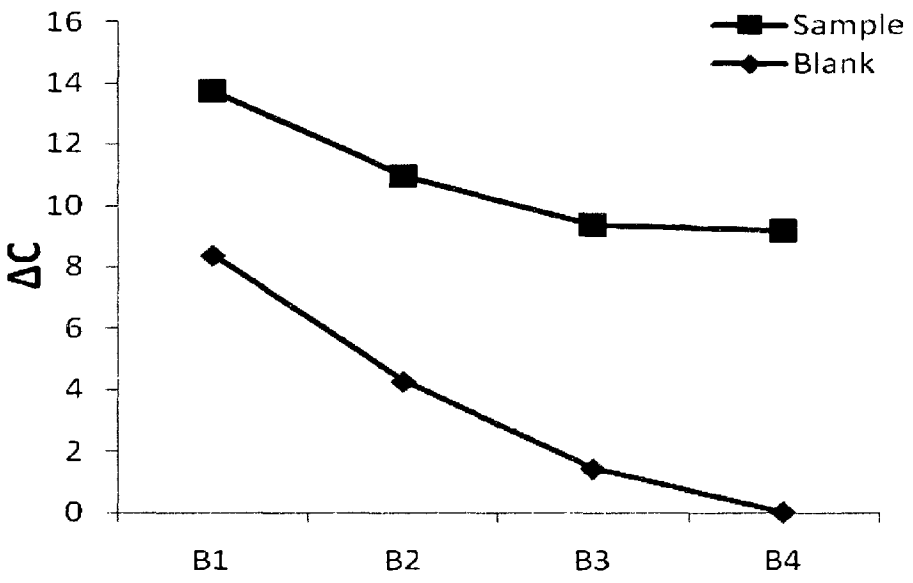

Figure 6.3. Effect of the length of blocking oligonucleotides on signal and background in hairpin-induced hairpin assay. B1 represents the use of Block-F-1 and Block R6-1. B2 represents the use of Block-F-2 and Block R6-2. B3 represents the use of Block-F-3 and Block R6-3. B4 represents the use of Block-F-4 and Block R6-4. The sequences of these blocking oligos are shown in Table 6.1. Standard deviation: 0.28 -0.62.

We also examined the impact of probe concentration and ligation time on analysis of streptavidin (10^{-13}M). Various concentrations of Strep-Probe-F1 and Strep-Probe-R6 probes from 1 pM to 500 pM were used. Although the background increased consistently with increase of probe concentrations, the increase in signal was higher until the probe concentrations reached 100 pM **(Figure 6.4)**.

The impact of the ligation time was studied by analysis of samples at fixed amount of streptavidin (10^{-13}M) or blank with various ligation times from 5 min to 30 min (**Figure 6.5**). The longer time allowed more products of ligation, increasing the background. But the ligation time did not show much affect on the detection of streptavidin. The ligation time of 10 min was chosen for analysis of streptavidin.

After optimization of the above parameters, we applied the principle to analysis of solutions containing varying concentrations of streptavidin (5×10^{-17} M to 1×10^{-9} M) (**Figure 6.6**). A linear dynamic range of over 5 orders of magnitude (5×10^{-17} M to 1×10^{-11} M) was obtained, and the method was able to distinguish the solutions containing protein levels at 2-fold difference. The value of $\Delta\Delta C_t$ started decreasing from 1×10^{-10} M, because there were not enough probes to provide at least two molecules to bind to each streptavidin molecule when the solution contained streptavidin in excess of 1×10^{-10} M. A detection limit of 3×10^{-17} M, defined as the concentration equivalent to three times the standard deviation of the background level, was reproducibly obtained for homogeneous analysis of streptavidin. This detection limit represents the ability of the method to detect as few as 20 molecules in 1 μL.

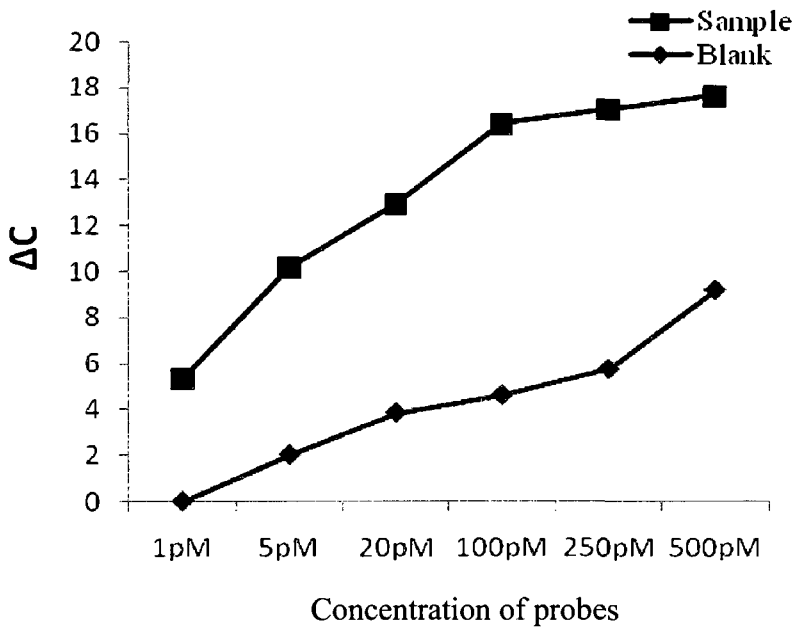

Figure 6.4. Effect of the concentration of probes on signal and background in hairpin-induced hairpin assay. Standard deviation: 0.19 -0.78.

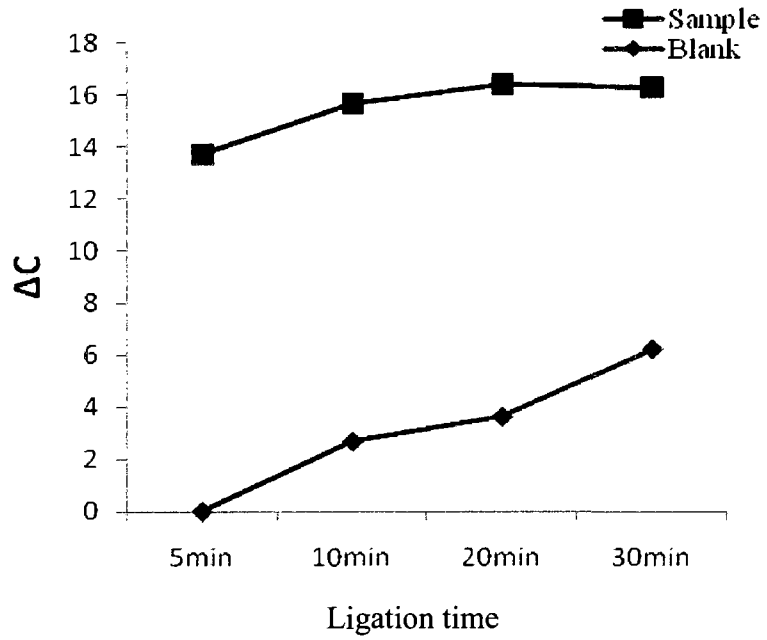

Figure 6.5. Effect of the ligation time on signal and background in hairpin-induced hairpin assay. Standard deviation: 0.31 -0.64.

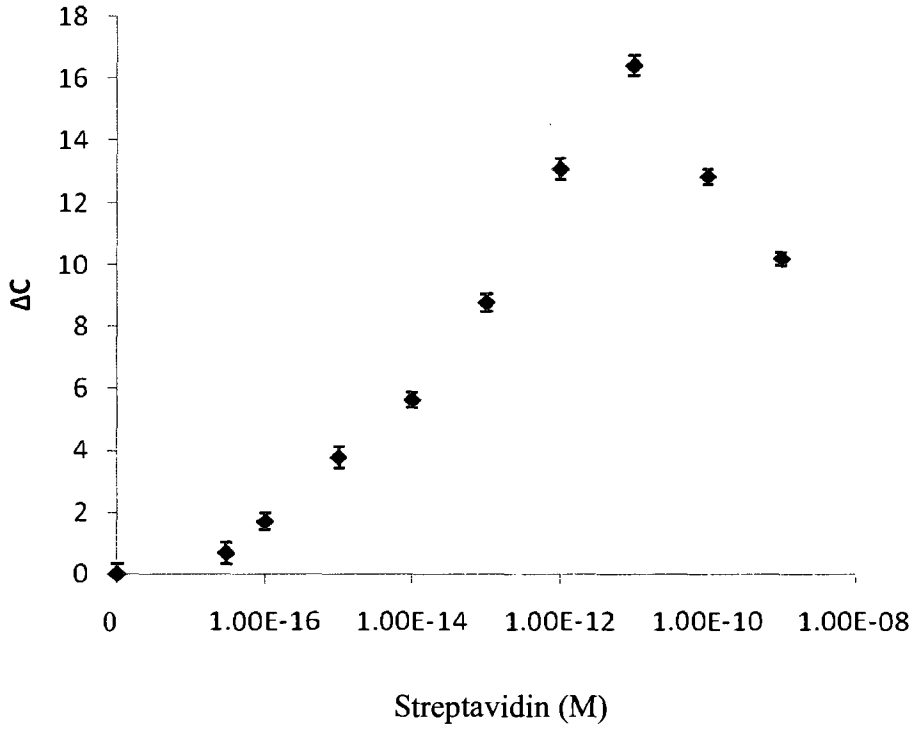

Figure 6.6. Analysis of streptavidin by binding-induced hairpin assay

6.3.3 Analysis of PDGF-BB by using aptamer as probe

Building on the success of the detection of streptavidin with extreme sensitivity, we expanded the principle to analysis of PDGF-BB by using aptamers as affinity ligands. Aptamers are short oligonucleotides that are capable of recognizing various molecular targets with high affinity and specificity (11, 12). A pair of probes was prepared by linking the above probe for streptavidin analysis with the biotinylated aptamer using the streptavidin as the intermediate molecule. Since the conjugated oligonucleotides were the same as those in the analysis of

streptavidin, we focused on the performance of probes with six or seven stem bases in the presence of various pairs of blocking oligoncleotides. The results are shown in **Figure 6.7**. The impact of blocking oligonucleotides led to similar trends in analysis of PDGF-BB by using probes with six or seven stem bases. However, the probes with six stem bases provided best sensitivity when the pair of blocking oligonucleotides, Block-F3 and Block-R6-3, was used. We optimized the initial concentration of probes for analysis of PDGF-BB, and found the probes at 100 pM resulted in the largest $\Delta\Delta C_t$ (**Figure 6.8**).

The method was demonstrated to be able to detect 5×10^{-16} M PDGF-BB. A linear dynamic range of over 4 orders of magnitude (1×10^{-15} M to 1×10^{-11} M) was achieved (**Figure 6.9a**). To demonstrate the applicability of the method for biological samples, the PDGF-BB spiked into mammalian cell lysate was analyzed. A similar calibration curve was obtained compared to results from the analysis of PDGF-BB in incubation buffer (**Figure 6.9b**).

While PDGF-BB was detected with high sensitivity, other PDGF isomers AA and AB could not be detected because the aptamer binds to the B chain of PDGF with high affinity, but not to the A chain of PDGF (13).

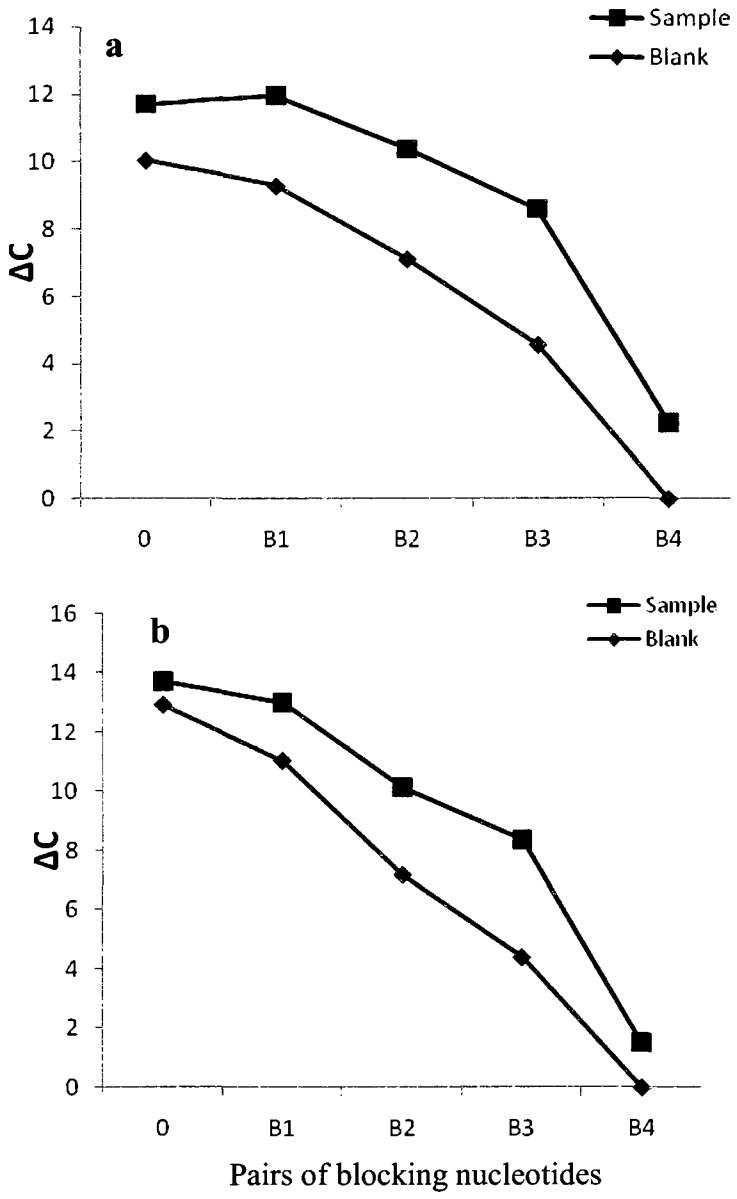

Figure 6.7. Effect of the length of blocking oligonucleotides on the analysis of PDGF-BB by using probes with 6 stem bases (a) or 7 stem bases (b). In (a), B1, B2, B3, and B4 represent Block-F-1and Block R6-1, Block-F-2 and Block R6-2, Block-F-3 and Block R6-3, and Block-F-4 and Block R6-4, respectively. In (b), B1, B2, B3, and B4 represent Block-F-1and Block R7-1, Block-F-2 and Block R7-2, Block-F-3 and Block R7-3, and Block-F-4 and Block R7-4, respectively. 0 means no blocking oligonucleotide was used. Sequences of the blocking oligos are shown in Table 6.1. Standard deviation: 0.21 -0.59.

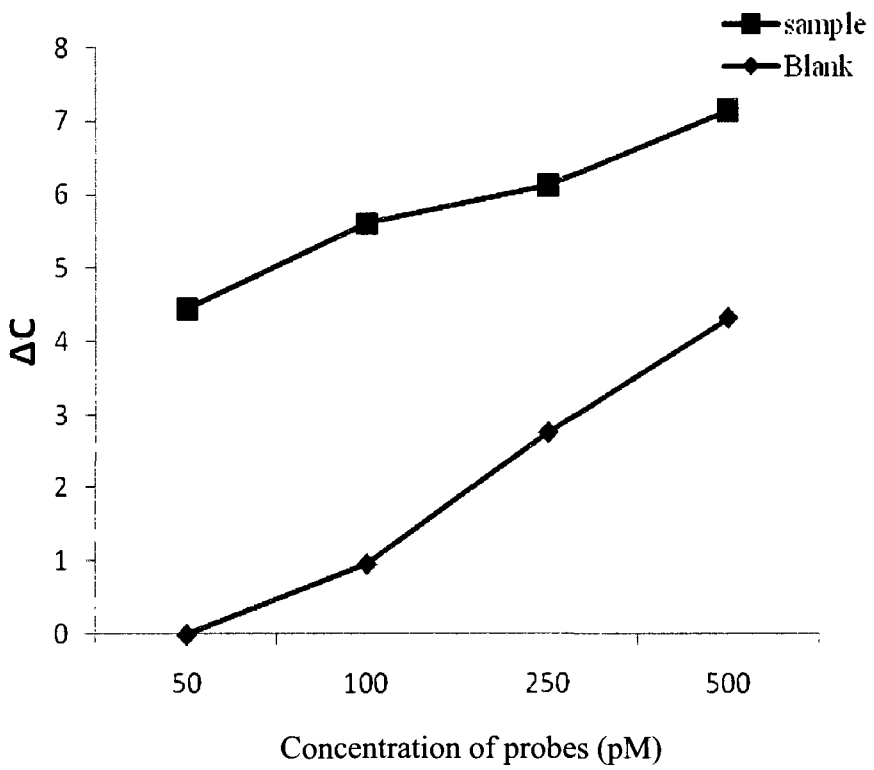

Figure 6.8. Effect of the probe concentration on analysis of PDGF-BB. Standard deviation: 0.18 -0.52.

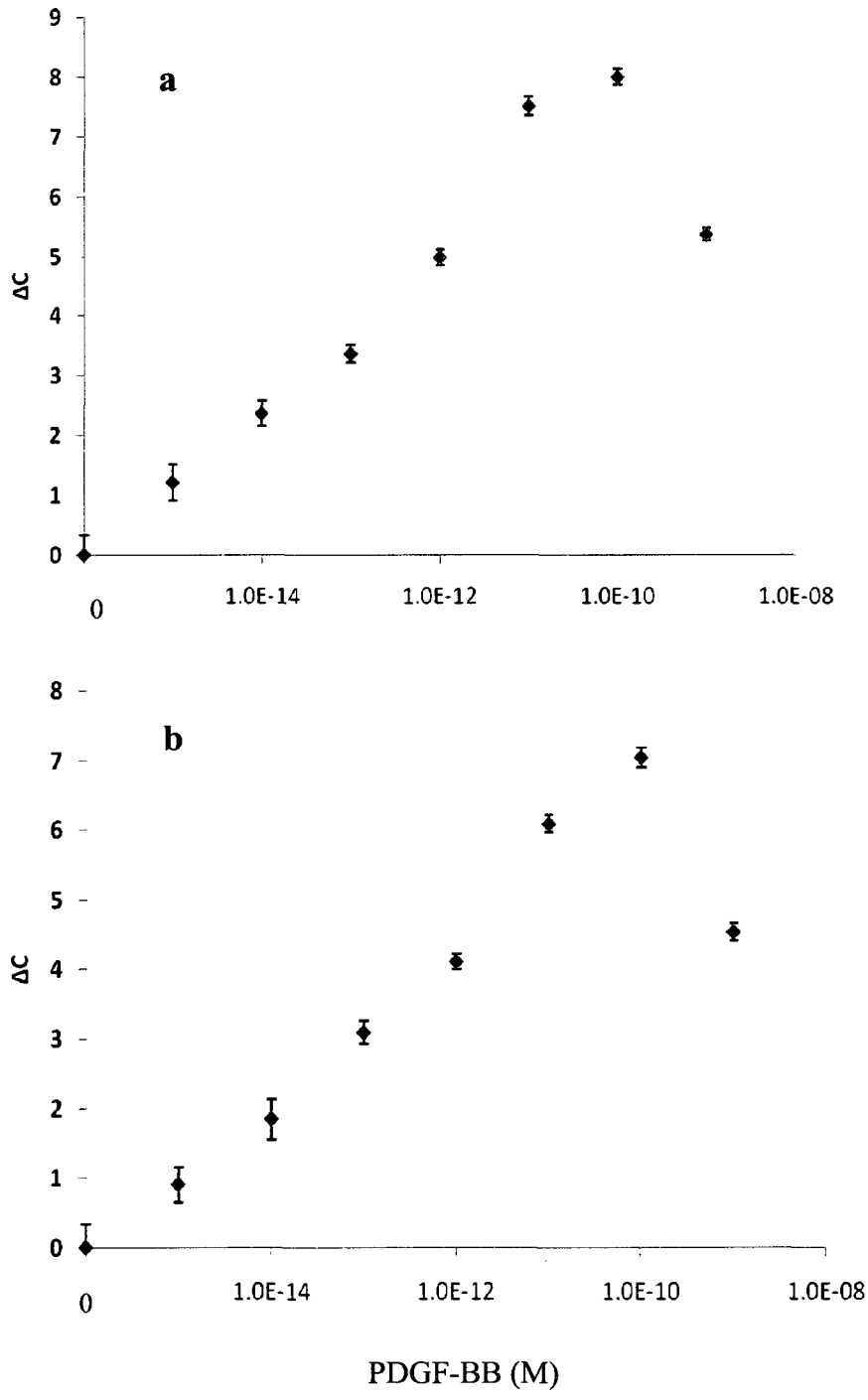

Figure 6.9. Analysis of PDGF-BB in 1×PBS (a) and cell lysate (b) by binding-induced hairpin assay

6.3.4 Analysis of PSA

Antibodies are also able to serve as affinity ligands in the binding-induced hairpin ligation assay. To prepare the antibody-based probes for analysis of PSA, we attached the streptavidin probes to biotinylated antibodies by using streptavidin as a connector. The performance of probes with six or seven stem bases was also studied in the presence of various pairs of blocking oligonucleotides. While probes with six stem bases produced the best sensitivity for detection of both streptavidin and PDGF-BB, the probes with seven stem bases led to the better results in analysis of PSA (**Figure 6.10**). These results suggested that larger loop induced in analysis of PSA required a longer stem sequence to efficiently form the hairpin structure. Similarly, the concentration of probes and ligation time were optimized to obtain the best sensitivity (**Figure 6.11**).

We were able to detect 1×10^{-16}M PSA, which represents the ability of the method to detect as low as 60 PSA molecules in 1 μL. A linear dynamic range of over 5 orders of magnitude (1×10^{-15}M to 1×10^{-10}M) was obtained (**Figure 6.12a**). When the method was applied to detect the spiked PSA in diluted goat serum, similar sensitivity and dynamic range were achieved (**Figure 6.12b**).

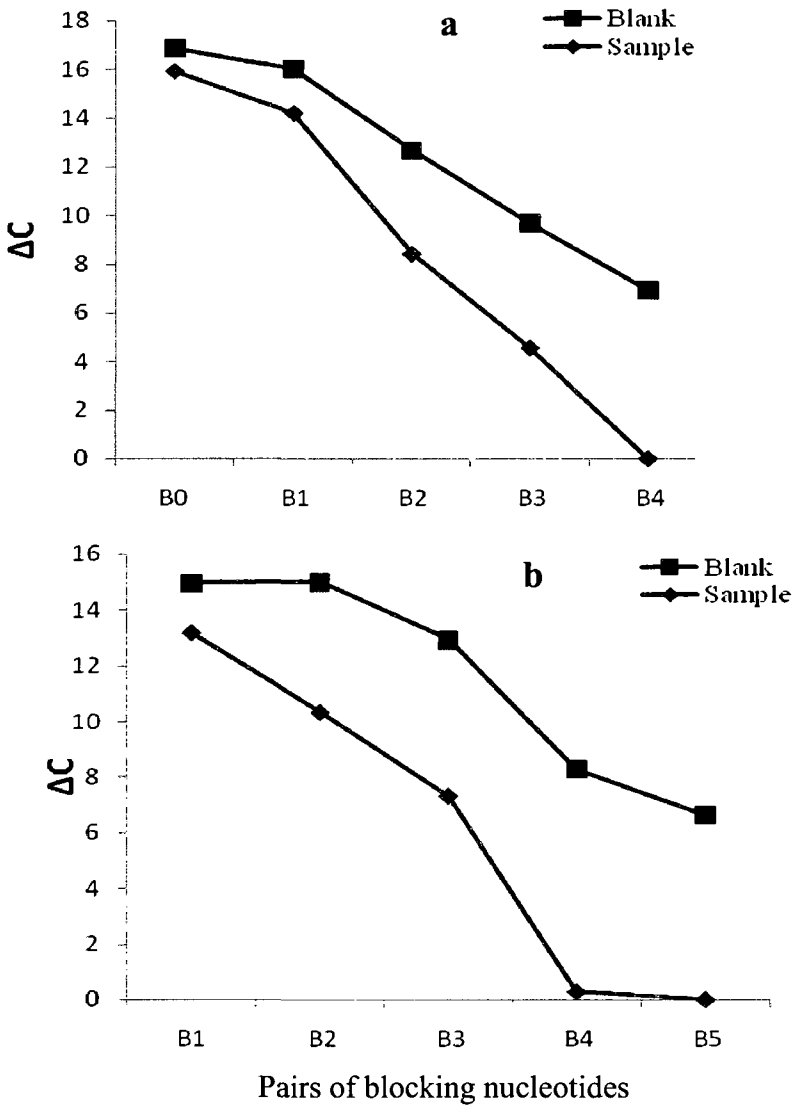

Figure 6.10. Effect of the length of blocking oligonucleotides on the analysis of PSA by using probes with 6 stem bases (a) or 7 stem bases (b). In (a), B1, B2, B3, and B4 represent Block-F-1and Block R6-1, Block-F-2 and Block R6-2, Block-F-3 and Block R6-3, and Block-F-4 and Block R6-4. In (b), B1, B2, B3, B4, and B5 represent Block-F-1and Block R7-1, Block-F-2 and Block R7-2, Block-F-3 and Block R7-3, Block-F-4 and Block R7-4, and Block-F5 and Block-R7-4. 0 means no blocking oligonucleotide was used. Sequences of the blocking oligos are shown in Table 6.1. Standard deviation: 0.29 -0.84.

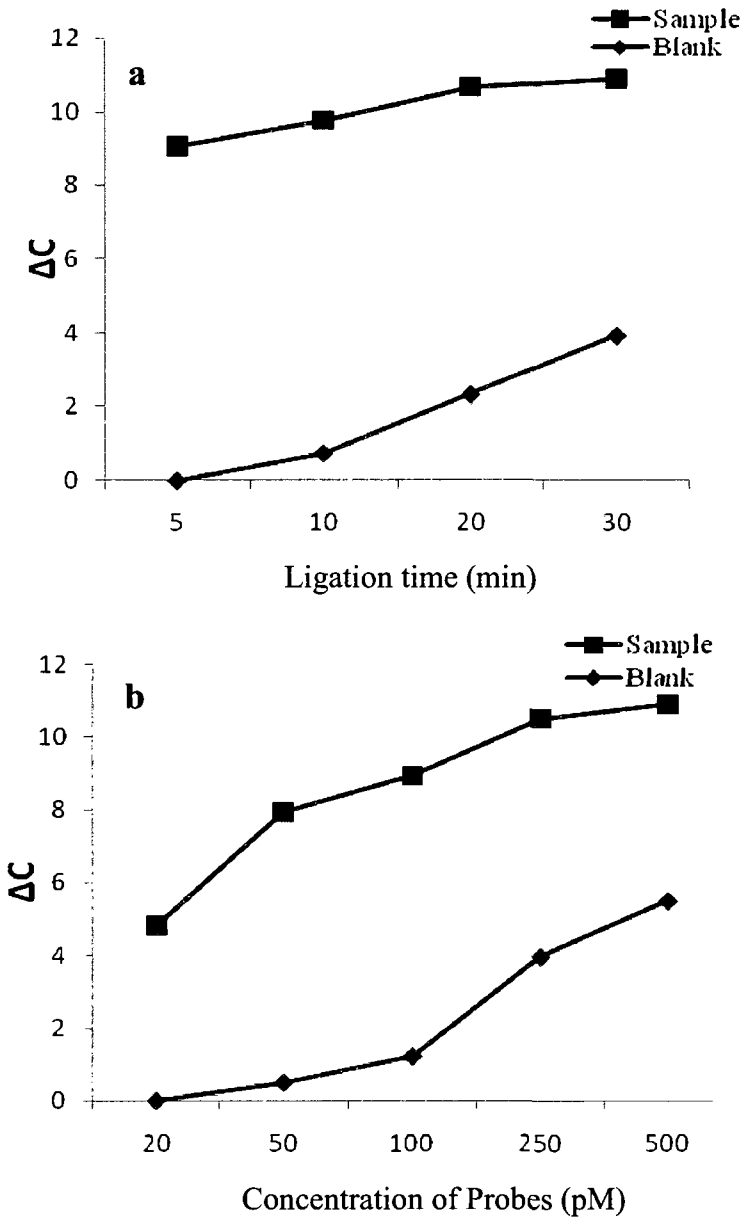

Figure 6.11. Effect of the ligation time (a) and probe concentration (b) on the analysis of PSA. Standard deviation: 0.16 -0.55.

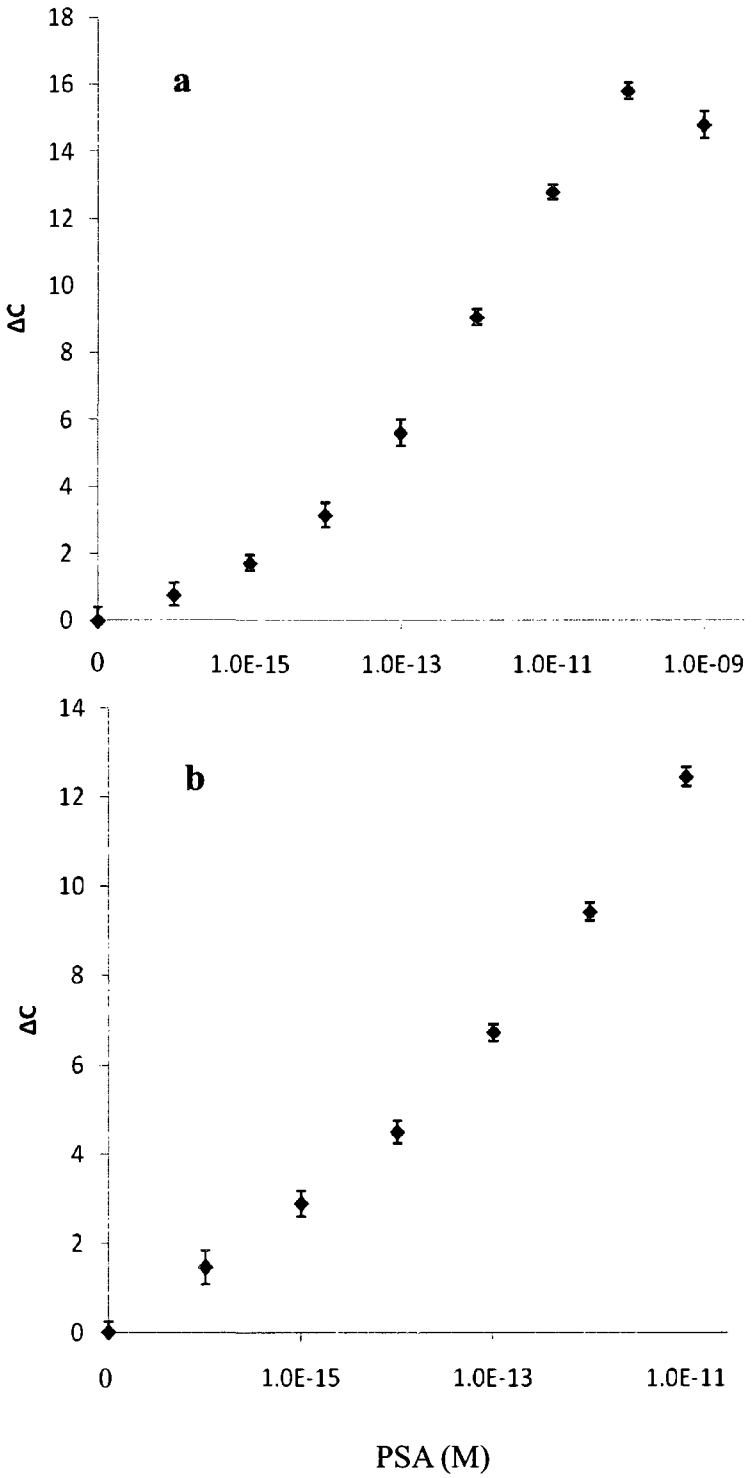

Figure 6.12. Analysis of PSA in 1×PBS (a) and goat serum (b) by binding-induced hairpin assay

6.4 Discussion and Conclusions

The results have demonstrated a new strategy to construct a hairpin structure as a result of molecular binding. Hairpin structures could be formed once complementary sequences are present in a single nucleotide molecule. In addition to the presence of complementary sequences, the binding-induced hairpin structures resulted in the integration of separate probes with the target protein into a single complex molecule. Therefore, the formation of binding-induced hairpin structures enables the analysis of proteins in homogeneous solution. The adaptation of the DNA ligation technique converted the formation of hairpin structures into the synthesis of a new oligonucleotide, which allowed us to detect the target protein using the technique for nucleic acid detection, real-time PCR. The method possesses similar potential sensitivity to the detection of nucleic acids. Three proteins were detected with a sensitivity of about 10^3- to 10^5-fold higher than the general pM detection limit of ELISA. The sensitivity of the method is comparable to another ligation assay involving real-time PCR (14, 15). Because the occurrence of binding-induced hairpin structures also requires the two probes to bind to a single target molecule simultaneously, the method has similar specificity to other sandwich format assays. The applicability of the method was demonstrated by analysis of proteins in cell lysate or serum.

Various ligands could be employed to create the probes, depending on the target and the availability of ligands. In order to achieve better sensitivity, ligands with higher affinity are preferred, because these ligands allow a larger portion of

the target molecules involved into the hairpin structure. The nucleotides in probes should be long enough to allow the hybridization of the stem sequence. The length of nucleotides could be optimized by experiments. The nucleotides used in probes having 77 bases total in the loop were capable of analysis of three protein targets by using various types of ligands. The stem sequences in probes play a crucial role in the determination of the sensitivity of analysis. The length and G-C content of the stem sequences could be determined by a combination of theoretical estimation and experimentation. After optimization, the stem sequences need only minor adjustments for various assays. Because of the longer complementary sequence of blocking nucleotides and their higher concentrations present in solution, the blocking oligonucleotides could effectively reduce the independent background hybridization of free probes, thereby eliminating the interference of background.

The detection schemes for the binding-induced hairpin structure are not limited to the ligation assay used in this study. Many fluorescence techniques could be employed to monitor the hairpin formation. A pair of fluorophores or quantum dots could be attached to the free ends of probes; therefore, the formation of the hairpin structure would be amenable for FRET. The stem formation of hairpin structure could also be detected by double-stranded DNA dyes, such as SYBR green.

In addition to protein detection, the binding-induced hairpin assay should enable the detection of various macromolecule targets, such as lipids,

polysaccharides, or whole cells. The events that allow two probes to be brought together in a single complex molecule, such as the interaction of two biomolecules, also could be monitored by binding-induced hairpin. Furthermore, after simple modifications, the binding-induced hairpin assay should also be suitable for the detection of macromolecules within living cells.

6.5 References

1. G. Varani, *Annu. Rev. Biophys. Biomol. Struct.*, 1995, 24, 379-404.
2. C. E. Pearson and R. R. Sinden, *Curr. Opin. Struct. Biol.*, 1998, 8, 321-330.
3. G. Bonnet, O. Krichevsky and A. Libchaber, *Proc. Natl. Acad. Sci. U S A.*, 1998, 95, 8602-8606.
4. G. Bonnet, S. Tyagi, A. Libchaber and F. R. Kramer, *Proc. Natl. Acad. Sci. U S A.*, 1999, 96, 6171-6176.
5. S. Tyagi and F. R. Kramer, *Nat. Biotechnol.*, 1996 14, 303-308.
6. S. Tyagi, D. P. Bratu and F. R. Kramer, *Nat. Biotechnol.*, 1998, 16, 49-53.
7. S. Tyagi, S. A. E. Marras and F. R. Kramer, *Nat. Biotechnol.*, 2000, 18, 1191-1196.
8. D. L. Sokol, X. Zhang, P. Lu and A. M. Gewirtz, *Proc. Natl. Acad. Sci. U S A.*, 1998 95, 11538-11543.
9. D. Whitcombe, J. Theaker, S. P. Guy, T. Brown and S. Little, *Nat. Biotechnol.*, 1999, 17, 804-807.
10. L. Diatchenko, Y. F. Lau, A. P. Campbell, A. Chenchik, F. Moqadam, B. Huang, S. Lukyanov, K. Lukyanov, N. Gurskaya, E. D. Sverdlov and P. D. Siebert, *Proc. Natl. Acad. Sci. U S A.* 1996, 93, 6025-6030.
11. A. D. Ellington and J. W. Szostak, *Nature*, 1990, 346, 818-822.
12. C. Tuerk and L. Gold, *Science*, 1990, 249, 505-510.
13. L. S. Green, D. Jellinek, R. Jenison, A. Ostman, C. H. Heldin and N. Janjic, *Biochemistry*, 1996, 35, 14413-14424.

14. S. Fredriksson, M. Gullberg, J. Jarvius, C. Ollson, K. Pietras, S. M. Gustafsdottir, A. Ostman and U. Landergren, *Nat. Biotechnol.*, 2002, 20, 473-477.

15. E. Schallmeiner, E. Oksanen, O. Ericsson, L. Spångberg, S. Eriksson, U. Stenman, K. Pettersson, U. Landegren, *Nat. Methods*, 2007, 4, 135-137.

Chapter Seven

Conclusions and Synthesis

7.1 Introduction

Proteins are essential components of organisms and are involved in a wide range of biological functions (1, 2). The occurrences of various cancers and diseases may involve altered protein expression and distribution (3-5). The detection of certain proteins could potentially serve as diagnostic tests for specific diseases (6-8). The early detection of a disease can significantly facilitate its ultimate control and treatment (9, 10). Therefore, there is substantial interest in the detection of proteins at ultra-low levels, because numerous important biological markers for cancer, infectious diseases, or biochemical processes are present at very low levels during the early stages of disease development (11, 12). Moreover, a few molecules of a particular protein are sufficient to trigger a disease or to affect the biological functions of cells. Methods with extreme sensitivity and high specificity are therefore required.

Tremendous advances have been achieved in the development of protein detection technologies, such as ELISA, protein microarray, immunosensors and mass spectrometry-based technologies (14-18). Although some of these methods have provided improved sensitivity, most of them are only able to detect abundant proteins.

Recent advances in nucleic acid amplification technologies and nanotechnologies have greatly contributed to the development of ultrasensitive

technologies for protein detection (19). The amplification of oligonucleotides conjugated to the affinity probes indirectly improves the sensitivity of protein detection by increasing the number of detection molecules. The employment of nano/micro materials conjugated to affinity probes enhances the measurement signals by using the unique electrical, optical, and catalytic properties of these novel materials. However, most of these methods are generally useful for detection of an individual or several proteins.

Detection of specific proteins at ultra-low levels is still particularly challenging. While nucleic acids can be amplified by PCR to improve the sensitivity, there is no comparable technique to chemically amplify proteins. Furthermore, a myriad of proteins are present in cells, and their abundances range by more than 10^6-fold (12, 13). Therefore, the determination of specific proteins at ultralow levels is usually challenged by the presence of a huge excess of other more abundant molecules.

This investigation was focused on the development of novel bioanalytical techniques enabling the detection of proteins with extreme sensitivity, and high specificity and throughput. The key results and a synthesis of the experimental findings are summarized below.

7.2 Advancement in Knowledge

7.2.1 Chapter 2: Developing tunable aptamer capillary electrophoresis and demonstrating its application to multiple protein analysis

An aptamer-based CE method termed tunable aptamer CE was developed for multiple protein analysis. The key concept is tuning the electrophoretic

mobility of proteins with DNA aptamers to achieve efficient separation of multiple proteins. The unique properties of aptamers impart them with the ability to serve as effective charge modulators, modifying the electrophoretic mobility of specific proteins. In free-zone CE, aptamers migrate through the capillary at a similar mobility. The single peak produced by various aptamers leaves more space for protein separation. Aptamers are highly negatively charged, and each nucleotide carries near -1 charge under the pH conditions typically used for CE separation. In contrast, the size of a nucleotide is much smaller than that of a protein. The binding of an aptamer to a protein produces a strong impact on the mass-to-charge ratio of the protein. Moreover aptamers could also be easily designed to desired lengths. As a result, the electrophoretic mobility of specific proteins could be rationally controlled by binding to aptamers of varying nucleotide length. In addition to the adaptation of aptamers as charge modulators, another important benefit of aptamer binding to the proteins is the incorporation of fluorescent aptamers as probes to enable laser induced fluorescence (LIF) detection of the proteins that are otherwise not amenable to high sensitivity LIF detection. The simultaneous determination of pM levels of IgE, HIV-RT, thrombin, and PDGF-BB was achieved in a single CE analysis.

7.2.2 Chapter 3: Demonstrating the ability of the tunable aptamer capillary electrophoresis to separate and detect protein isomers

The tunable aptamer CE was demonstrated for the differentiation and detection of PDGF-AB and PDGF-BB isomers. Using an aptamer that binds to the B chain but not the A chain of PDGF, it was able to tweak the electrophoretic

mobilities of the PDGF isomers for their separation. PDGF-AB bound to a single aptamer was well resolved from PDGF-BB bound to two aptamer molecules. Simultaneous determination of 50 pM of two isomers was accomplished in a single analysis. PDGF-AB has been found to be able to serve as a connector, bringing receptor α and fluorescent aptamer into a single complex molecule. As a result, the formation of a receptor α–PDGF-AB–aptamer complex enabled the detection of the receptor α in a noncompetitive affinity assay. In comparison, a competitive assay has been developed for the determination of receptor β. The assay takes advantage of the variation of the PDGF-BB aptamer complex formation upon the competition between the receptor β and fluorescent aptamer in binding to the PDGF-BB. Detection limits were 0.5 nM for PDGF receptor α and 5 nM for receptor β. Determination of PDGF isomers and their receptors in diluted serum samples showed no interference from the sample matrix.

7.2.3 Chapter 4: Developing affinity aptamer amplification assay and demonstrating its application to ultrasensitive detection of HIV-RT

A new approach for the detection of minute amounts of proteins was developed, termed the affinity aptamer amplification assay. It is based on the integration of affinity aptamer recognition, CE separation, and PCR amplification. The aptamer was first introduced to bind to the target protein, forming protein-aptamer complex. The protein-aptamer complex was then separated from the unbound aptamer by CE. Fractions were collected at 30 s intervals and each fraction was subjected to PCR analysis. Amplification of the protein-bound aptamer by PCR dramatically improved the sensitivity of the analysis of the

corresponding target protein. This method was applied to the determination of trace amounts of HIV-RT, and was able to detect 30 fM of HIV-RT in a 10 nL sample, representing approximately 180 molecules of the protein. The method exhibited high specificity for the target protein, due to the specific recognition of the aptamer and the CE separation.

7.2.4 Chapter 5: Expanding the affinity aptamer amplification assay as a generalized approach for multiple protein detection

The affinity aptamer amplification assay was further expanded as a generalized approach for multiple protein detection. Its capability for multiple protein analysis is attributed to the powerful separation ability of CE and the unique specificity of PCR amplification. The typical free-zone CE allows various aptamers to migrate through the capillary at a similar mobility, but protein-aptamer complexes migrate faster than aptamers. Therefore, it is possible to find a boundary of the migration time for the fraction collection. The fractions collected before the boundary contained only protein-aptamer complexes, and not unbound aptamers. The detection of proteins is achieved by the amplification of aptamers dissociated from complexes using pairs of primers that are designed specifically for the corresponding aptamers. Simultaneous determination of fM levels of IgE, HIV-RT and thrombin was achieved in a single analysis. The separation between the individual protein-aptamer complexes is not required. The method has great potential for analysis of other proteins.

7.2.5 Chapter 6: Developing the binding-induced hairpin assay and demonstrating its application to ultrasensitive detection of streptavidin,

PDGF-BB, and PSA

A new strategy for the construction of probes was developed for the determination of trace amounts of proteins or other macromolecules in homogeneous solutions. A pair of probes was created through the conjugation of oligos to affinity ligands. While affinity ligands are able to bind to target proteins, oligos contain the complementary stem sequences at their free ends. In the absence of target, the probes are present separately because the stem sequences are designed to be so short that hybrids of oligos are unable to exit at the temperature of the analysis. When a pair of probes encounters a target molecule, the binding of the pair of probes brings the two probes into a single complex molecule. The stem sequences of oligos in the single complex molecule are brought into close proximity. The subsequent hybridization of stem sequences allows the formation of a hairpin structure. Because this hairpin structure is induced upon the binding of probes to the target protein, it is termed as binding-induced hairpin. The formation of binding-induced hairpin structures enables the analysis of proteins in homogeneous solution. The adaptation of the DNA ligation technique converted the formation of hairpin structures into the synthesis of a new oligonucleotide, allowing the detection of the target protein by using the technique for nucleic acid detection, such as real-time PCR. The assay offered the similar potential sensitivity to the detection of nucleic acids. Three proteins were detected with a sensitivity of about 10^3-to 10^5- fold higher than the general pM detection limit of ELISA.

7.3 Conclusions

Three novel bioanalytical techniques for the determination of trace amounts of proteins have been developed in this investigation. In addition to the use of affinity ligands (aptamers and antibodies) as recognizing molecules for target proteins, other unique properties of aptamers and antibodies were explored in the development of these techniques, including serving as templates of PCR amplification in the affinity aptamer amplification assay, working as charge modulators in the tunable aptamer amplification assay, and providing loop and stem sequences of the hairpin construction in the binding-induced hairpin assay. The application of these techniques to the ultrasensitive protein detection, multiple protein detection, and protein isomer detection was demonstrated. The results of this investigation provide exciting approaches with many potential applications, such as detection of low abundance proteins for proteomics research and medical diagnostics, studies of molecular interactions, biosensing, environmental analysis, and drug discovery.

7.4 Future Research

Building on the success of the development of three novel approaches for ultrasensitive protein analysis, further research needs to be conducted to improve the applicability and practicability of the methods. Regarding the affinity apatmer amplification assay, the methods could be applied to analysis of more target proteins or other molecular targets. If aptamer complexes of other macromolecular targets, such as lipids and polysaccharides, could be separated

from unbound aptames by CE, the detection of these targets could be achieved. Furthermore, the ability of the method to perform multiple protein detection could be further demonstrated by simultaneous analysis of more target proteins in a single analysis. The differentiation and detection of protein isomers or of a family of proteins are always challenging. Therefore, it is very interesting and useful to explore further the ability of tunable aptamer CE to separate protein isomers or family proteins, if more aptamers are selected to bind to protein isomers or proteins in a family. The binding-induced hairpin assay was only initially developed in this investigation. A lot of work is required to further improve and expand this exciting technique. The measurement of the formation of binding-induced hairpins is not limited to enzyme-based ligation and PCR amplification. Many fluorescence techniques could be easily employed to monitor the hairpin formation, such as FRET, and double-stranded DNA binding dyes. Likewise, in addition to the protein detection, the binding-induced hairpin assay enables the detection of various macromolecule targets, such as lipids, polysaccharides, or whole cells. Furthermore, the principle can be applied to the study of the interaction of two biomolecules, and the detection of molecular targets within living cells.

7.5 References

1. G. A. Petsko and D. Ringe, *Protein Structure and Function,* New Science Press, London, 2004.
2. R. K. Murray, D. K. Granner, P. A. Mayes and V. W. Rodwell, *Harper's Illustrated Biochemistry,* McGraw-Hill Companies, New York, 2003.
3. A. A. Alaiya, B. Franzen, G. Auer and S. Linder, *Electrophoresis,* 2000, 21, 1210-1217.
4. A. Alaiya, M. Al-Mohanna and S. Linder, *J. Proteom. Res.,* 2005, 4, 1213-1222.
5. P. R. Srinivas, B. S. Kramer and S. Srivastava, *Lancet Oncol.,* 2001, 2, 698-704.
6. A. V. Rapkiewicz, V. Espina, E. F. Petricoin III and L. A. Litotta, *Eur. J. Cancer,* 2004, 40, 2604-2612.
7. J. Hernandez and I. M. Thompson, *Cancer,* 2004, 101, 894-904.
8. S. Korfias, G. Stranjalis, A. Papadimitriou, C. Psachoulia, G. Daskalakis, A. Antsaklis and D. E. Sakas, *Curr. Med. Chem.,* 2006, 13, 3719-3731.
9. R. Etzioni, N. Urban, S. Ramsey, M. McIntosh, S. Schwartz, B. Reid, J. Radich, G. Anderson and L. Hartwell, *Nat. Rev. Cancer*, 2003, 3, 1-10.
10. J. D. Wulfkuhe, L. A. Liotta and E. F. Petricoin, *Nat. Rev. Cancer*, 2003, 3, 267-275.
11. G. S. Omenn, *Proteomics*, 2006, 6, 5662-5673.
12. N. L. Anderson and N. G. Anderson, *Mol. Cell Proteomics,* 2002, 1, 845-867.
13. S. Hanash, *Nature*, 2003, 422, 226-232.

14. E. Engvall and P. Perimann, *Immunochemistry,* 1971, 8, 871-874.

15. P. B. Luppa, L. J. Sokoll and D. W. Chan, *Clin. Chim. Acta,* 2001, 314, 1-26.

16. A. Bange, H. B. Halsall and W. R. Heineman, *Biosen. Bioelectron.,* 2005, 20, 2488-2503.

17. M. F. Templin, D. Stoll, M. Schrenk, P. C. Traub, C. F. Vohringer and T. O. Joos, *Trends Biotechnol.,* 2002, 20, 160-166.

18. R. Aebersold and M. Mann, *Nature,* 2003, 422, 198-207.

19. H. Zhang, Q. Zhao, X.-F. Li and X. C. Le, *Analyst,* 2007, 132, 724-737.